

# East Asian Workshop on Exotic Hadrons 2024

— 东亚奇特强子态研讨会 —

Dec.8 - Dec.12 2024 / Nanjing, China

## Machine learning-based line shape analysis of exotic hadron candidates

**Denny Lane Sombillo**

*National Institute of Physics, University of the Philippines Diliman*

[LM Santos, VAA Chavez, DLBS, JPG \(2025\) 52 015104](#)

[DAO Co, VAA Chavez, DLBS, arXiv:2403.18265](#) Accepted in PRD

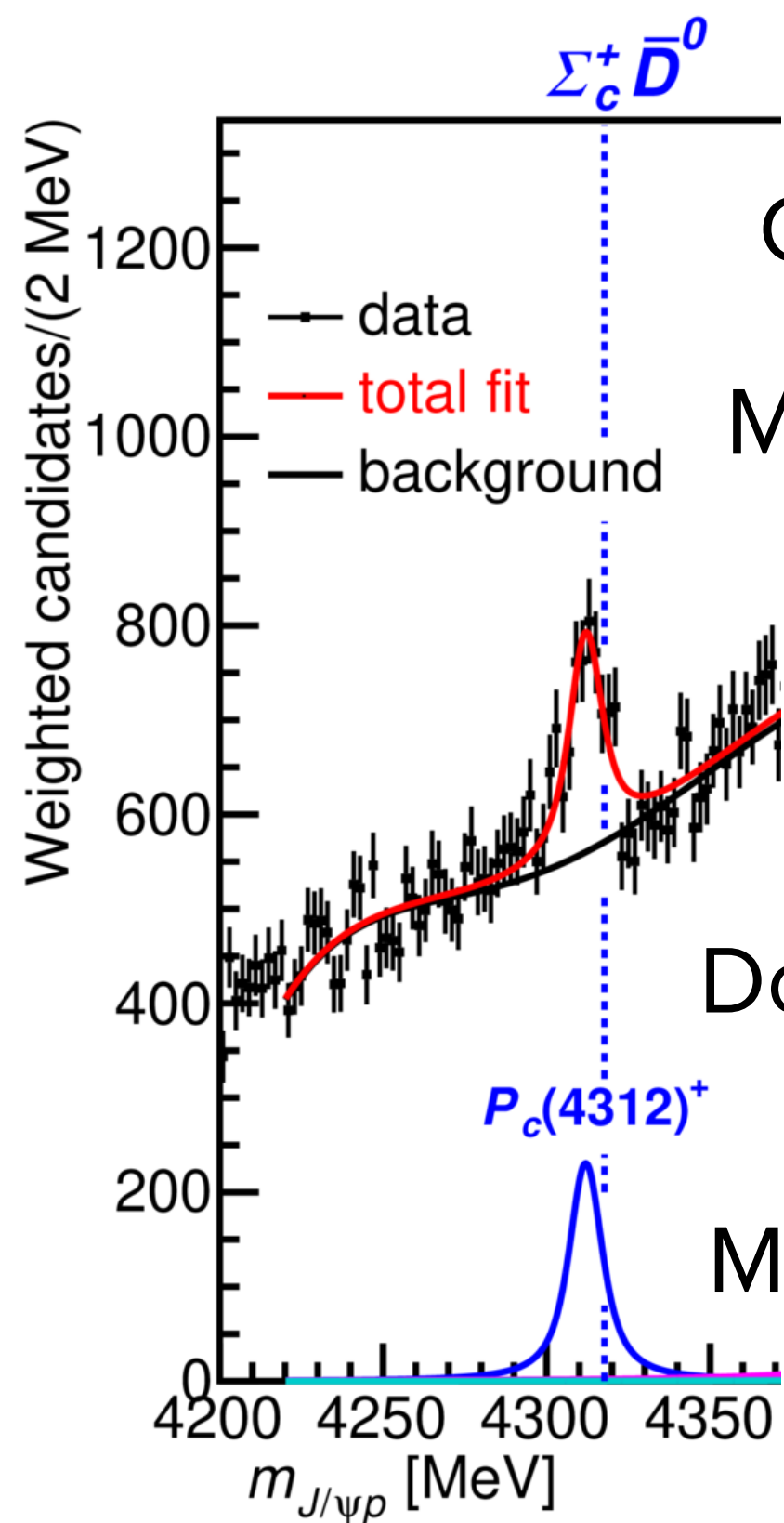
[DLBS, Y Ikeda, T Sato, A Hosaka PRD 102 016024 \(2020\)](#)

[DLBS, Y Ikeda, T Sato, A Hosaka Few-Body Syst. 62, 52 \(2021\)](#)



# Hadron spectroscopy - line shape interpretation

- Many observations of possible new states.
- Some are near hadron-hadron thresholds.
- Experiments give us the line shape.
- How do we interpret/ classify them?



Compact: [A Ali, AY Parkhomenko, PLB 793 \(2019\)](#)

Molecular: [ML Du, V Baru, FK Guo, C Hanhart, UG Meißner, J A Oller, Q Wang, PRL 124 072001 \(2020\)](#)

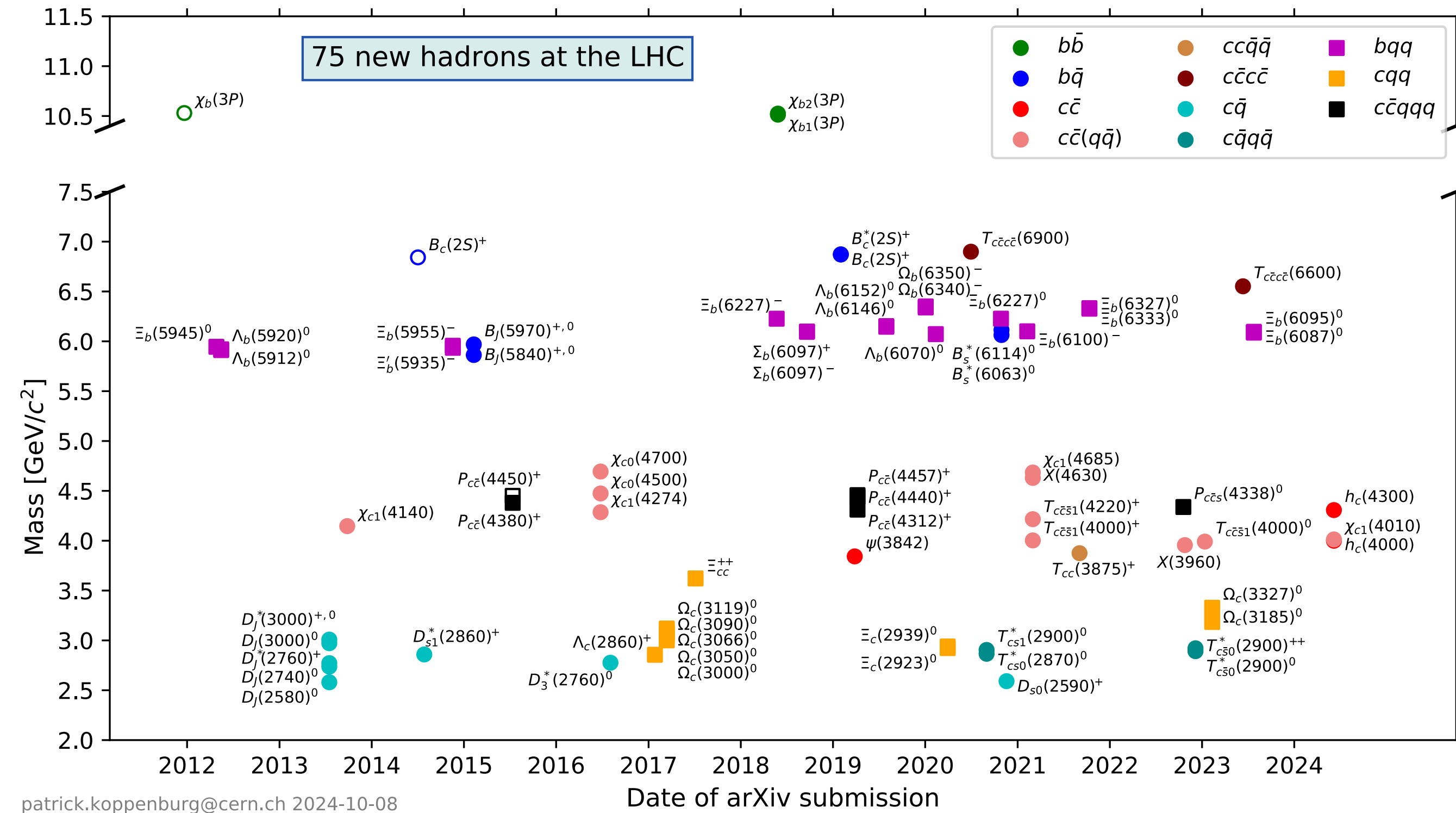
Virtual: [JPAC, PRL 123 092001 \(2019\)](#)

Double TS: [SX Nakamura, PRD 103 L111503 \(2021\)](#)

Molecule coupled to compact:

[Y Yamaguchi, H García-Tecocoatzi, A Giachino, A Hosaka, E Santopinto, S Takeuchi, M Takizawa, PRD 101 091502\(R\) \(2020\)](#)

[LHCb, PRL 122 222001 \(2019\)](#)



patrick.koppenburg@cern.ch 2024-10-08

# Hadron spectroscopy - line shape interpretation

Why use machine learning in line shape analysis?

Line shape interpretation - classification problem

Deep neural network (DNN) as a universal approximator (universal map).

[K Hornik, M Stinchcomber, H White, Neural Net., 2 5 \(1989\)](#)

DNN can be trained to map input line shape space into output interpretation space.

Linear transformation + non-linear activations and squashing

$$z_j^{(0)} = W_{ij}^{(0)} x_i + b_j^{(0)}$$

$$h_j^{(1)} = \text{ReLU}(z_j^{(1)})$$

⋮

$$z_j^{(n)} = W_{ij}^{(n)} h_i^{(n)} + b_j^{(n)}$$

$$h_j^{(n+1)} = \text{ReLU}(z_j^{(n)})$$

⋮

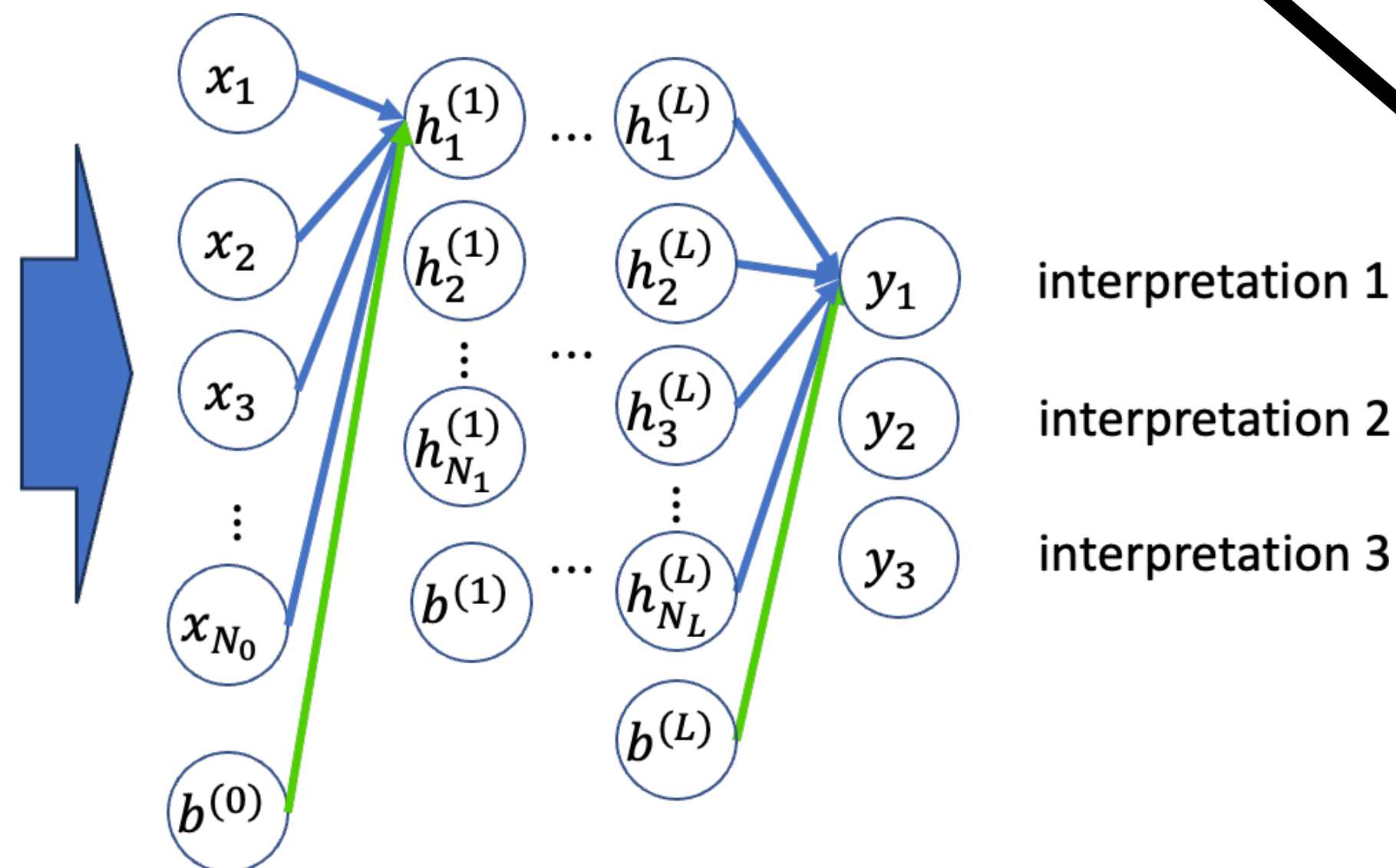
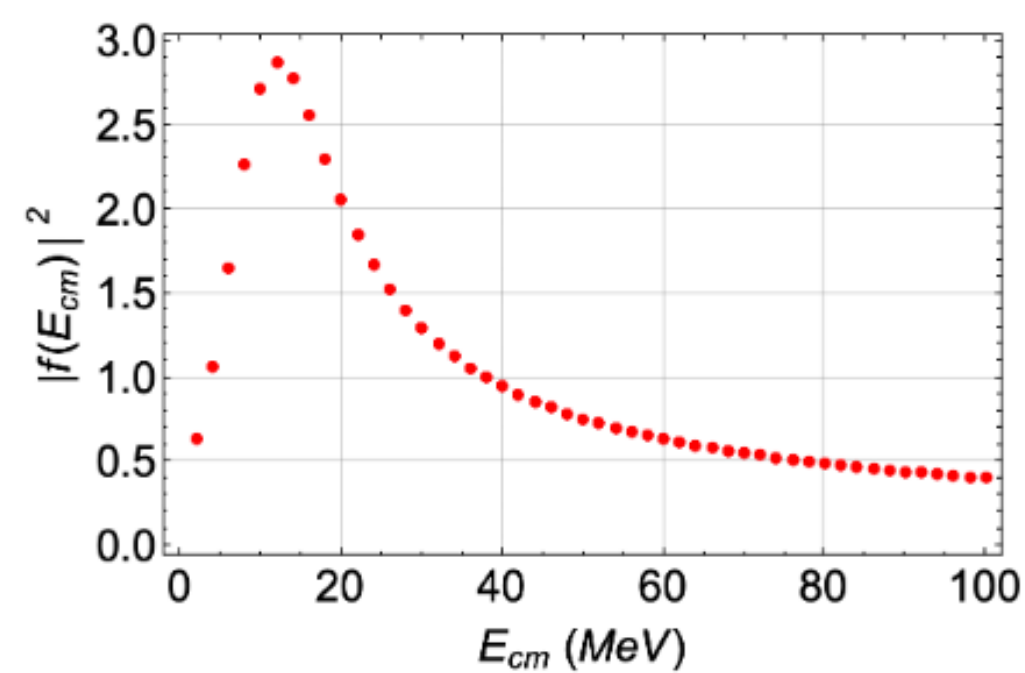
$$z_j^{(L)} = W_{ij}^{(L)} h_i^{(L)} + b_j^{(L)}$$

$$y_j = \frac{\exp(z_j^{(L)})}{\sum_i \exp(z_i^{(L)})}$$

Backpropagation to minimize the cost:

$$C(\hat{W}, \vec{b}) = \frac{1}{X} \sum_{\vec{x}} \vec{a}(\vec{x}) \cdot \log \left[ \vec{y}_{W,b}(\vec{x}) \right]$$

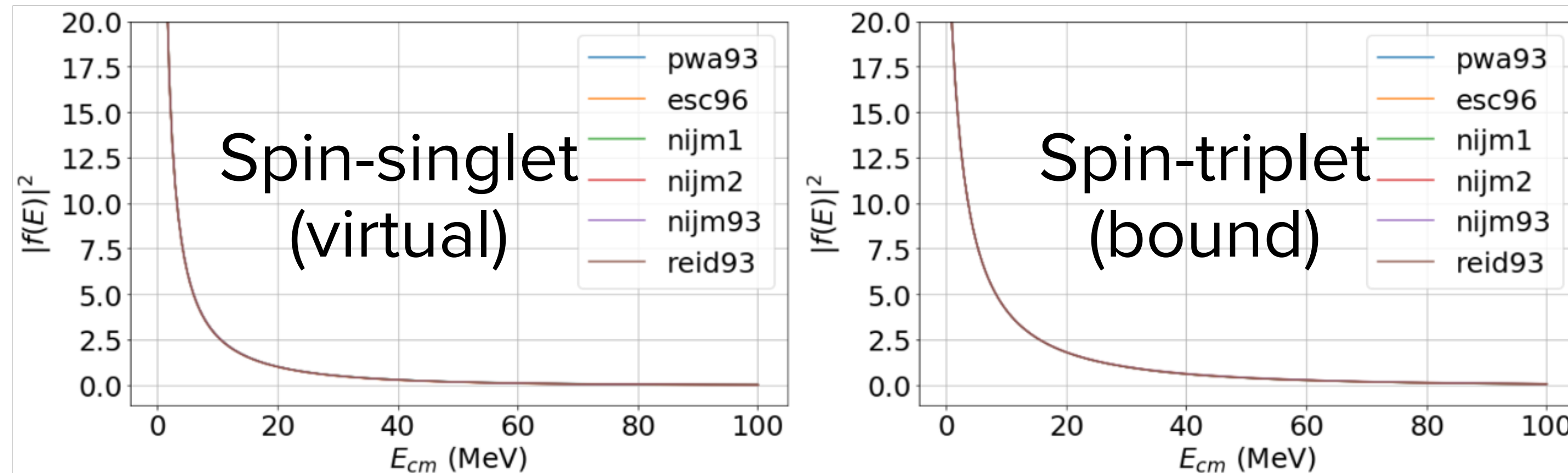
[DE Rumelhart, GE Hinton, RJ Williams, Nature 323, 533-536 \(1986\)](#)



# Deep learning: proof of principle

## Benchmarked on the known nucleon-nucleon bound state

Given only the s-wave cross section, the origin of enhancement can be unambiguously identified.



For near-threshold pole:  
 $k \cot \delta \sim -1/a$  (constant)

$$|f(k)|^{-2} = |k \cot \delta - ik|^2 \sim \frac{1}{a^2} + k^2$$

Not possible to distinguish bound vs virtual pole enhancements.

S-matrix can have distant singularities on the unphysical sheet.

Use different (unitary, analytic) backgrounds to help DNN distinguish bound and virtual enhancements.

$$S(k) = \exp \left[ 2i\delta_{bg}(k) \right] \frac{k + i\gamma}{k - i\gamma}; \quad \delta_{bg} = \alpha \tan^{-1} \left( \frac{k}{\beta} \right)$$

# Deep learning: proof of principle

DLBS, YI, TS, AH PRD 102 016024 (2020)  
DLBS, YI, TS, AH Few-Body Syst. 62, 52 (2021)

Optimize parameters of DNN using mock amplitudes:

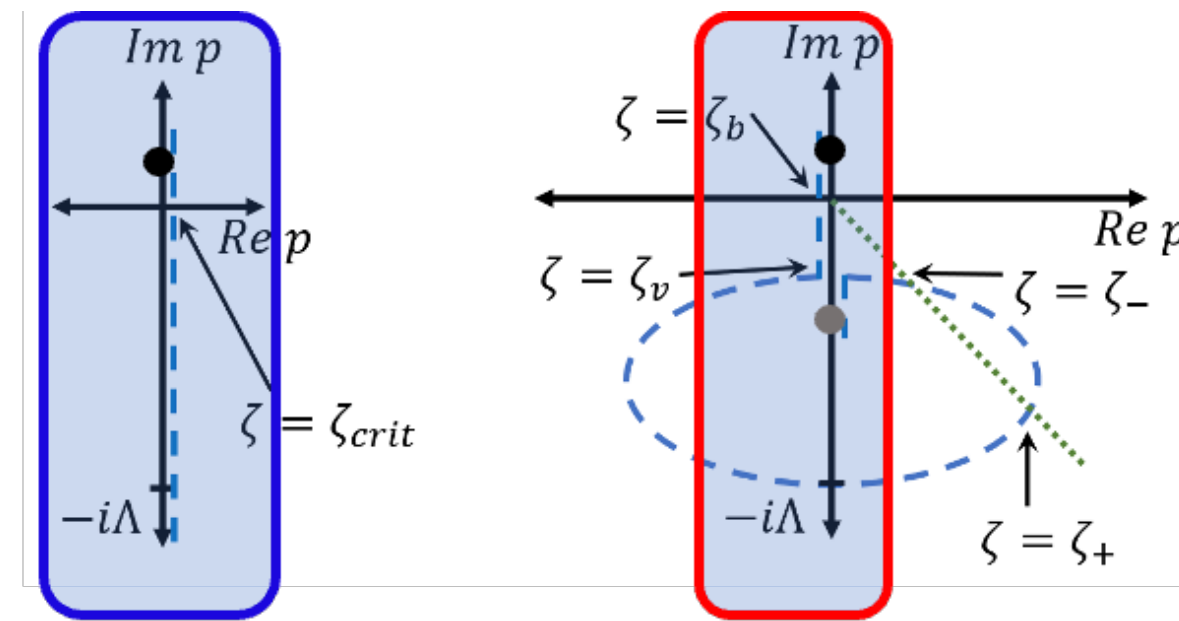
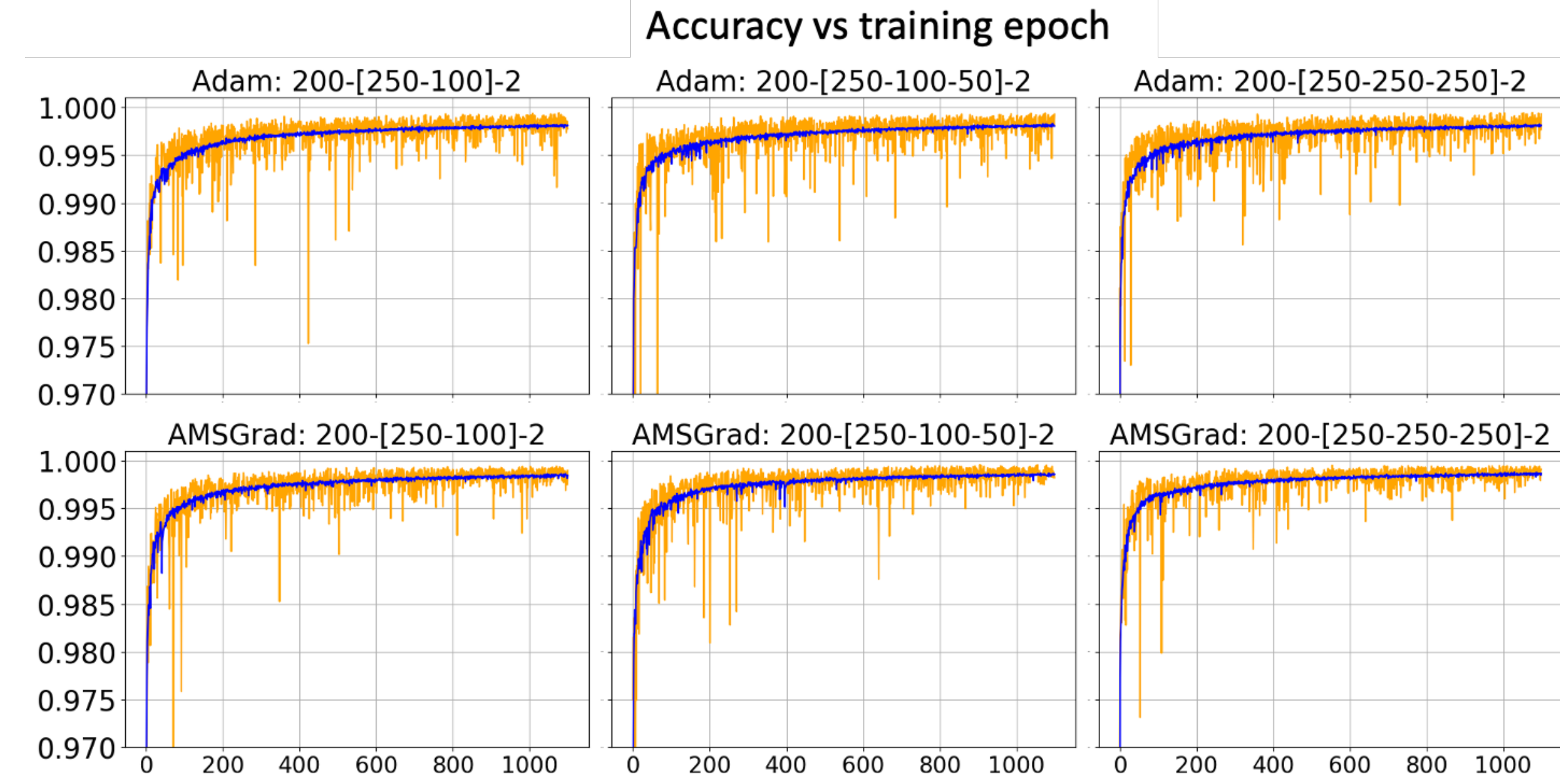
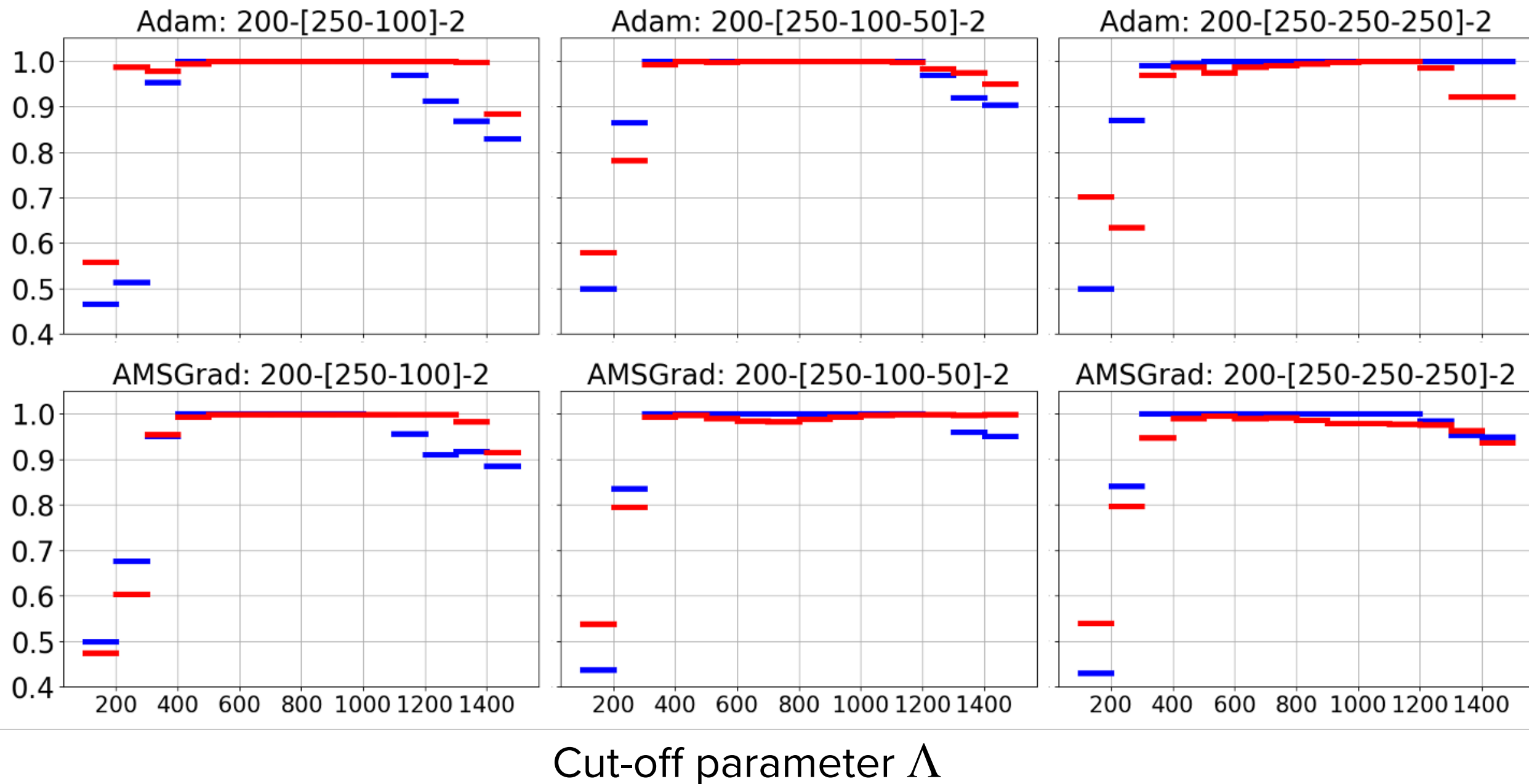
$$S(k) = \exp \left[ 2i\delta_{bg}(k) \right] \frac{k + i\gamma}{k - i\gamma}$$

3,200,000 training data

800,000 testing data

Validation using separable potential model

$$v(p, p') = \zeta \left( \frac{\Lambda^2}{p^2 + \Lambda^2} \right) \left( \frac{\Lambda^2}{p'^2 + \Lambda^2} \right)$$

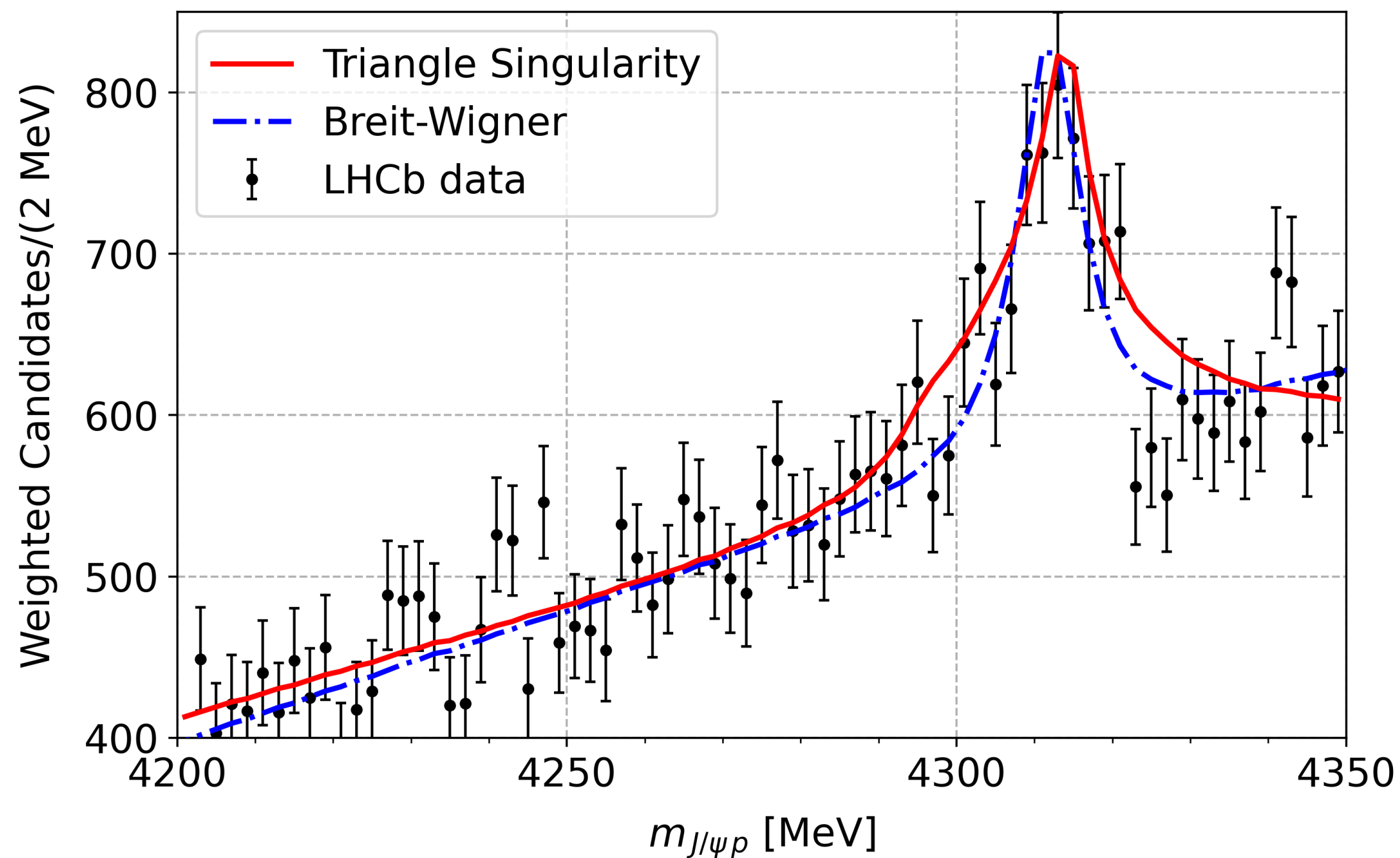
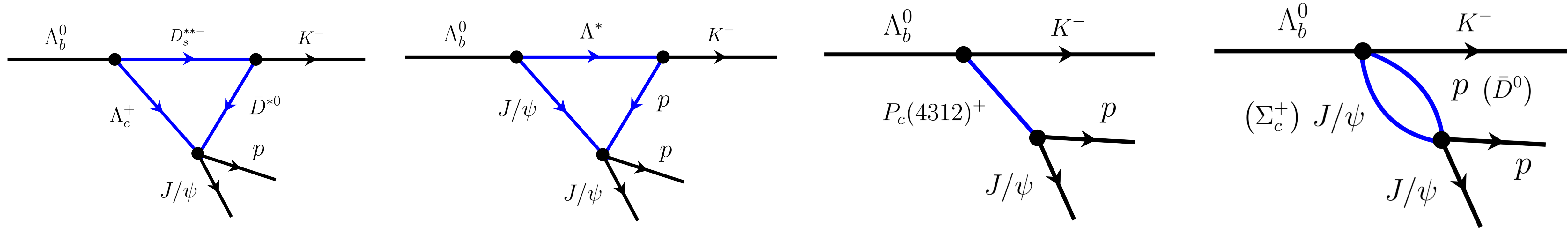


Energy independent coupling  $\zeta \rightarrow \text{constant}$   
Energy independent coupling  $\zeta \rightarrow (E - M_{sep})\zeta$

Trained and validated DNN deployed to probe the nucleon-nucleon

	PWA93	ECS96	NijmI	NijmII	Nijm93	Reid93
$^1S_0$	virtual	virtual	virtual	virtual	virtual	virtual
$^3S_1$	bound	bound	bound	bound	bound	bound

# Kinematical vs Dynamical enhancements



Can we train a DNN to discriminate different origin of enhancements?

- Triangle mechanism
- Coupled-channel effects
- True resonance

[DAO Co, VAA Chavez, DLBS, arXiv:2403.18265](#)

Accepted in PRD

If yes, then ML can supplement our analysis.

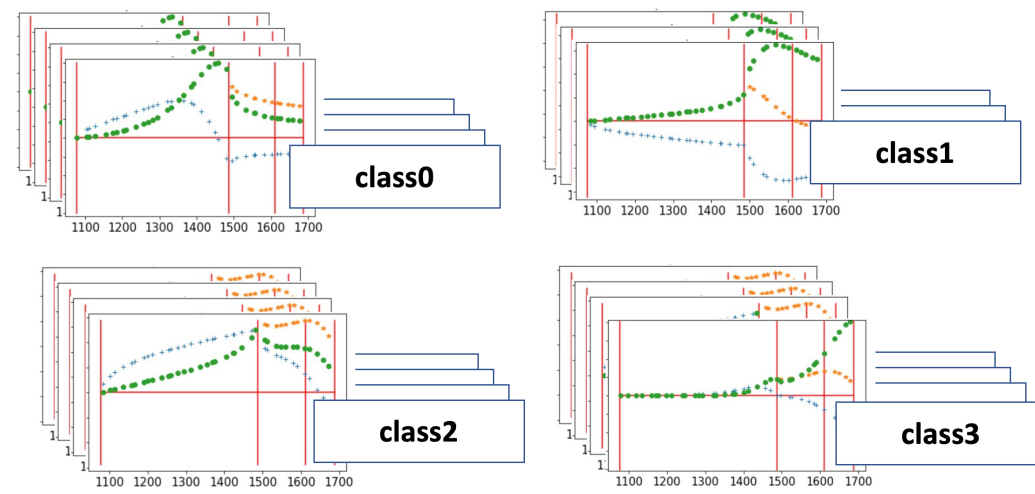
If no, then TS and pole enhancements are inherently ambiguous.

# ML framework

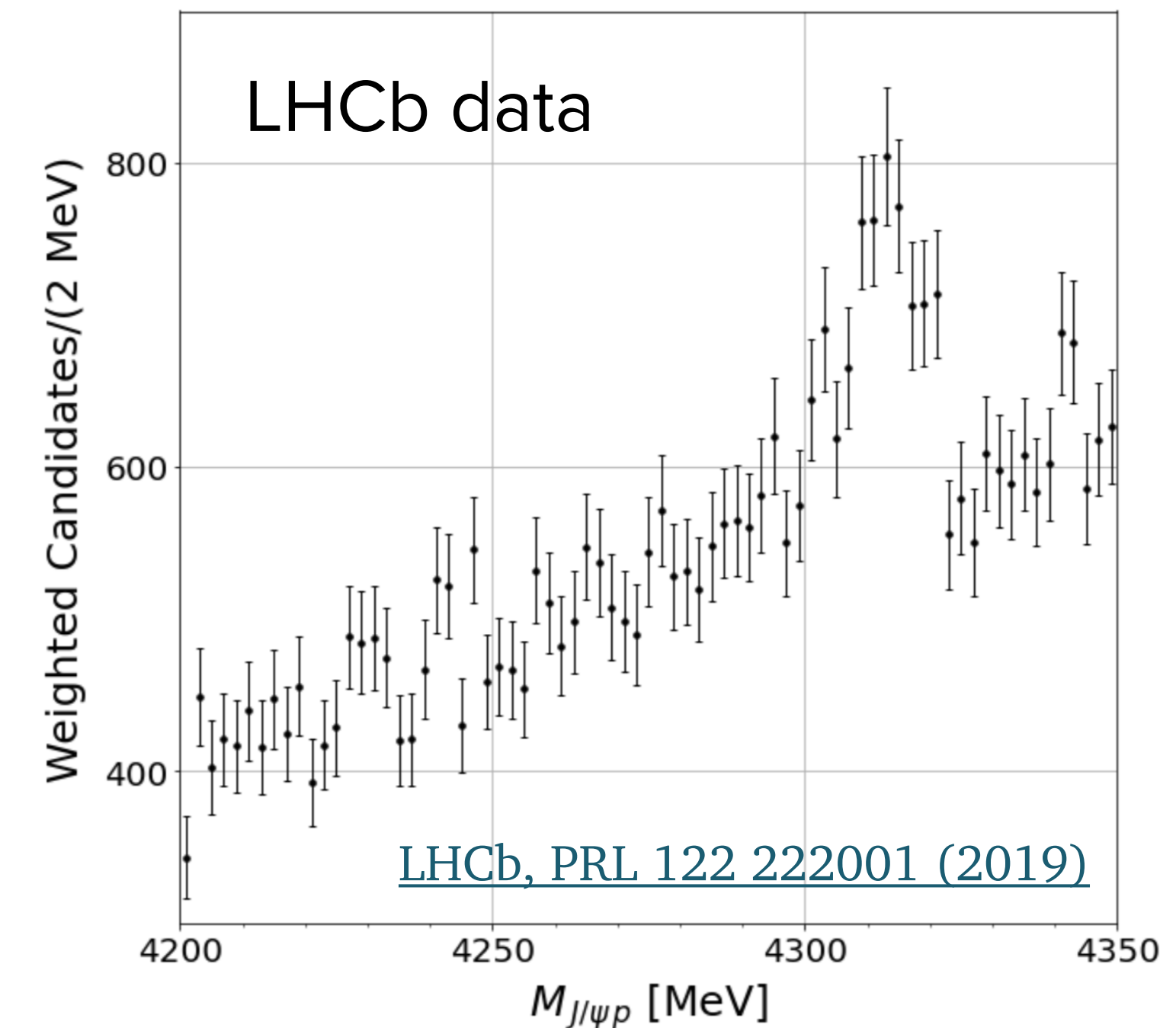
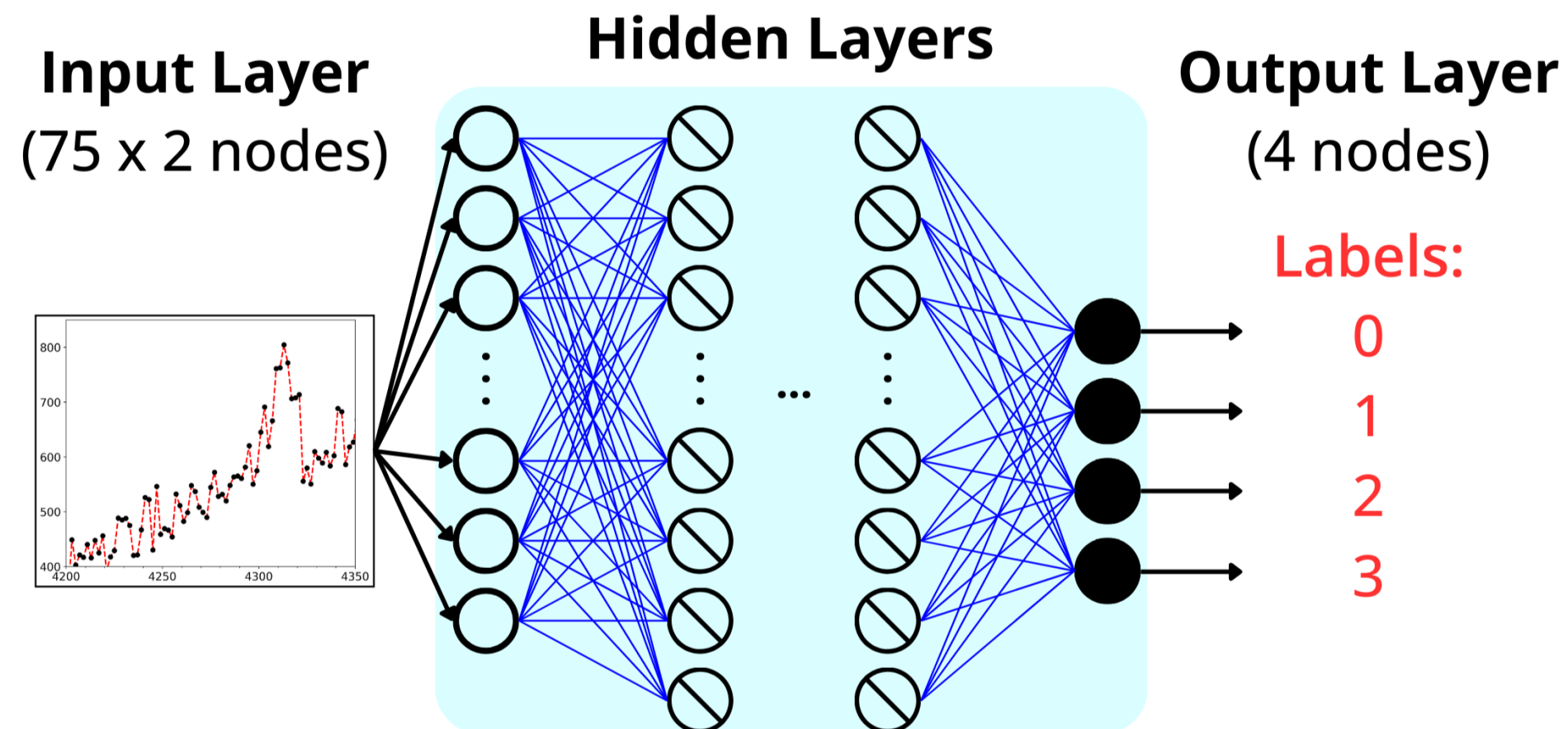
1. Choose the region of interest: [4200 MeV - 4350 MeV]

2. Generate the training dataset

- Triangle singularity
- Pole of S-matrix
  - 1 pole in 2nd RS
  - 1 pole in 4th RS
  - 1 pole each in 2nd and 3rd RS



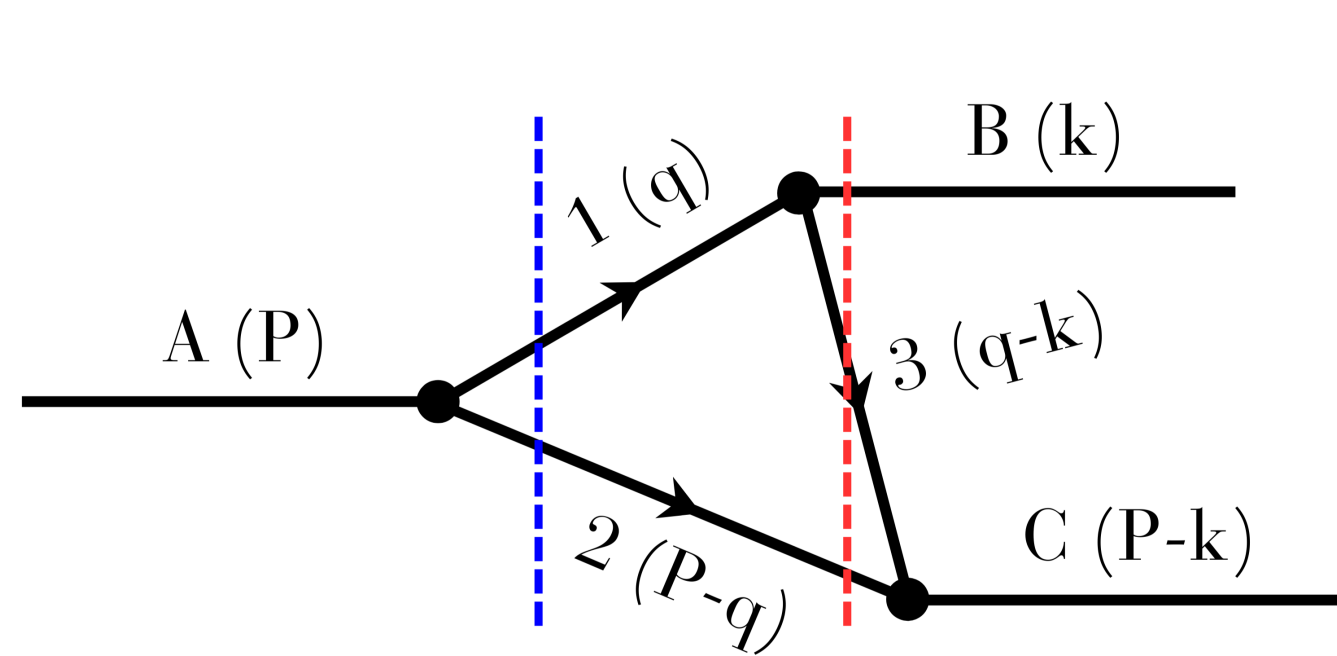
3. Design a set of DNN to solve the classification problem



4. Train, test, and validate the DNN

5. Use the trained DNN to interpret the experimental data

# (Single) Triangle mechanism



$$I(k) \propto \int_0^\infty \frac{q^2 f(q) dq}{P^0 - \sqrt{m_1^2 + q^2} - \sqrt{m_2^2 + q^2} + i\epsilon}$$

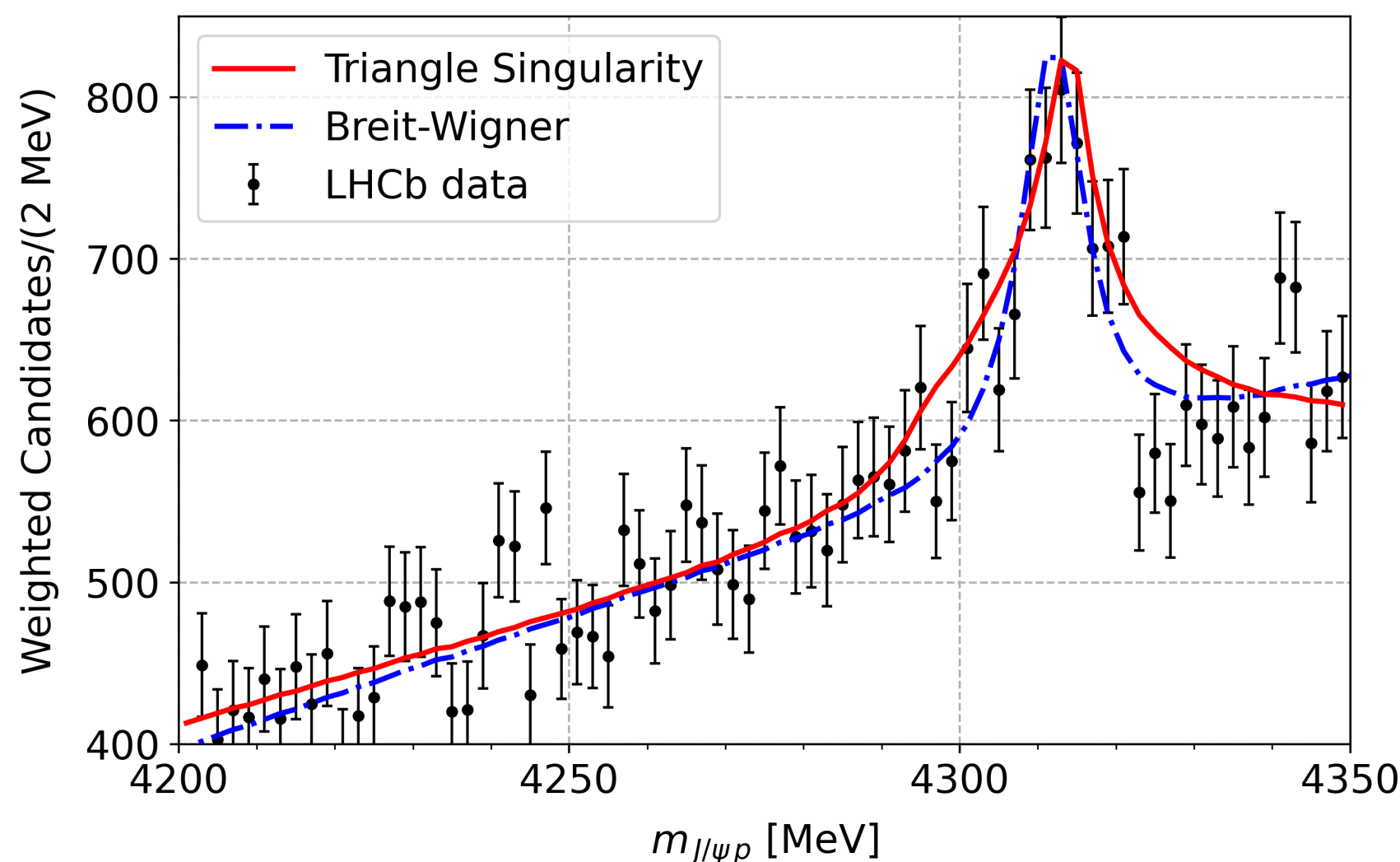
$$f(q) = \int_{-1}^1 \frac{dz}{E_C - \omega(q) - \sqrt{m_3^2 + q^2 + k^2 - 2qkz} + i\epsilon}$$

[M Bayar, F Aceti, FK Guo, E Oset, PRD 126 074039 \(2016\)](#)

[FK Guo, XH Liu, S Sakai, PPNP 122 103757 \(2020\)](#)

The amplitude has no singularity (no pole)

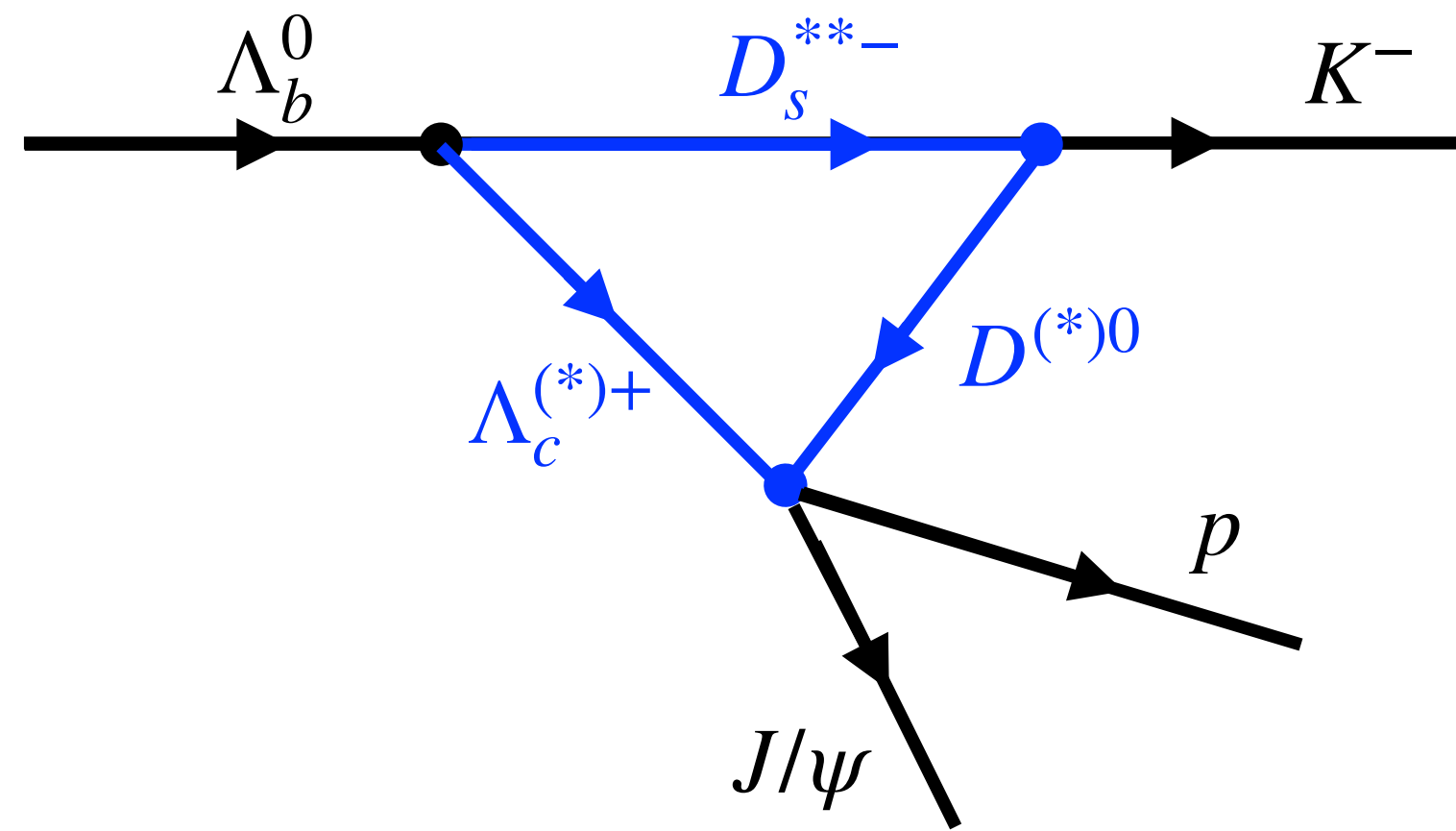
$$m_1^2 \in \left[ \frac{M_A^2 m_3 + M_B^2 m_2}{m_2 + m_3} - m_2 m_3, (M_A - m_2)^2 \right] \quad m_C^2 \in \left[ (m_2 + m_3)^2, \frac{M_A m_3^2 - M_B^2 m_2}{M_A - m_2} + M_A m_2 \right]$$



No need to introduce new hadron to explain the enhancement.

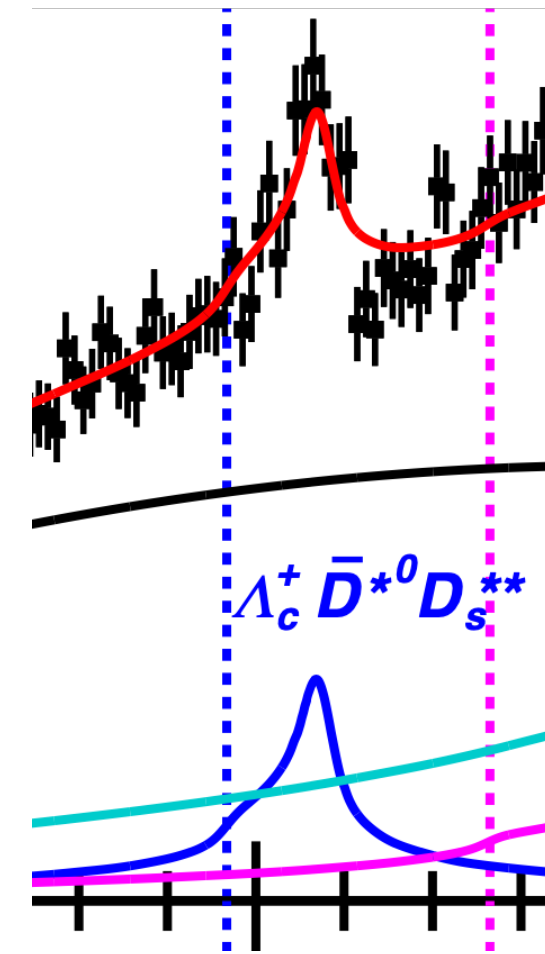
Mass condition - crucial in generating mock dataset

# (Single) Triangle mechanism

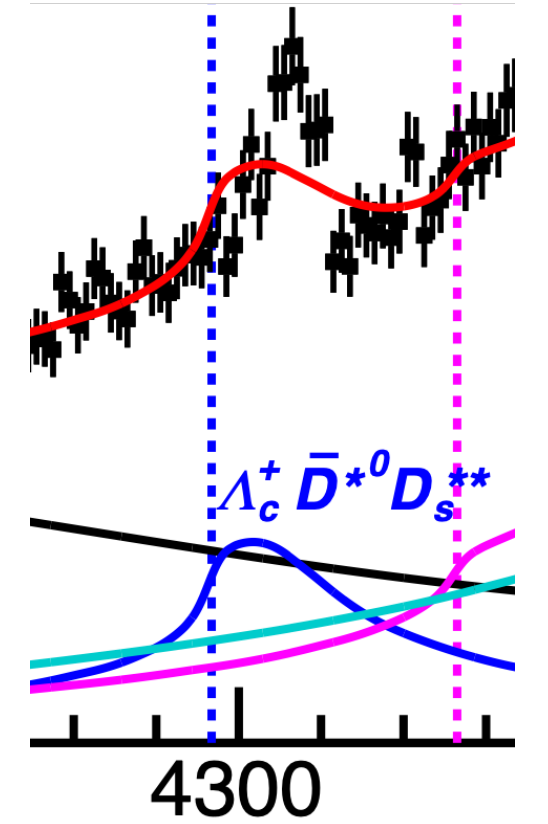


Good fit but with unrealistic  $\Gamma \sim 1\text{MeV}$  for  $D_s^{**}$

$D_s^{*-}(3288)$   
Not in PDG



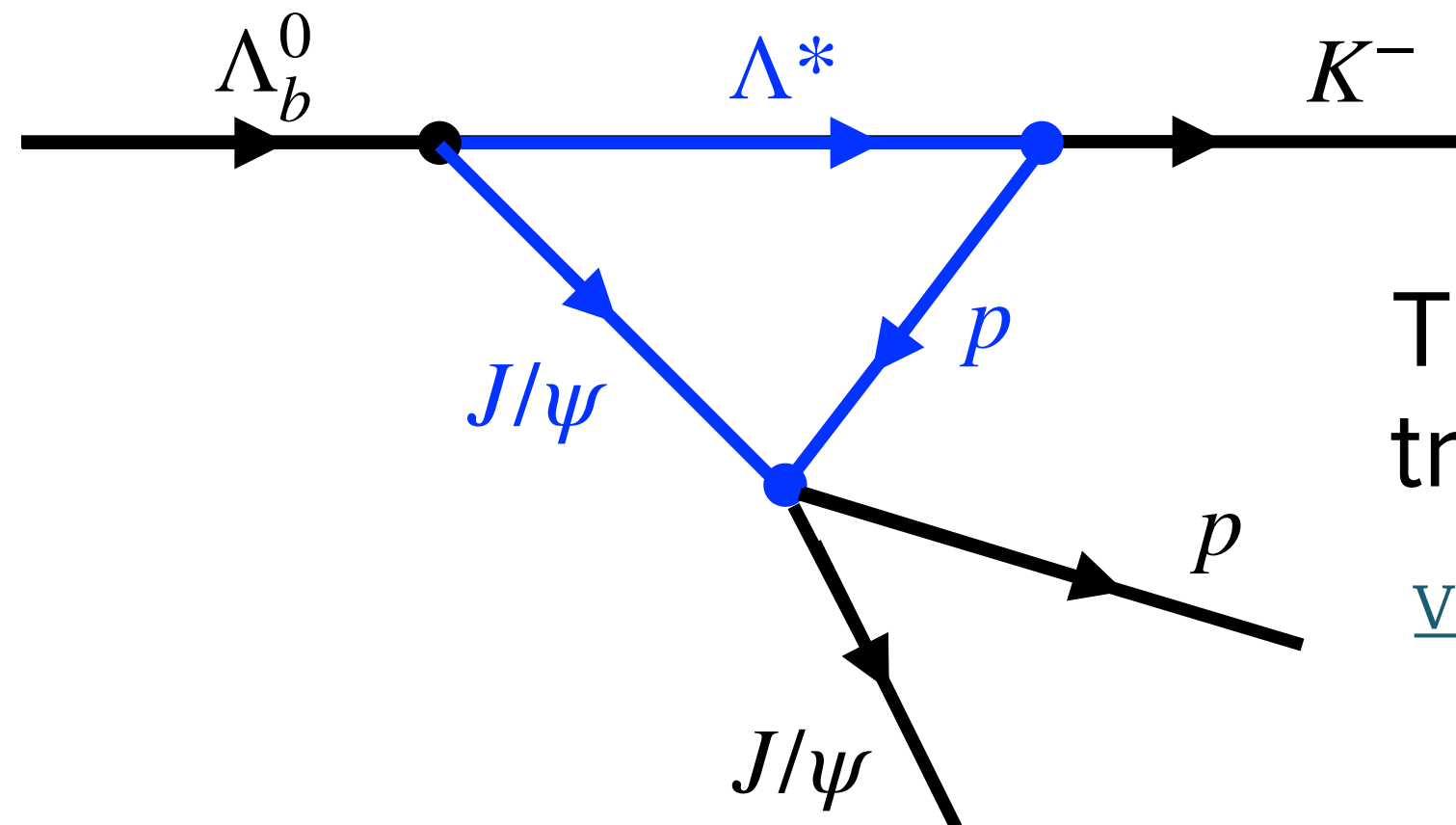
Bad fit with realistic  $\Gamma \sim 50\text{MeV}$  for  $D_s^{**}$



TS interpretation for the  $P_{c\bar{c}}(4312)^+$  - ruled out

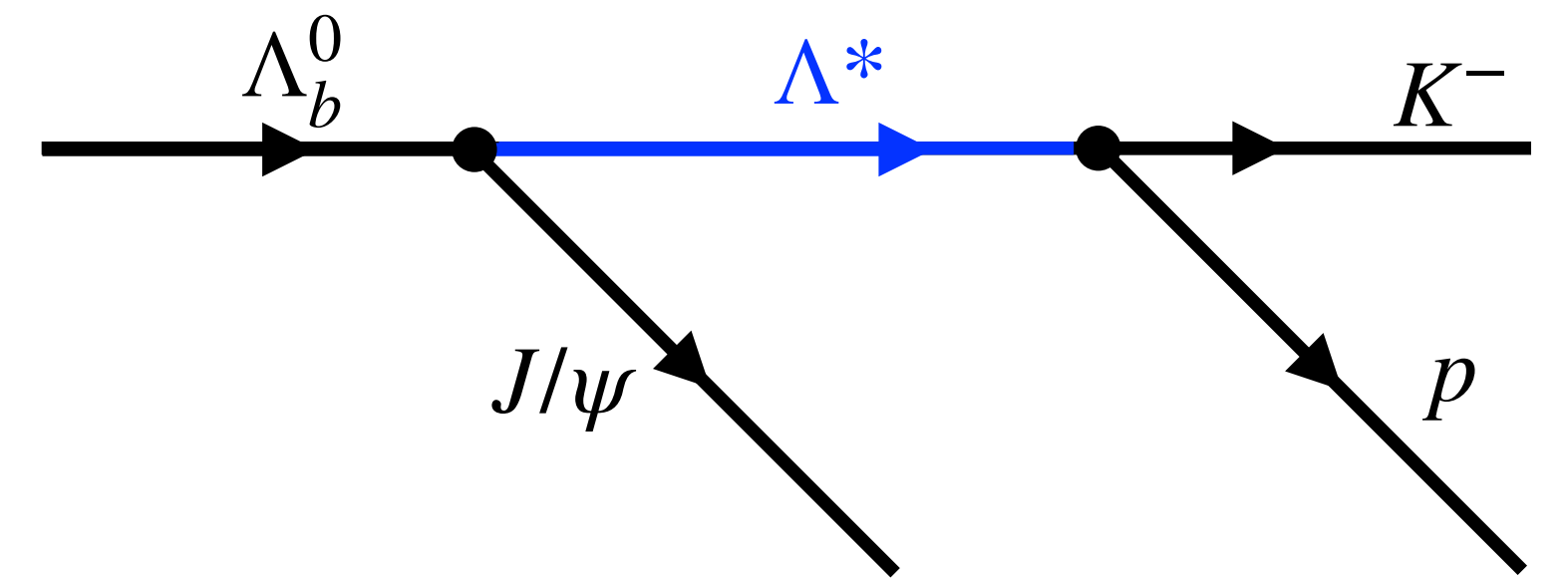
[LHCb, PRL 122 222001 \(2019\)](#)

## Other possible Triangle Mechanism



TS enhancement is drowned by the tree-level decay. (Schmid theorem)

[VR Debastiani, S Sakai, E Oset, EPJC, 79, 69 \(2019\)](#)



# General S-matrix parametrization

$$S_{11}(p_1, p_2) = \prod_m \frac{D_m(-p_1, p_2)}{D_m(p_1, p_2)}$$

[KJ Le Couteur, Proc. Roy. Soc \(London\) A256 \(1960\)](#)

[RG Newton J. Math. Phys. 2, 188 \(1961\)](#)

$$p_k \rightarrow q_k; \quad s = q_k^2 + \epsilon_k^2; \quad \omega = \frac{q_1 + q_2}{\sqrt{\epsilon_2^2 - \epsilon_1^2}} \quad \frac{1}{\omega} = \frac{q_1 - q_2}{\sqrt{\epsilon_2^2 - \epsilon_1^2}}$$

One pole per  $D_m(q_1, q_2)$  :  $\omega_m$

$$D_m(q_1, q_2) = D_m(\omega)$$

[M Kato, Ann. Phys., 31 1 \(1965\)](#)

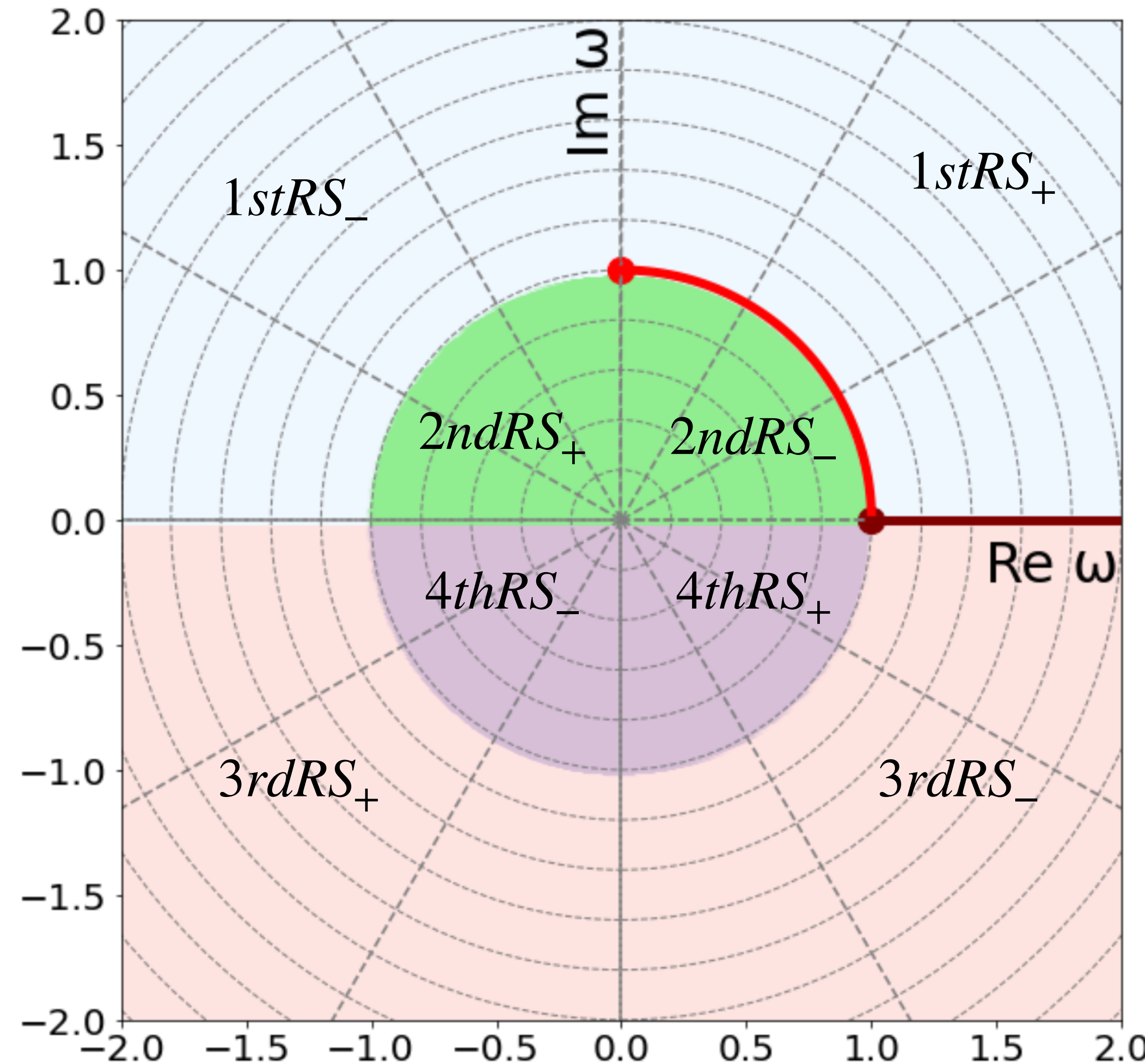
$$= \frac{1}{\omega^2} (\omega - \omega_m) (\omega + \omega_m^*) (\omega - \omega_{\bar{m}}) (\omega + \omega_{\bar{m}}^*)$$

$\omega_{\bar{m}}$  needed only to ensure  $\lim_{\omega \rightarrow \infty} S_{11} \rightarrow 1$ ;

$$|\omega_m \omega_{\bar{m}}| = 1$$

- Poles are introduced independently.
- Cusp at the threshold can be controlled via pole placement.

[LMS, DLBS PRC 108 045204 \(2023\)](#)



# General S-matrix parametrization

$$S_{11}(p_1, p_2) = \prod_m \frac{D_m(-p_1, p_2)}{D_m(p_1, p_2)}$$

[KJ Le Couteur, Proc. Roy. Soc \(Lo  
RG Newton J. Math. Phys. 2, 188](#)

$$p_k \rightarrow q_k; \quad s = q_k^2 + \epsilon_k^2; \quad \omega = \frac{q_1 + q_2}{\sqrt{\epsilon_2^2 - \epsilon_1^2}}$$

One pole per  $D_m(q_1, q_2)$ :  $\omega_m$

$$D_m(q_1, q_2) = D_m(\omega) \quad \text{M Kato, Ann. Phys., 31 1 (1965)}$$

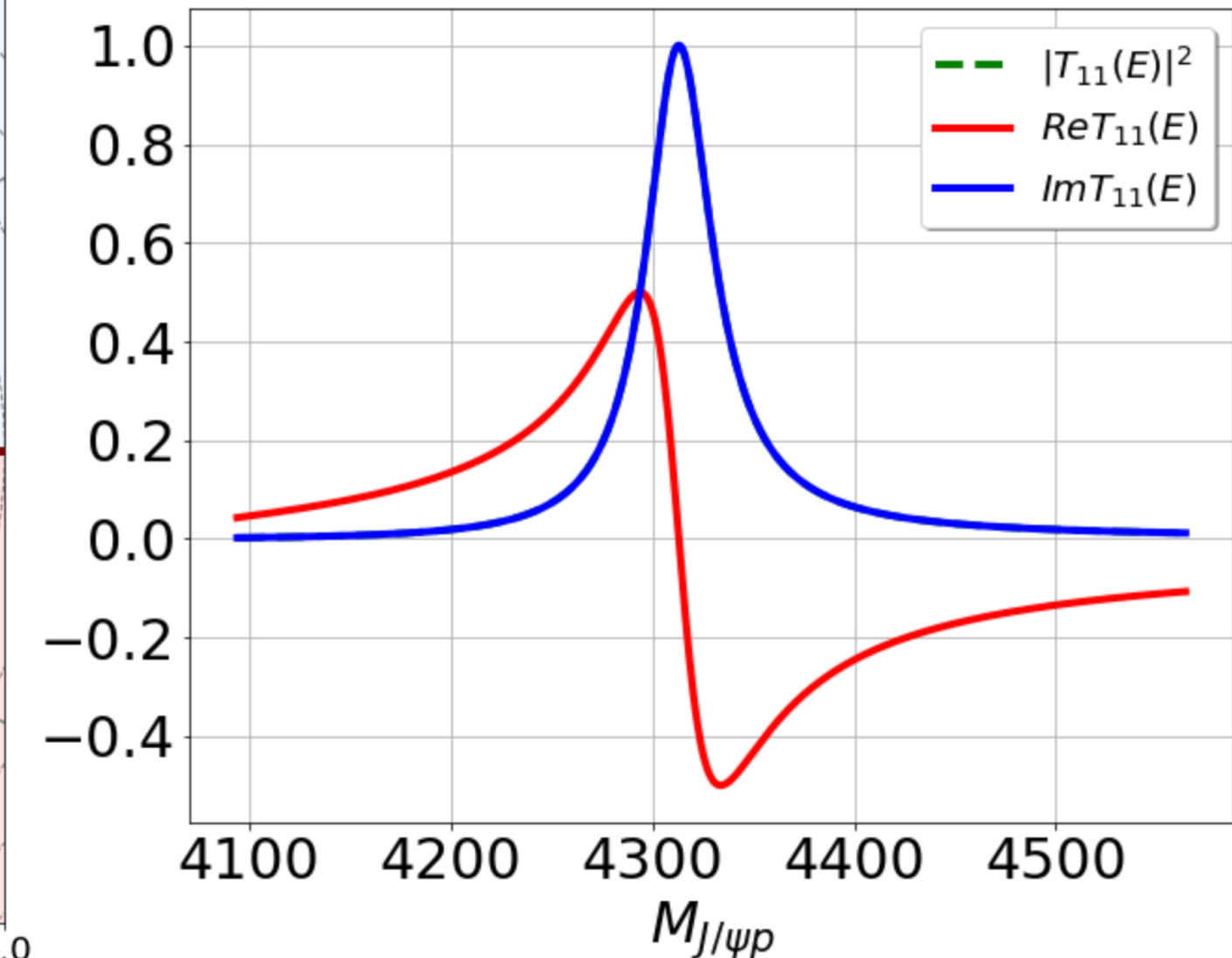
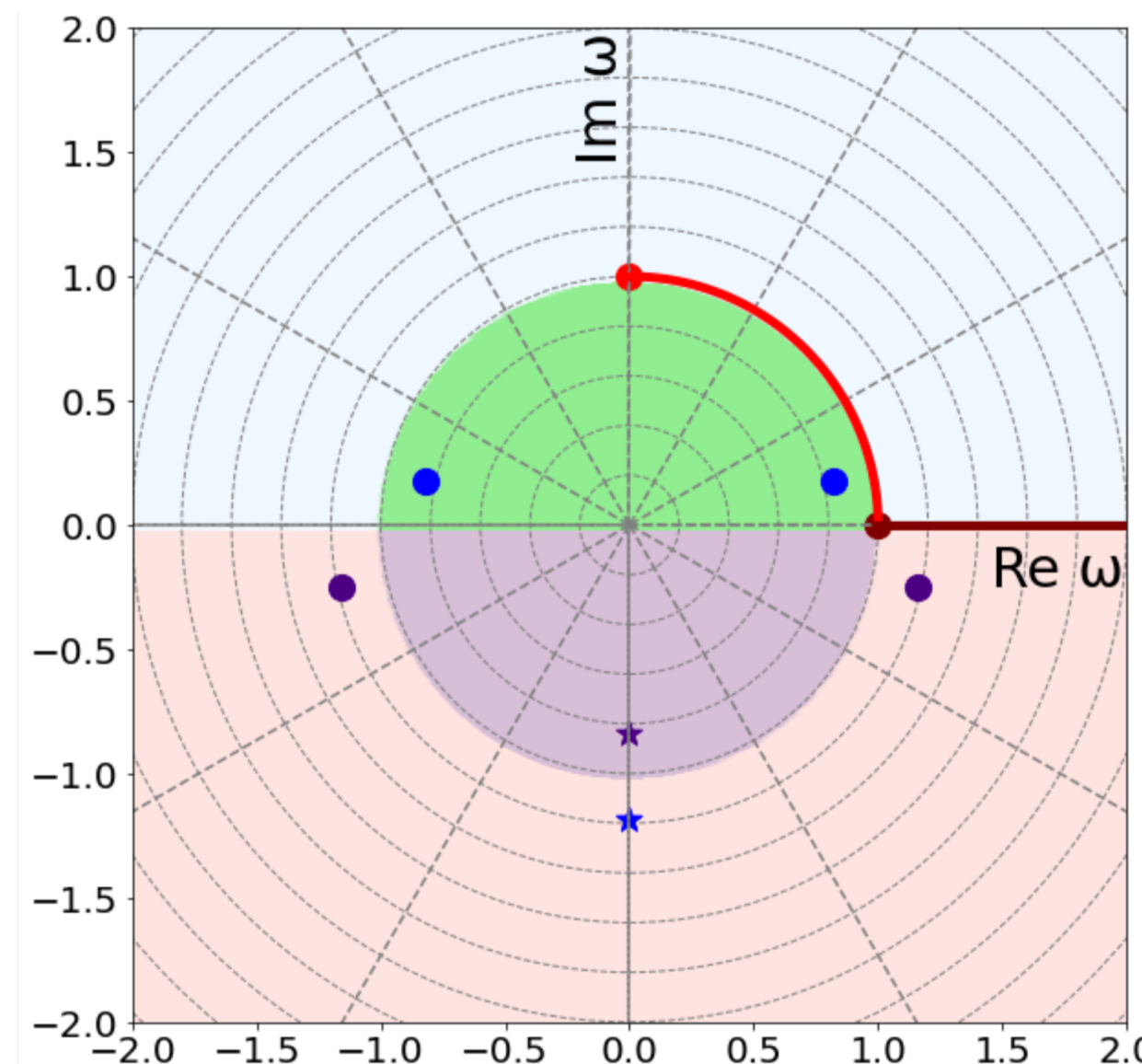
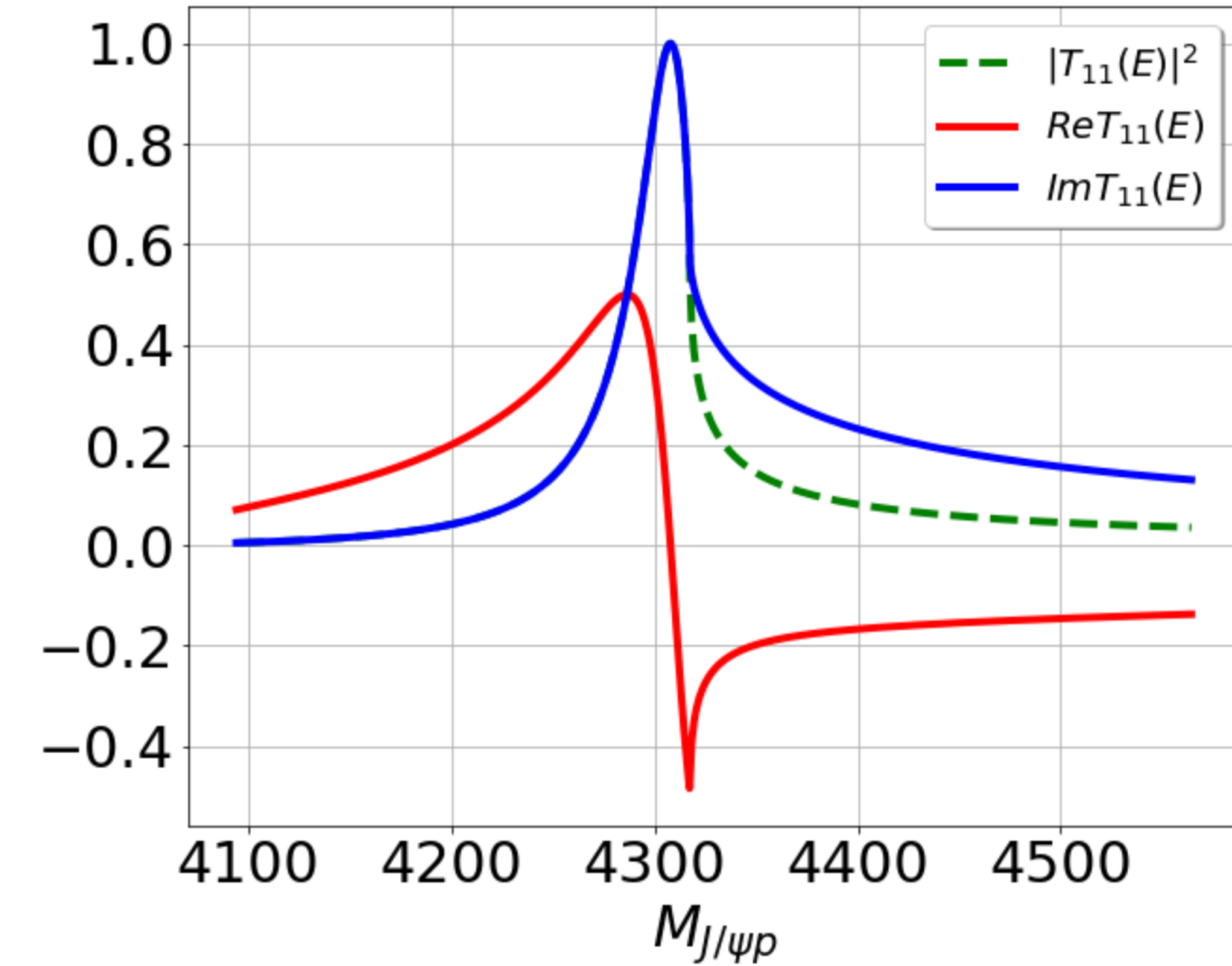
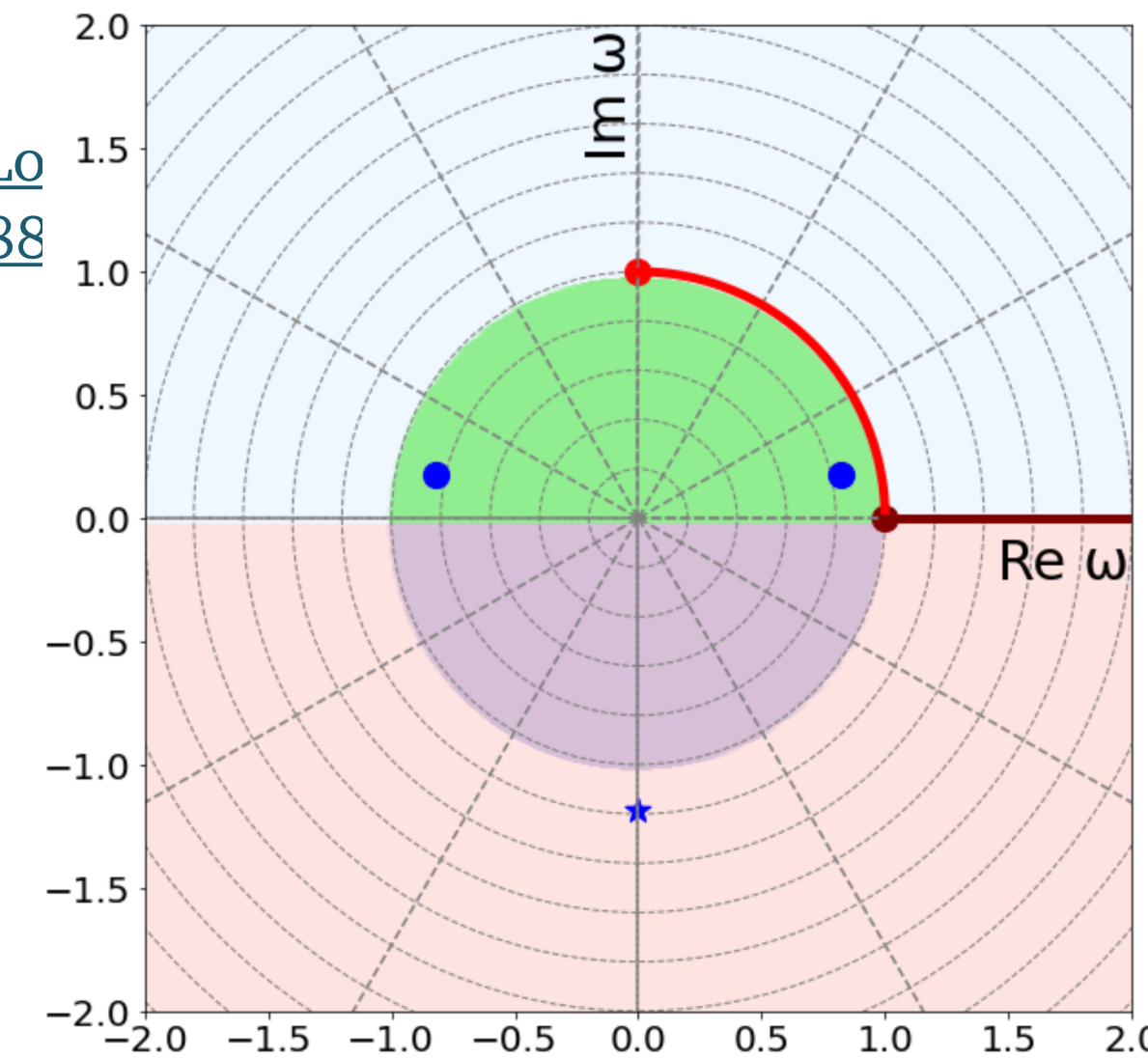
$$= \frac{1}{\omega^2} (\omega - \omega_m) (\omega + \omega_m^*) (\omega - \omega_{\bar{m}}) (\omega + \omega_{\bar{m}}^*)$$

$\omega_{\bar{m}}$  needed only to ensure  $\lim_{\omega \rightarrow \infty} S_{11} \rightarrow 1$ ;

$$|\omega_m \omega_{\bar{m}}| = 1$$

- Poles are introduced independently.
- Cusp at the threshold can be controlled via pole placement.

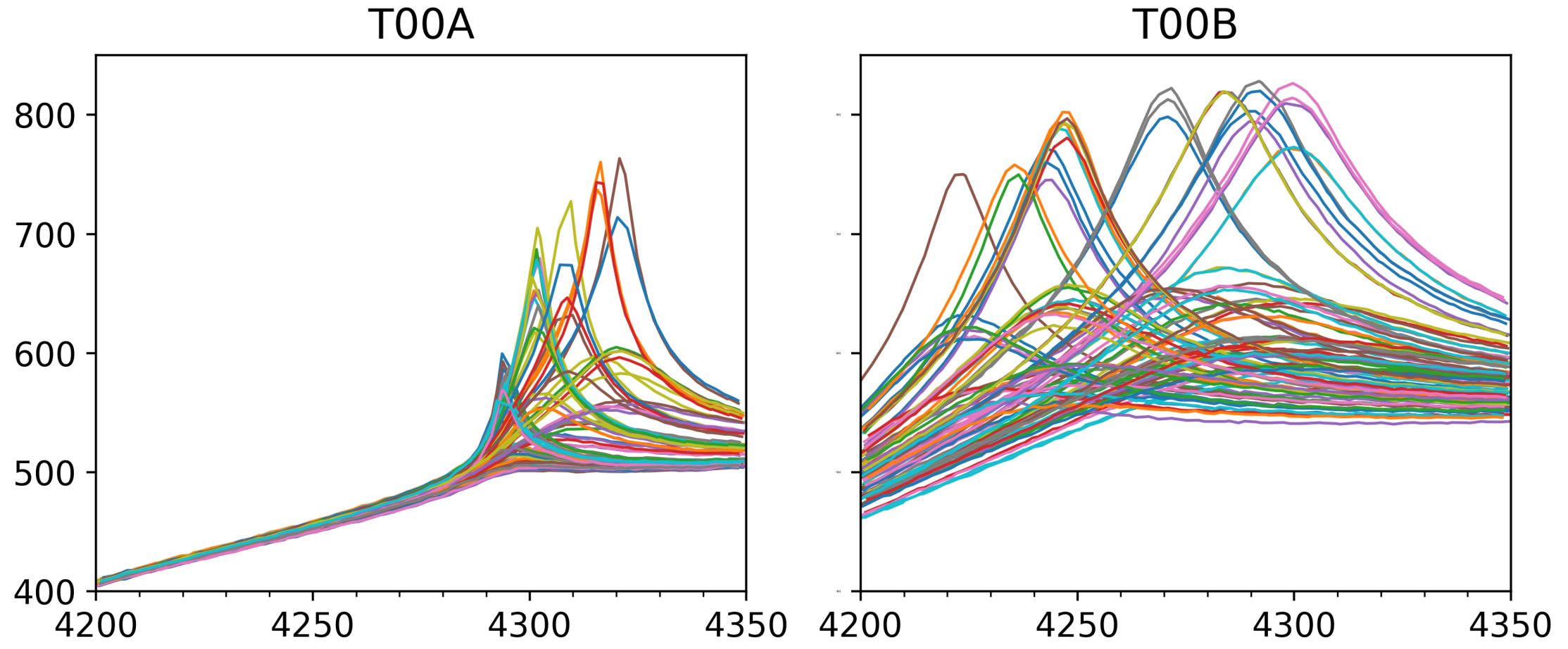
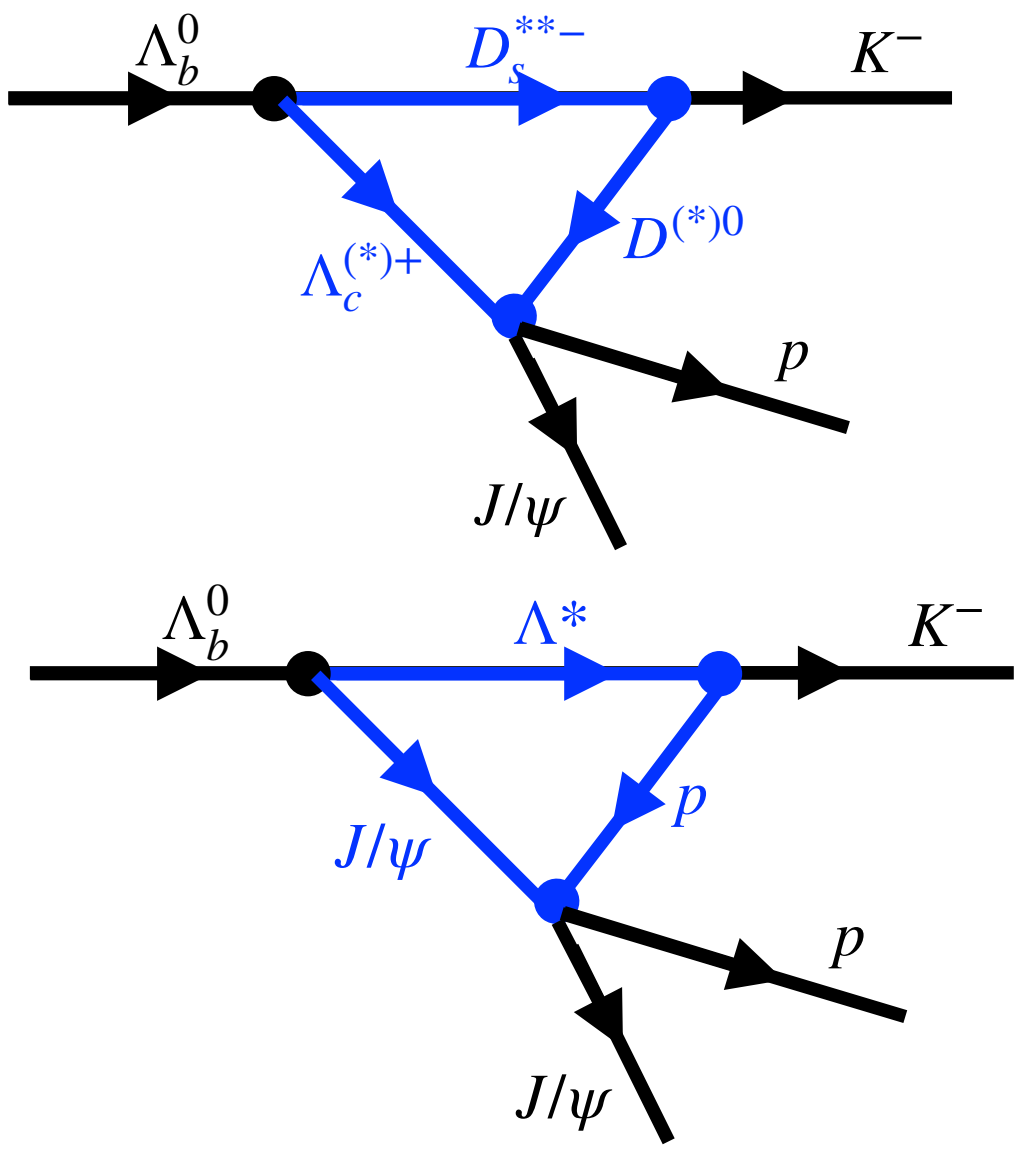
[LMS, DLBS PRC 108 045204 \(2023\)](#)



# Sample training datasets

## Triangle singularity

Parameter	Range of values [MeV]
$m_{\Lambda_b^0}$	$5619.60 \pm 0.17$
$m_{K^-}$	$493.677 \pm 0.016$
$m_{\Lambda_c^+}$	$2286.46 \pm 0.14$
$m_{\bar{D}^{*0}}$	$2006.85 \pm 0.05$
$m_{J/\psi}$	$3096.9 \pm 0.006$
$m_{D_s^{**}}$	[3209.80, 3315.00]
$m_{\Lambda^*}$	[2490.00, 2522.70]
$\Lambda$	[2000.0, 2500.0]
$\epsilon$	[1.0, 10.0]

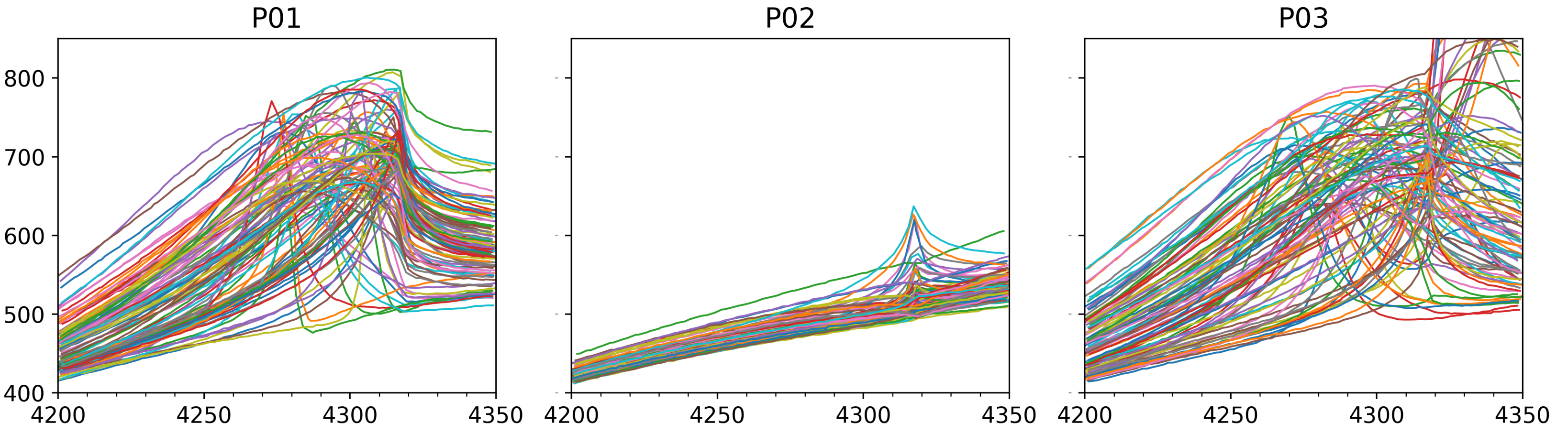


## Pole-based enhancements

$$\begin{cases} T_2 - 50 \leq \text{Re } E_{\text{pole}} \leq 4350 & \text{all RS} \\ -100 \leq \text{Im } E_{\text{pole}} < 0 & [bt] \text{ \& } [bb] \\ 0 < \text{Im } E_{\text{pole}} \leq 100 & [tb] \end{cases}$$

4 × 10,000  
Training dataset generated

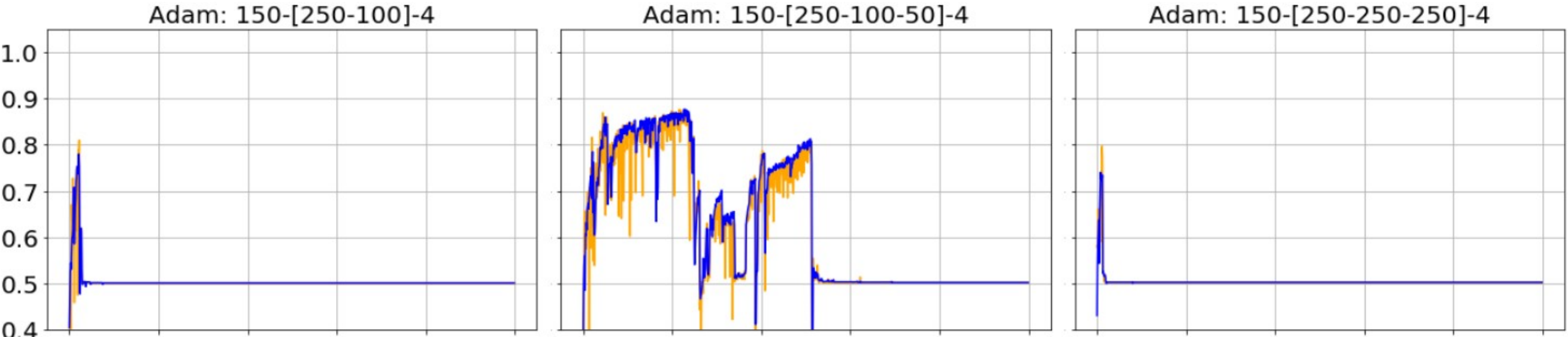
4 × 320  
Testing dataset generated



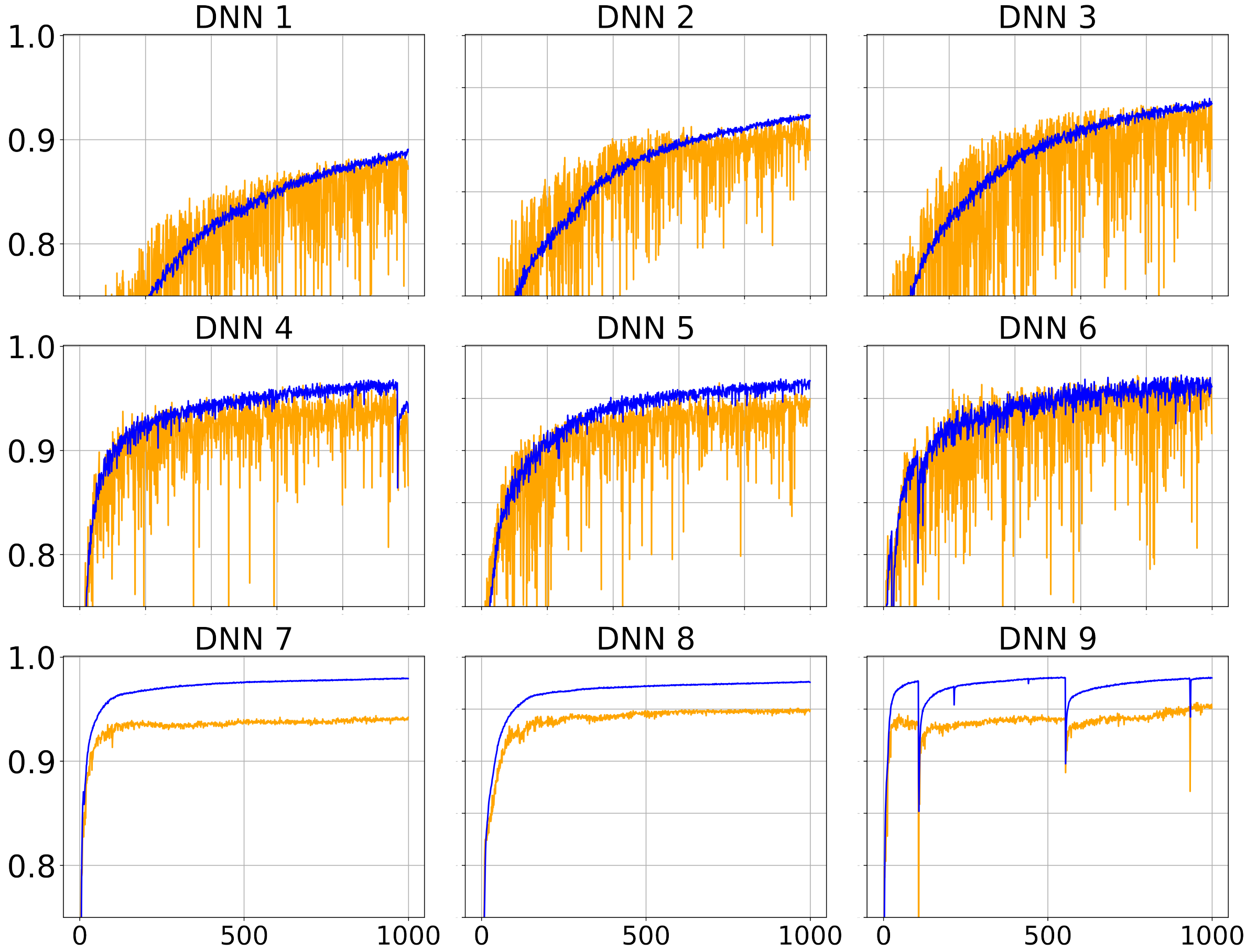
# Training performance

Model	Optimizer and Architecture
DNN 1	AdaGrad: 150-[250-100]-4
DNN 2	AdaGrad: 150-[250-100-50]-4
DNN 3	AdaGrad: 150-[250-250-250]-4
DNN 4	AMSGrad: 150-[250-100]-4
DNN 5	AMSGrad: 150-[250-100-50]-4
DNN 6	AMSGrad: 150-[250-250-250]-4
DNN 7	SMORMS3: 150-[250-100]-4
DNN 8	SMORMS3: 150-[250-100-50]-4
DNN 9	SMORMS3: 150-[250-250-250]-4

Other optimizers cannot even learn the classification task.

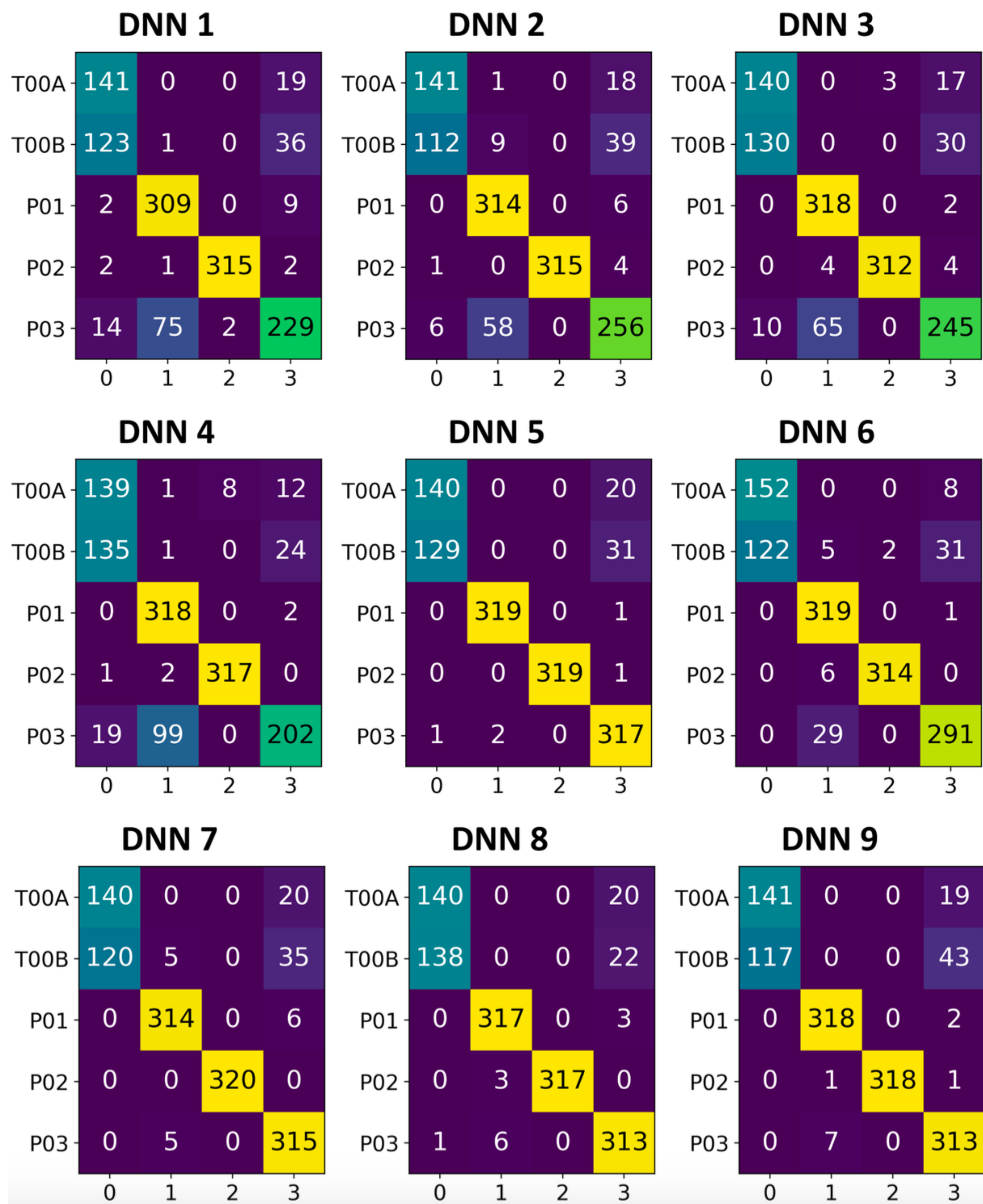


The classification task is non-trivial.



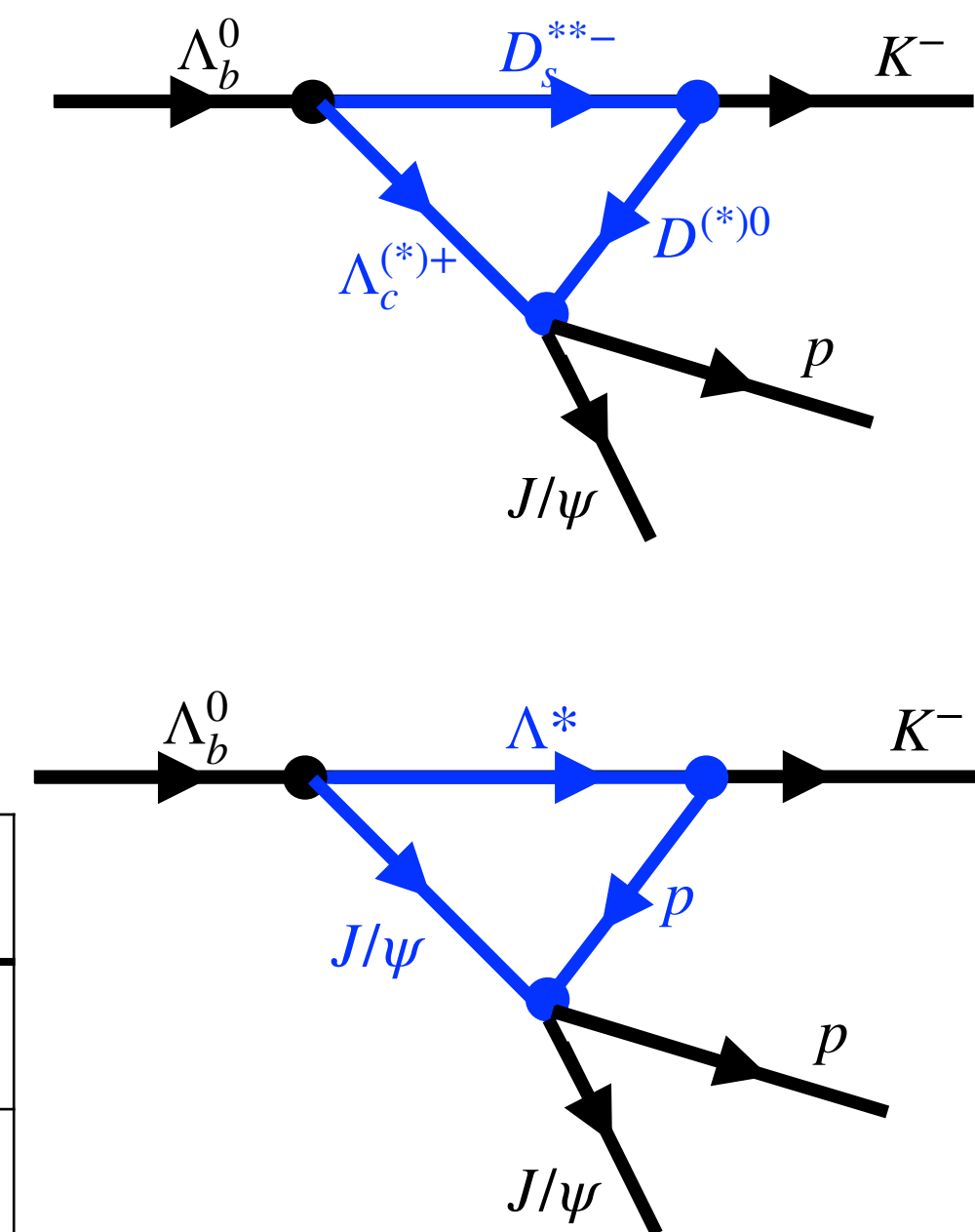
Training epoch vs accuracy

# Confusion Matrix



Generate a different set of 320 validation dataset per classification.

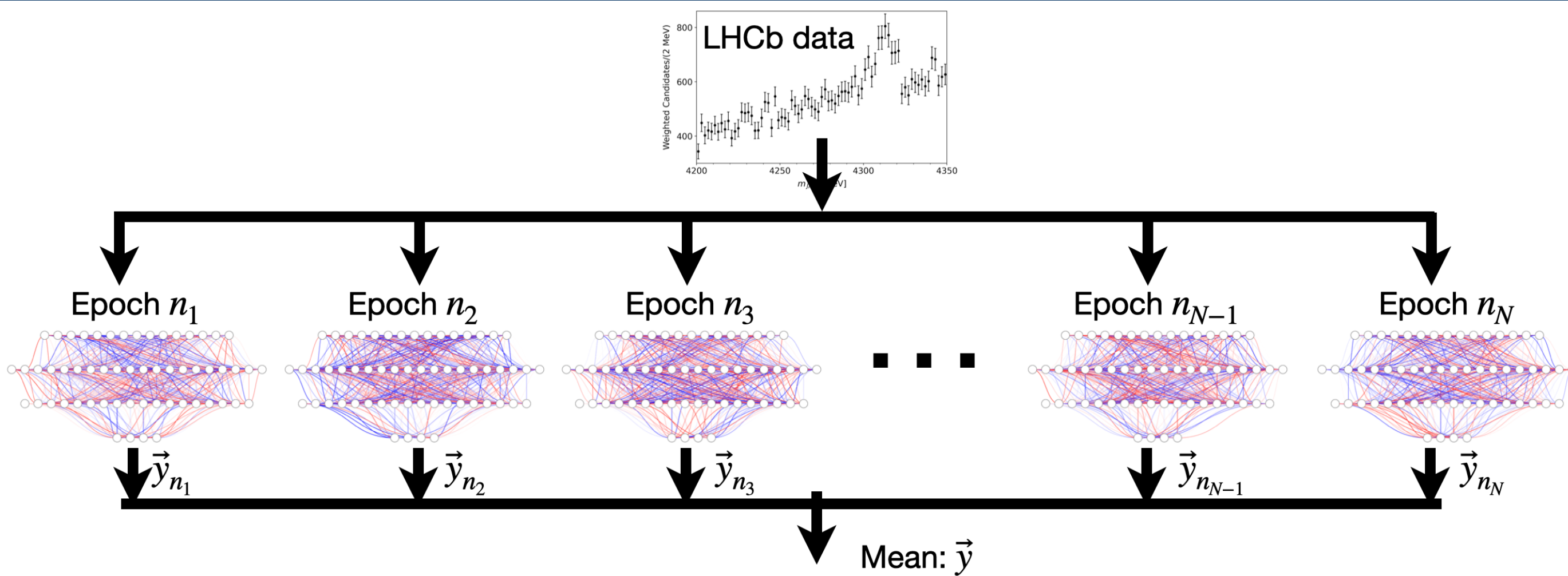
Label	Description
0	Triangle mechanism
1	1 pole in 2nd RS
2	1 pole in 4th RS
3	1 pole in 2nd and 1 pole in 3rd RSs



Slight confusion between TS and BW-like line shapes.

If the experimental data will favor either the TS or class 3, further analysis must be done.

# Inference stage (snapshot ensemble)



- Bootstrapped 3000 line shapes from the experimental data. (Uniform distribution)
- Feed to the DNN state at epoch  $n$
- Get the mean count

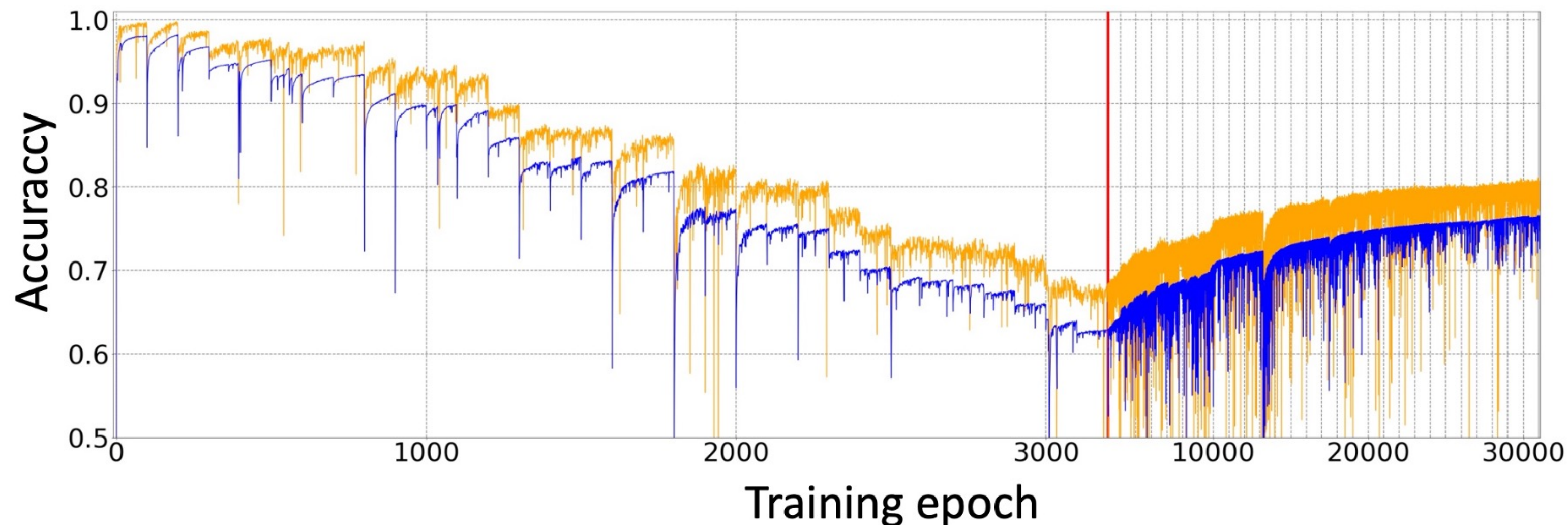
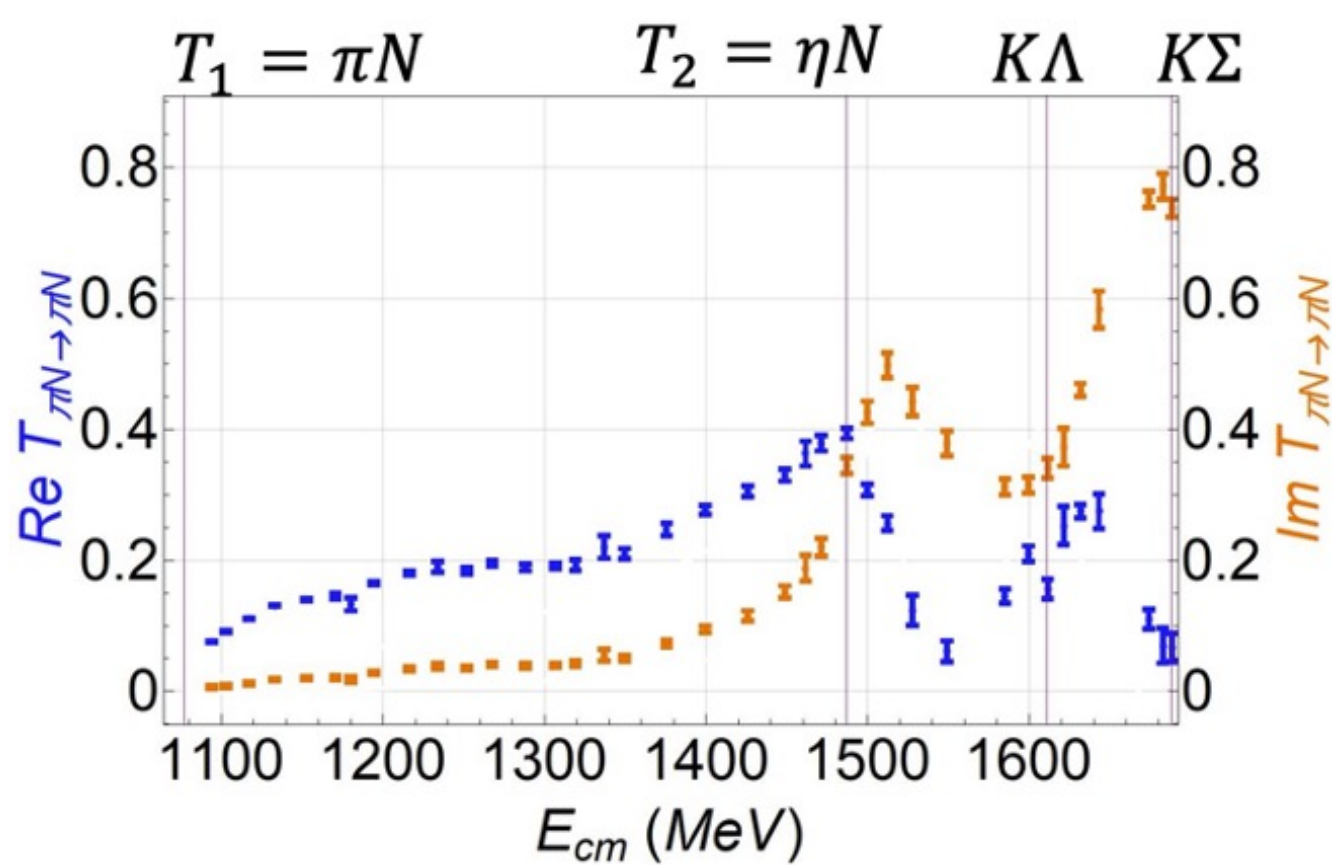
- TS is ruled out by pure line shape analysis!
- It is possible to distinguish kinematical cusp vs pole despite the presence of experimental uncertainty.
- The data favored the pole-based interpretation:  
1 pole in 2nd RS

Model	TS	1 pole in RS2	1 pole in RS4	1 pole each in RS2 & RS4
DNN 1	261	1930	0.248	804
DNN 2	18.4	1998	969	14.5
DNN 3	0.653	2960	0	36
DNN 4	0	2990	0	14.2
DNN 5	0	2660	0	337
DNN 6	0.436	2999	0	0.891
DNN 7	1	2590	0	414
DNN 8	0	2999	0	1.06
DNN 9	0	2970	0	127

[DAO Co, VAA Chavez, DLBS, arXiv:2403.18265](#)

# Probe deeper: Pole structure of $P_{c\bar{c}}(4312)^+$

DNN designed to probe the pole structure is difficult to train.



[DLBS, YI, TS, AH PRD 104 3 036001 \(2021\)](#)

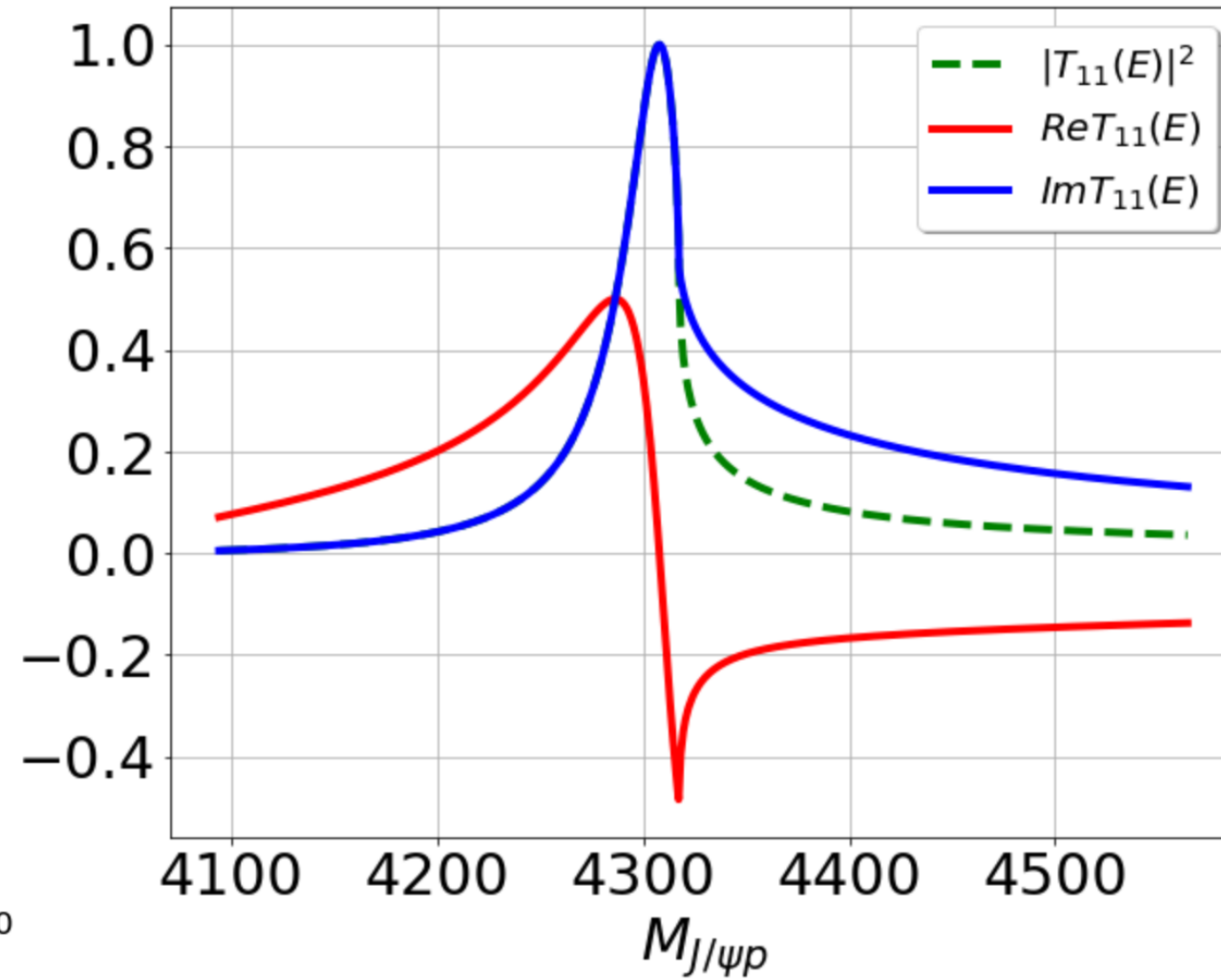
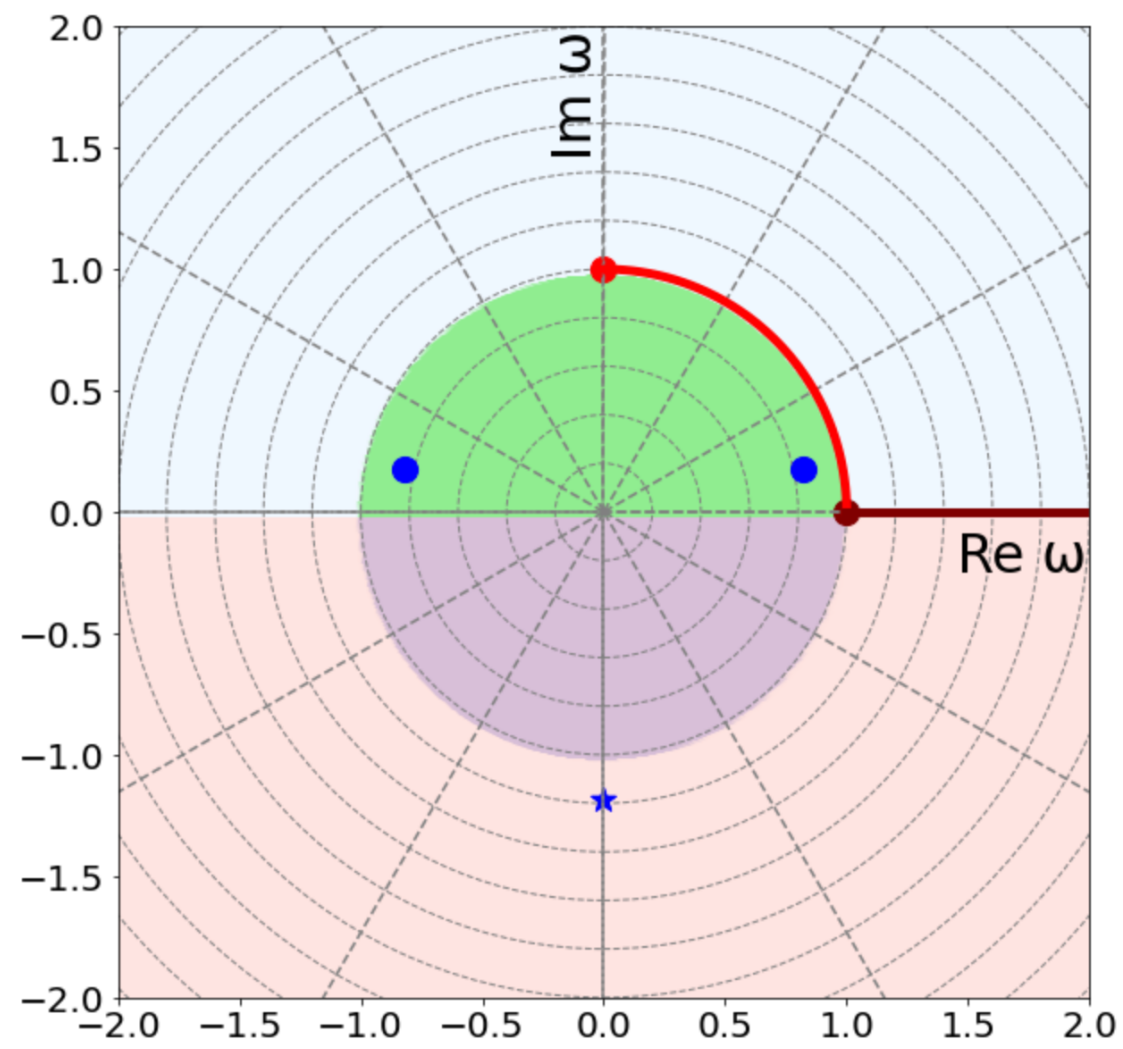
Label	S-matrix pole configuration
0	no nearby pole
1	1 pole in $[bt]$
2	2 poles in $[bt]$
$\vdots$	$\vdots$
32	1 pole in $[bt]$ , 2 poles in $[bb]$ and 1 pole in $[tb]$
33	1 pole in $[bt]$ , 1 pole in $[bb]$ and 2 poles in $[tb]$
34	1 pole in $[bt]$ , 1 pole in $[bb]$ and 1 pole in $[tb]$

There is an ambiguity in the line shape of  $T_{11}$ .

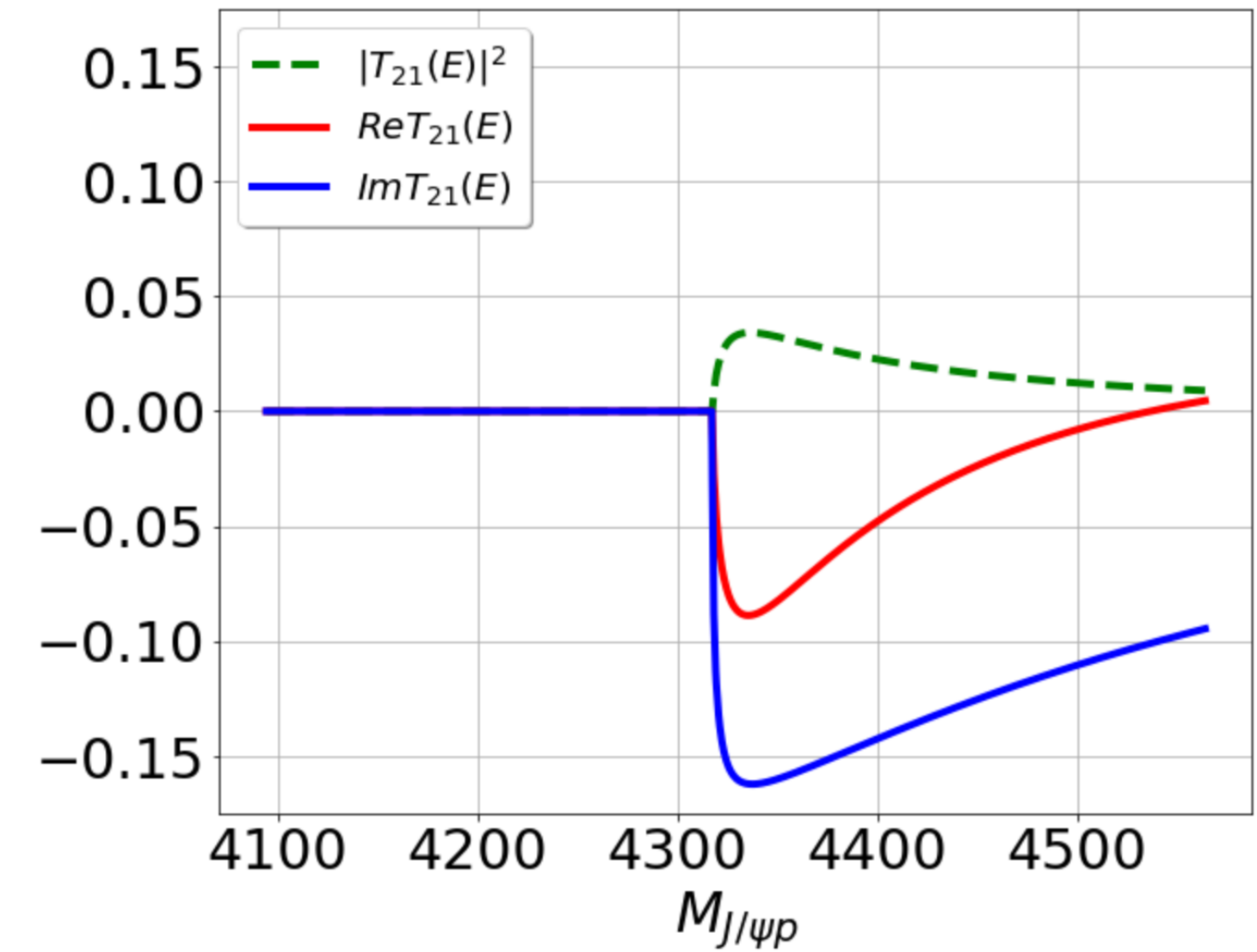
Different pole structures can give rise to the same line shape.

# Probe deeper: Pole structure of $P_{c\bar{c}}(4312)^+$

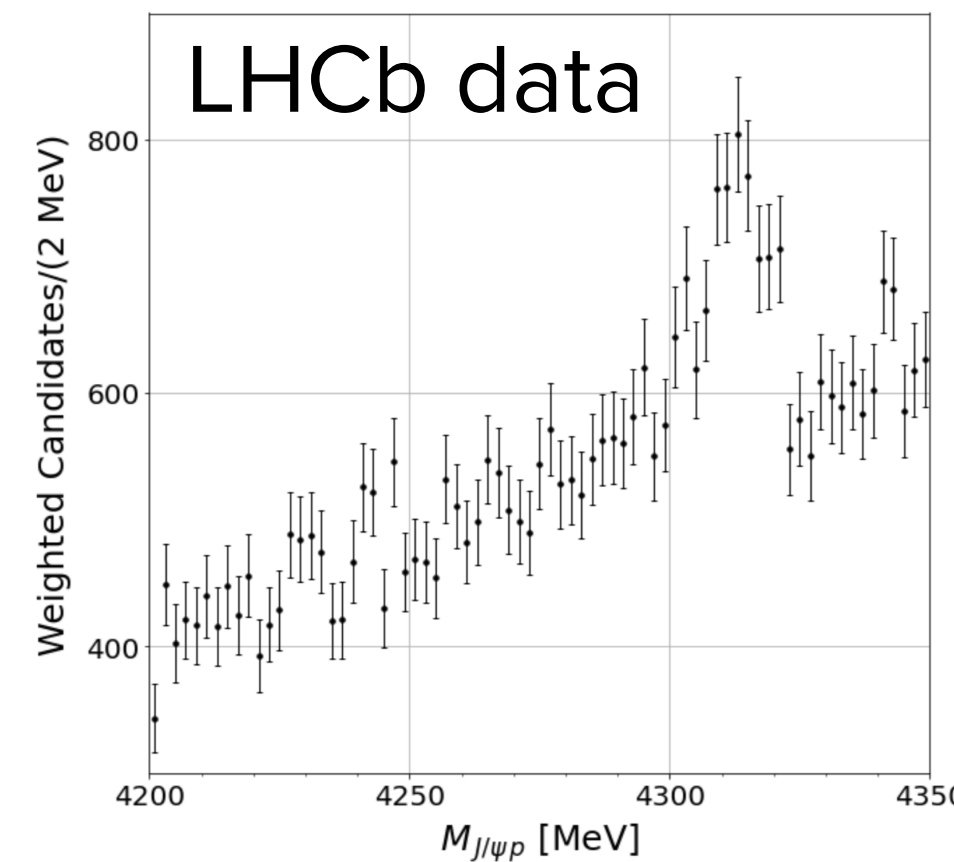
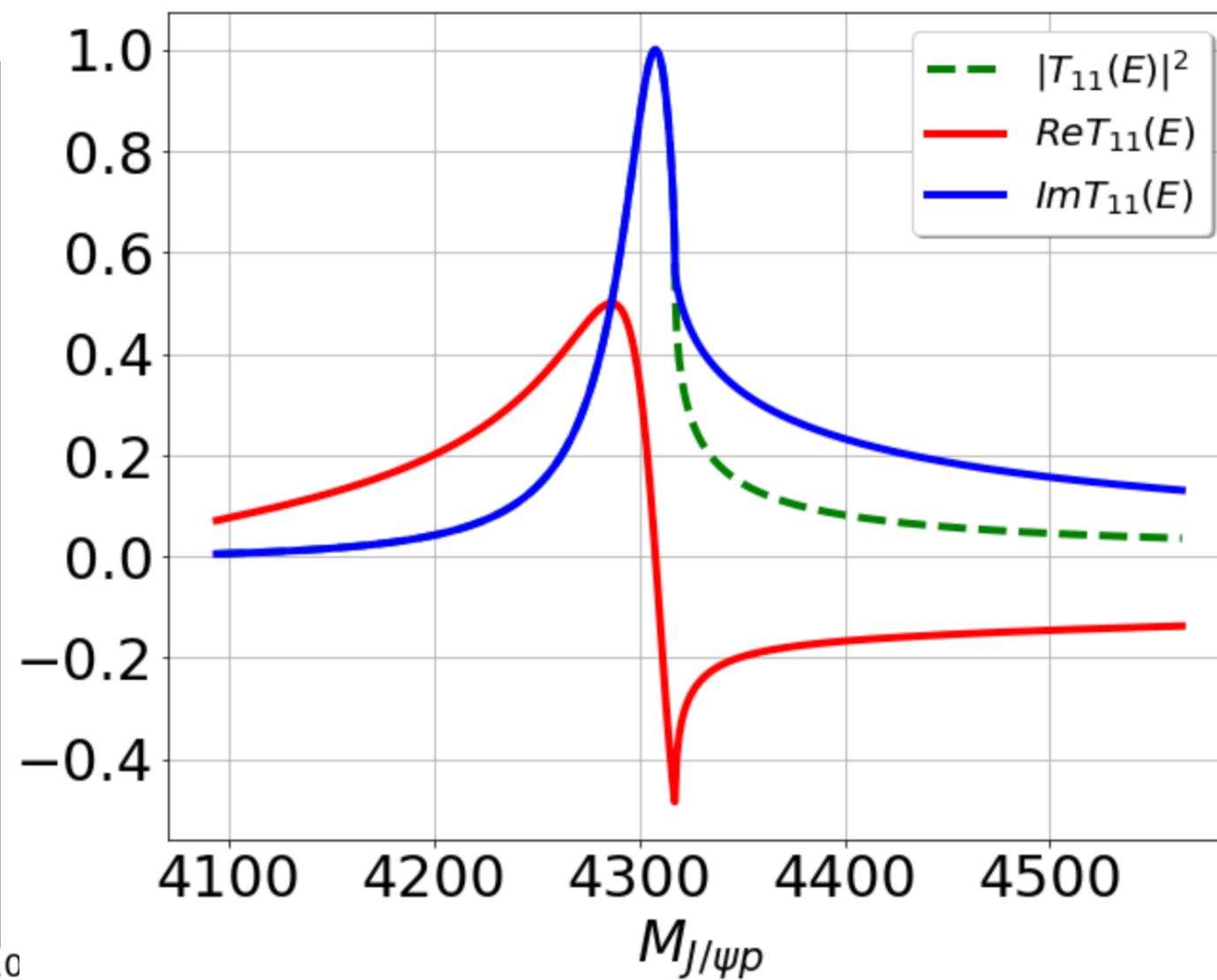
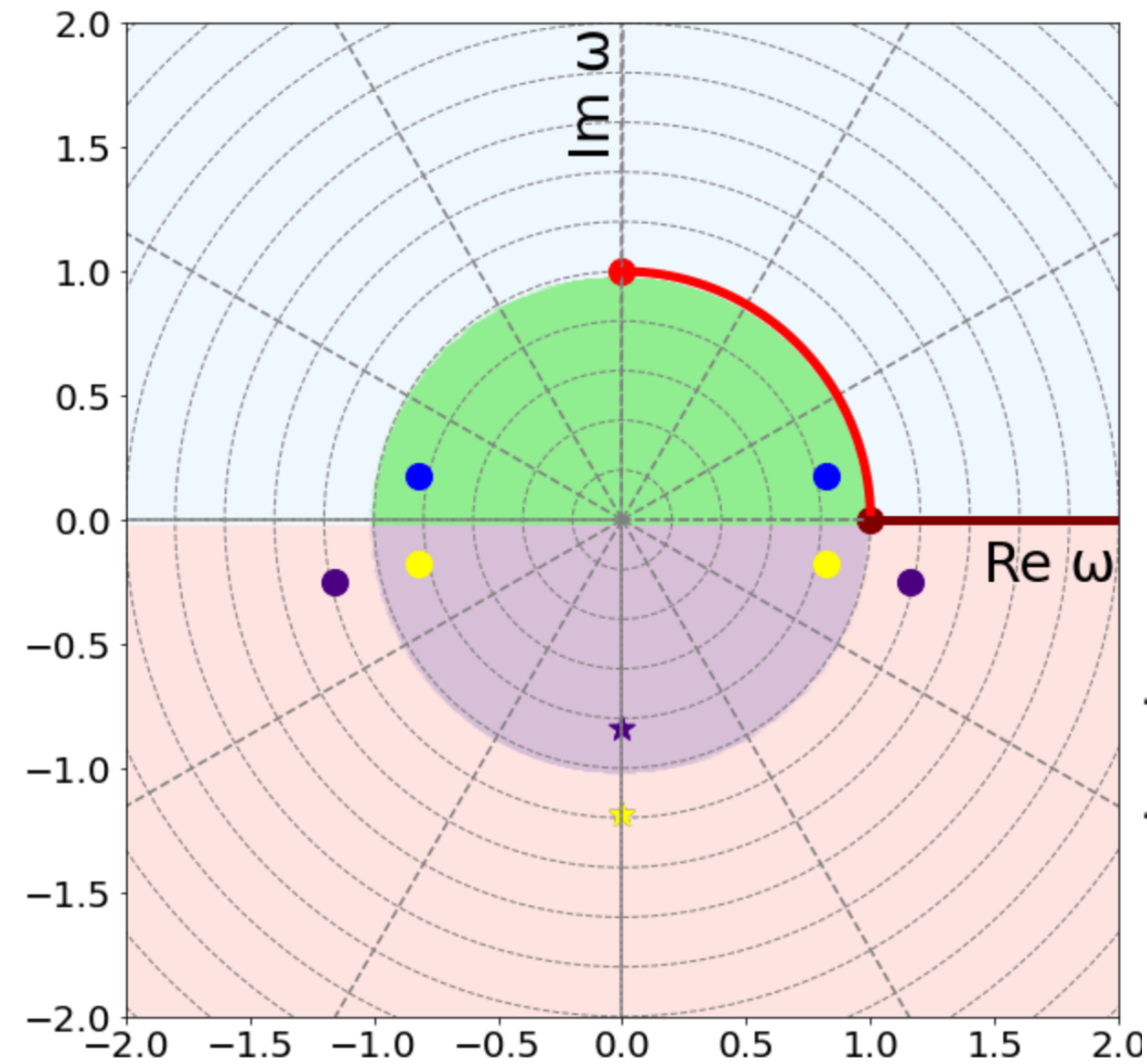
1 pole in the 2nd RS



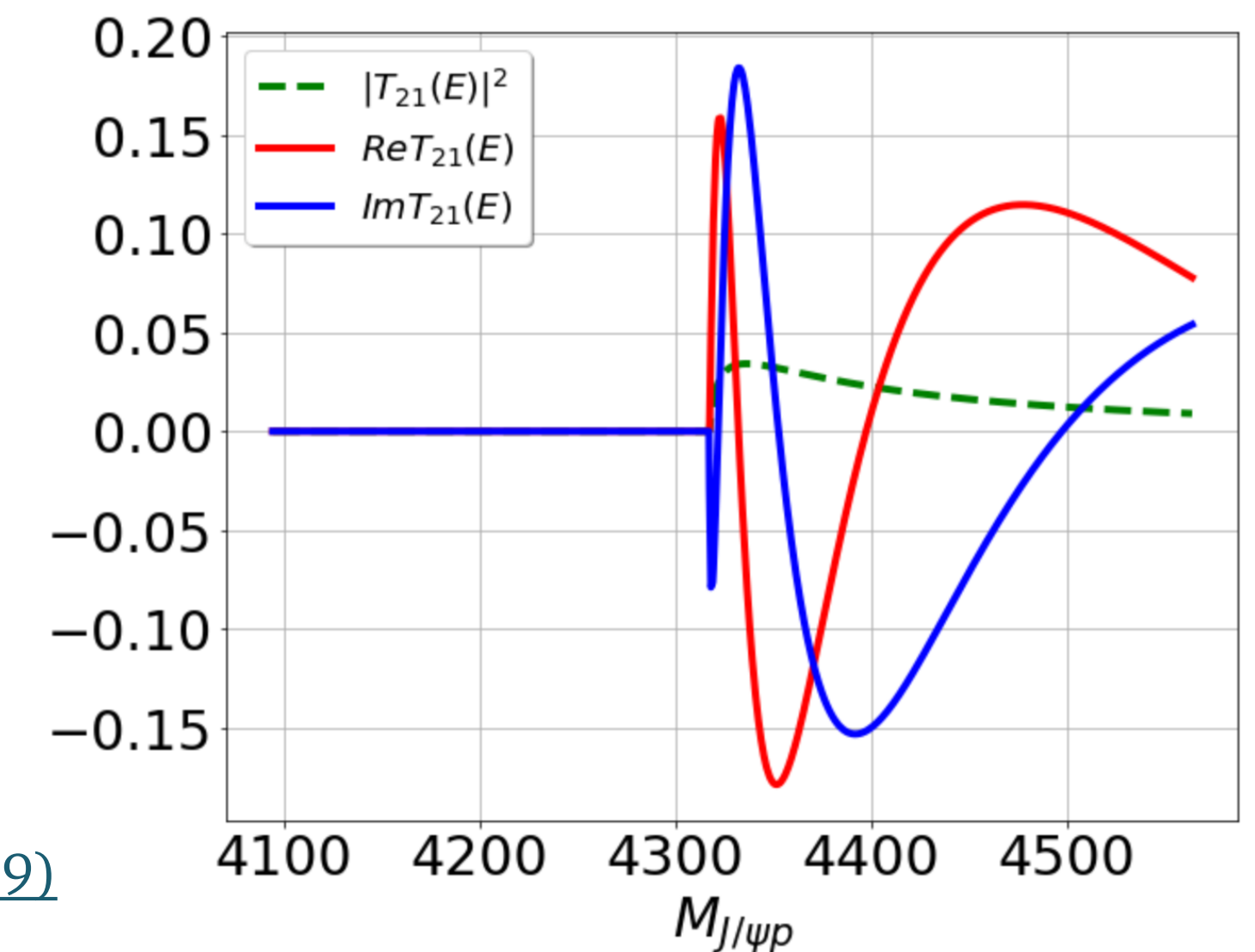
It is not enough to use one element of the T-matrix. We need to include the off-diagonal element.



1 pole in each RS



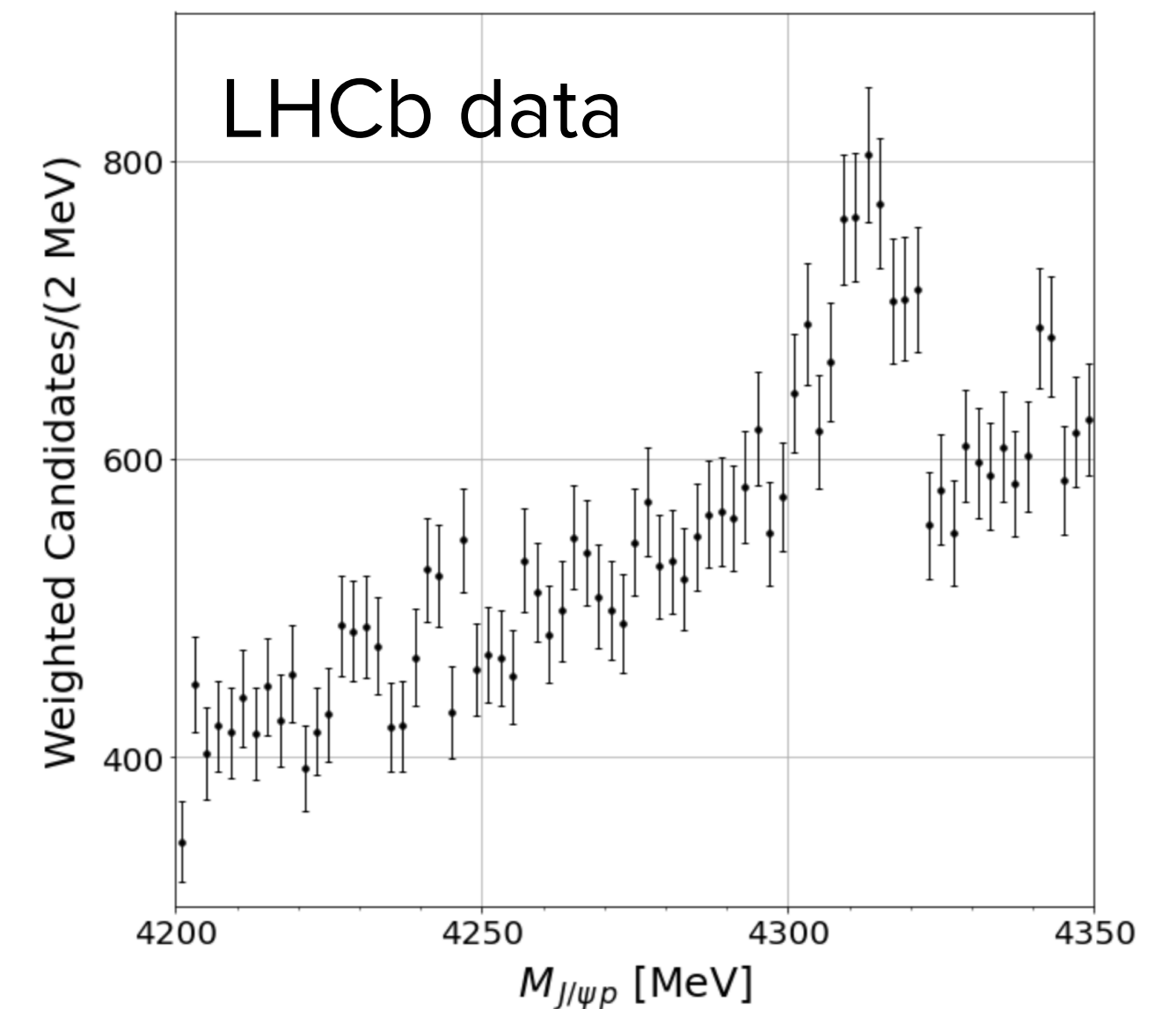
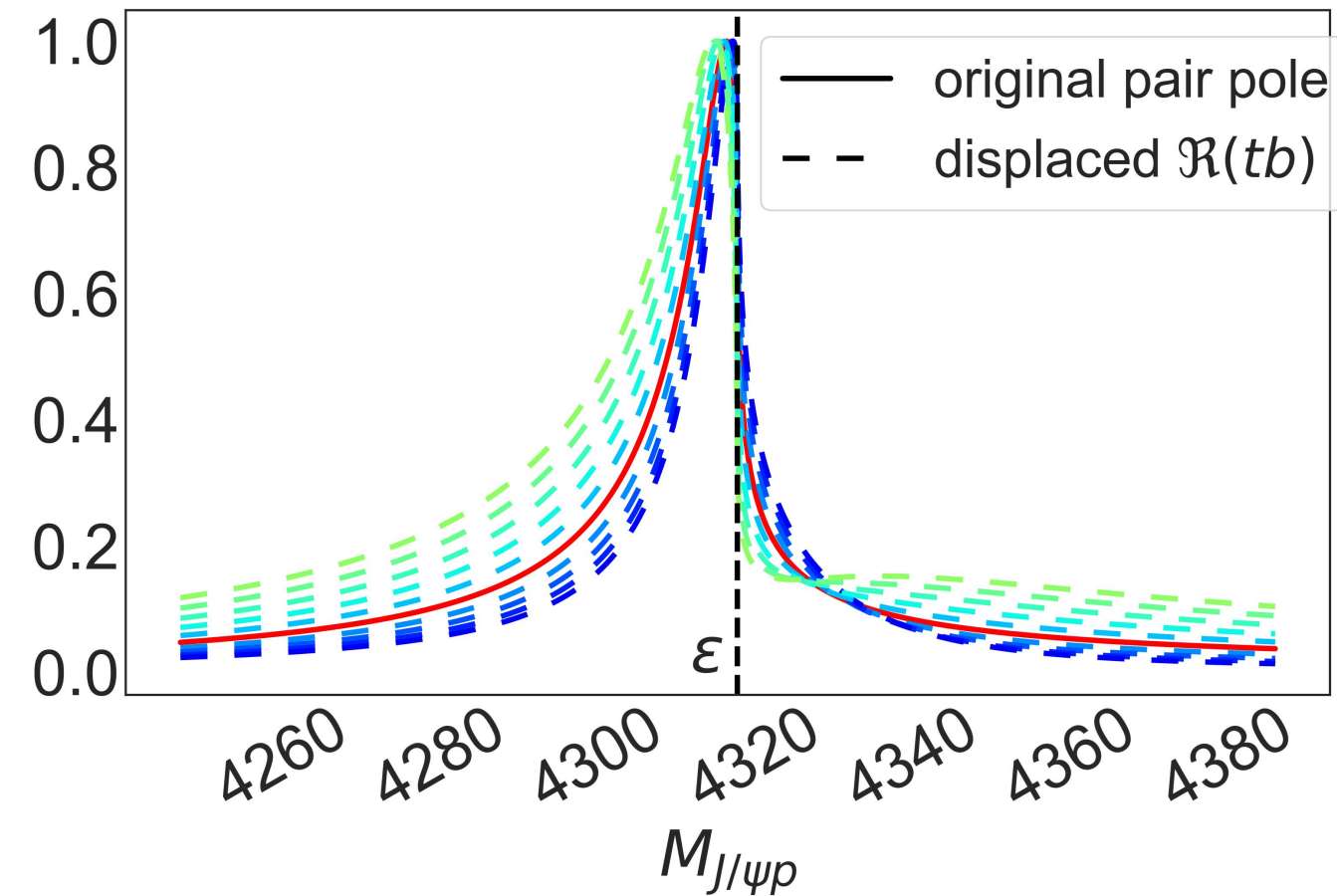
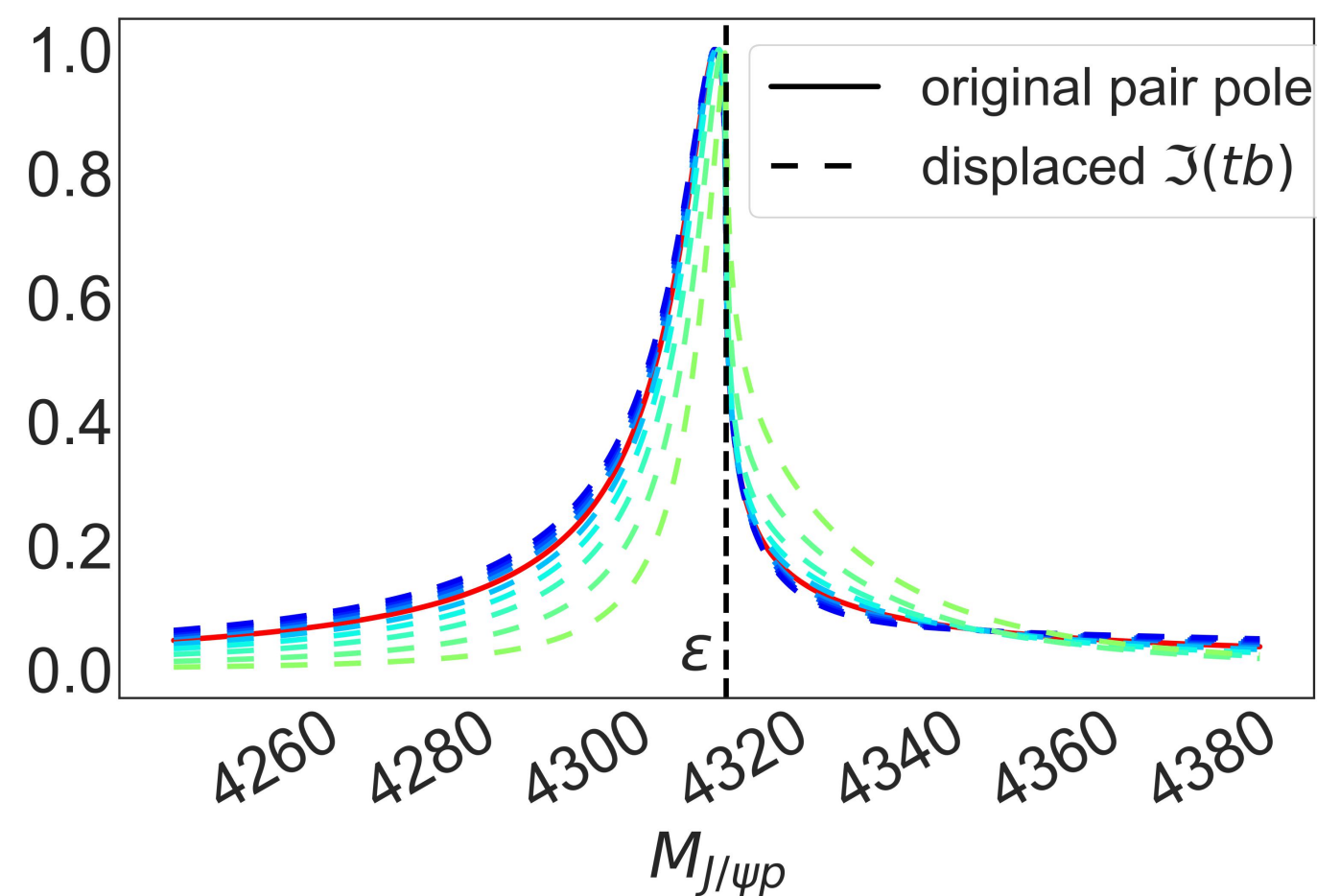
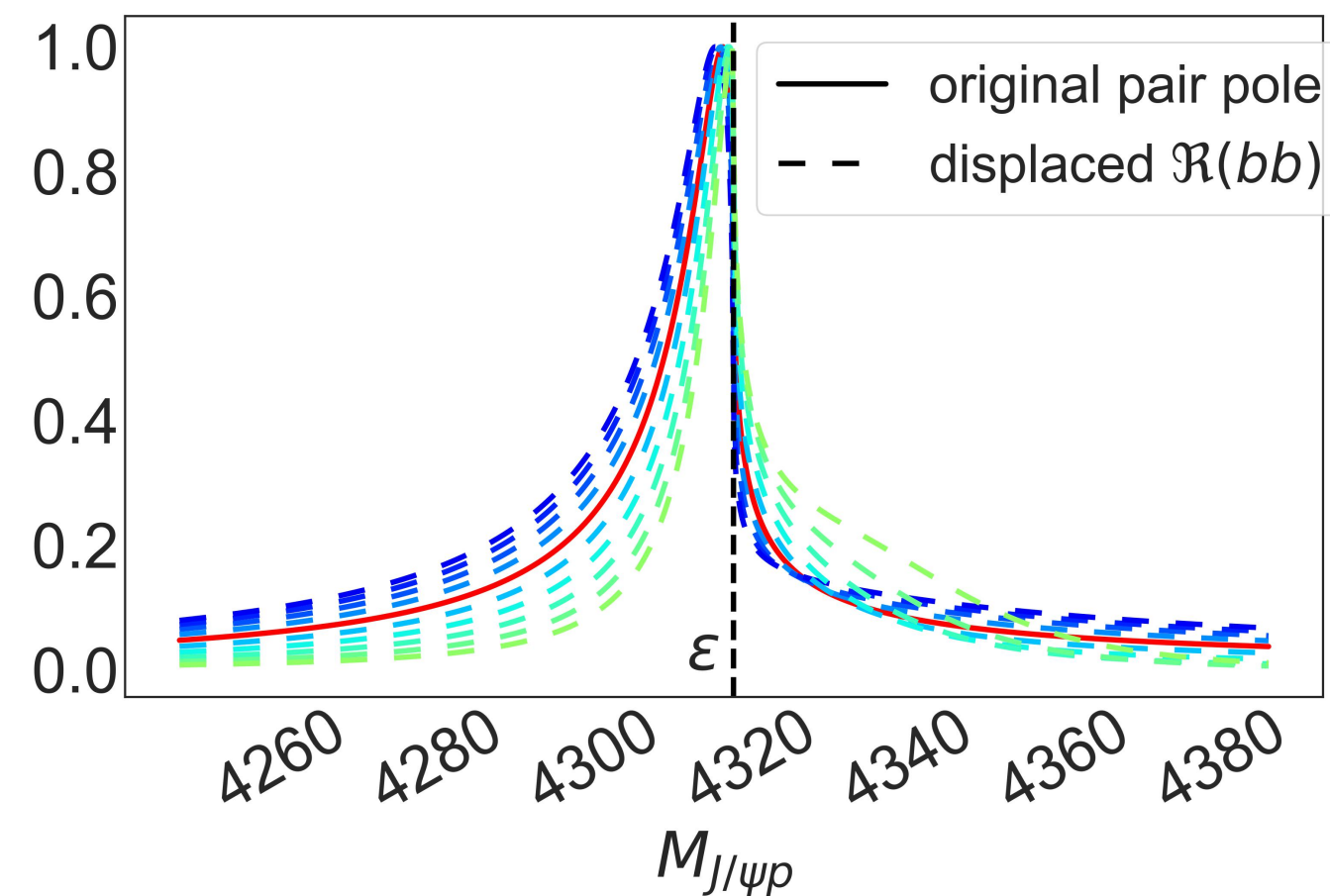
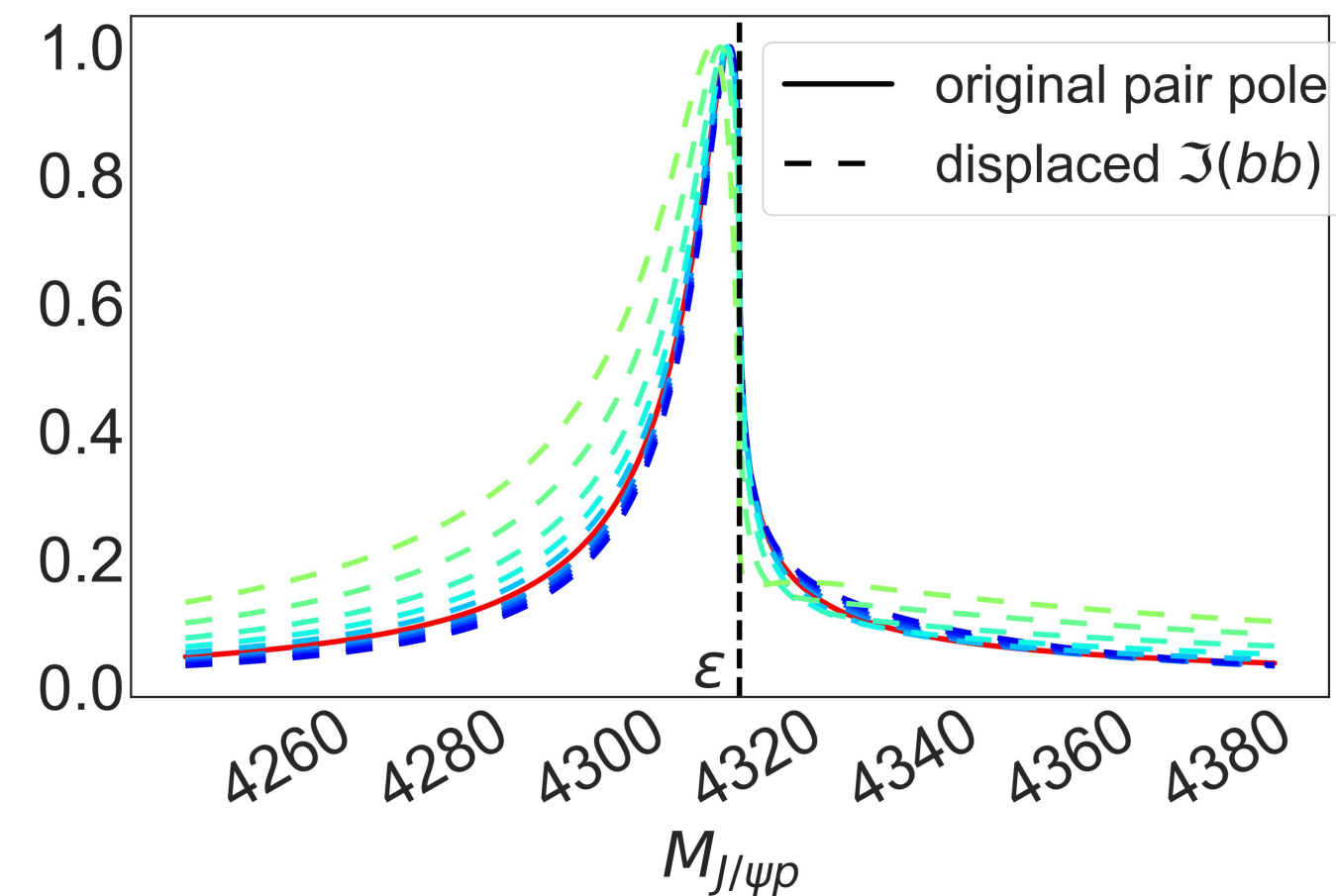
LHCb, PRL 122 222001 (2019)



LMS, DLBS PRC 108 045204 (2023)

# Probe deeper: Pole structure of $P_{c\bar{c}}(4312)^+$

Maybe unlikely to happen -  
to produce ambiguous pole structure, the poles must have  
the same position.



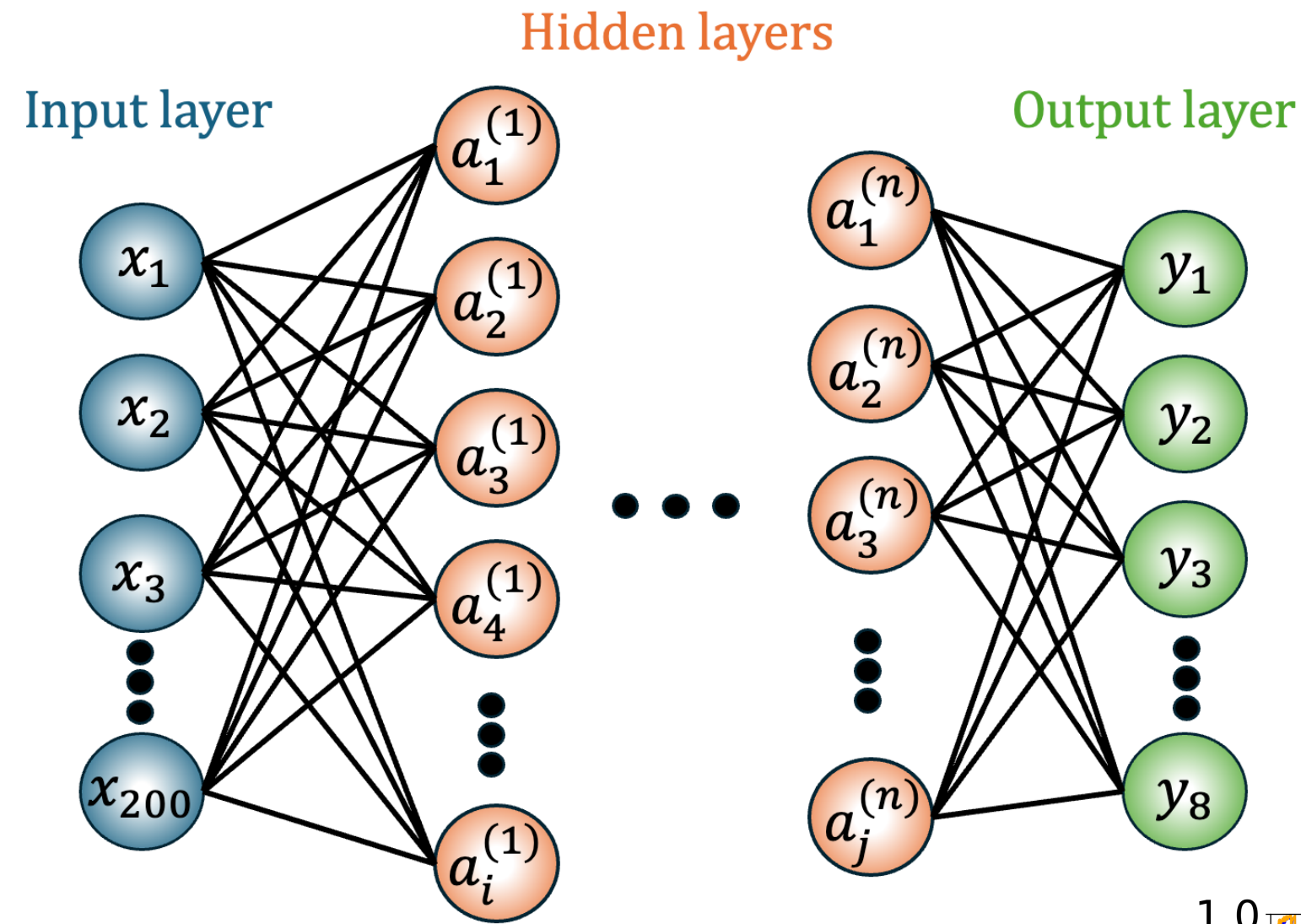
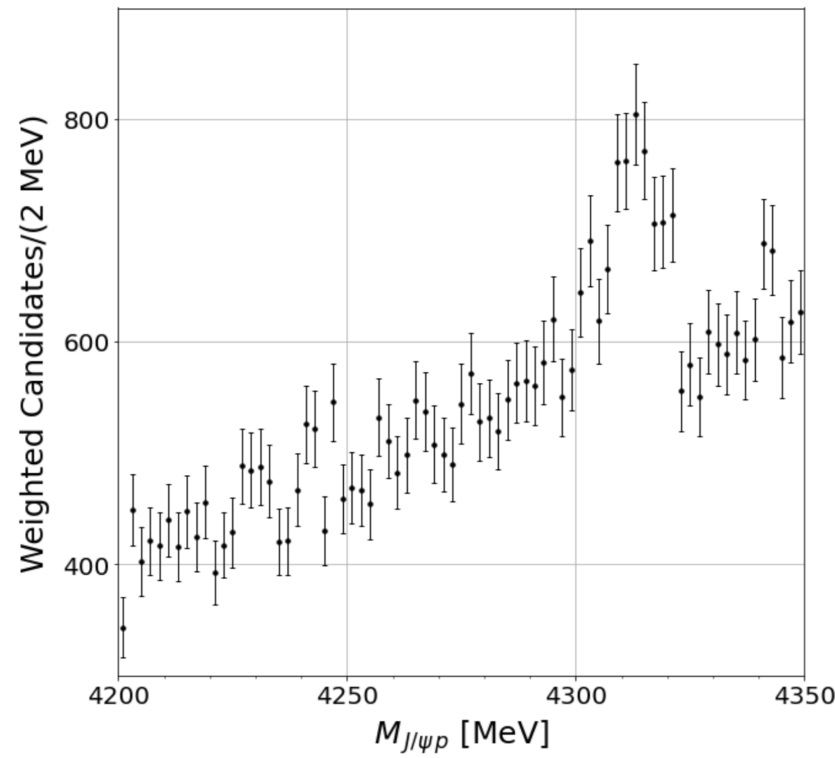
[LHCb, PRL 122 222001 \(2019\)](#)

Slight variation in the line shape

Experimental uncertainty might  
hide them.

[LMS, DLBS PRC 108 045204 \(2023\)](#)

# Probe deeper: Pole structure of $P_{c\bar{c}}(4312)^+$



Class label	$S$ -matrix pole configuration
0	1 pole on $[bt]$
1	1 pole on $[bb]$
2	1 pole on $[tb]$
3	1 pole on $[bt]$ and 1 pole on $[bb]$
4	1 pole on $[bb]$ and 1 pole on $[tb]$
5	1 pole on $[bb]$ , 1 pole on $[tb]$ , 1 pole on $[bt]$
6	2 poles on $[bb]$ , 1 pole on $[tb]$
7	1 pole on $[bb]$ , 2 poles on $[tb]$

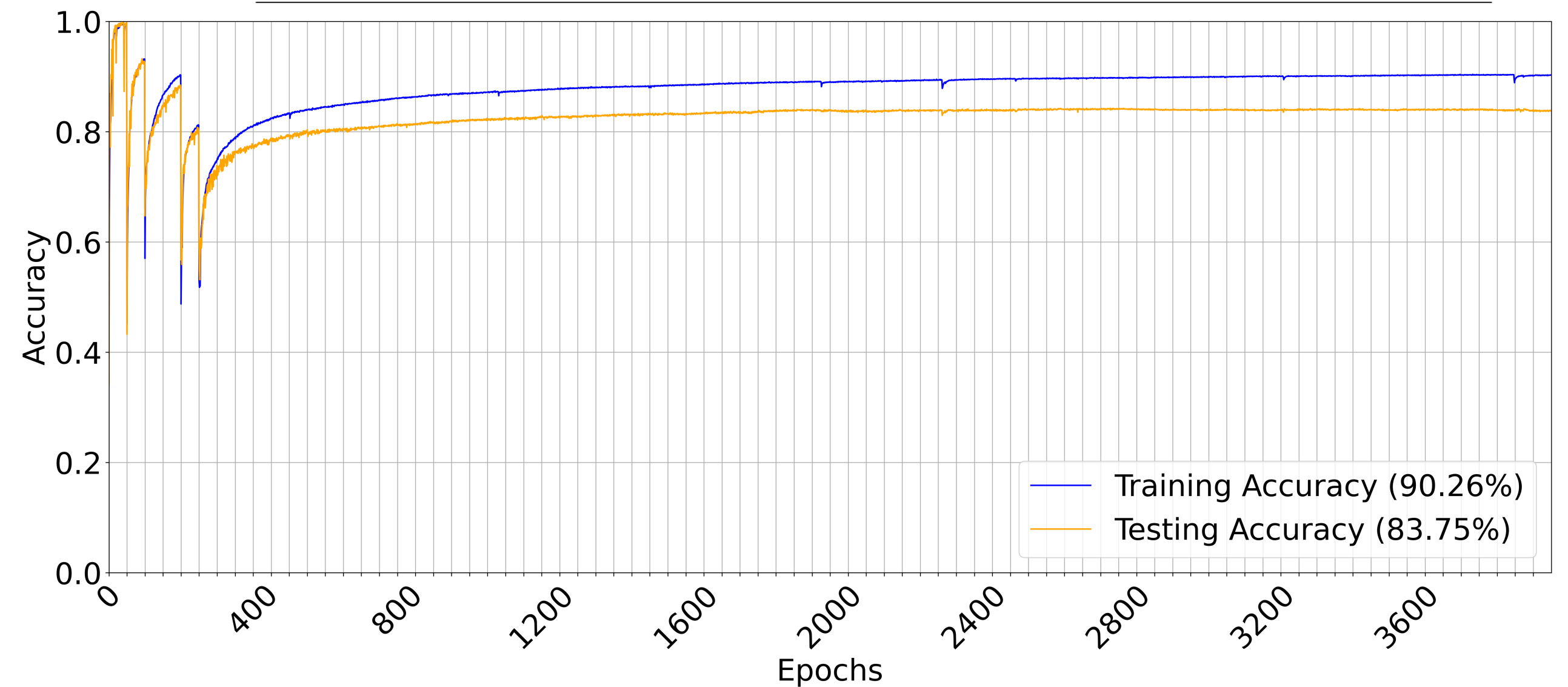
$$\frac{dN}{d\sqrt{s}} = \rho(s) \left[ |F(s)|^2 + B(s) \right];$$

$$F(s) = \alpha_1 T_{11}(s) + \alpha_2 T_{21}(s)$$

$$S_{11}(\omega) = \prod_m \frac{D_m(-1/\omega)}{D_m(\omega)} \quad S_{11}S_{22} - S_{12}S_{21} = \prod_m \frac{D_m(-\omega)}{D_m(\omega)}$$

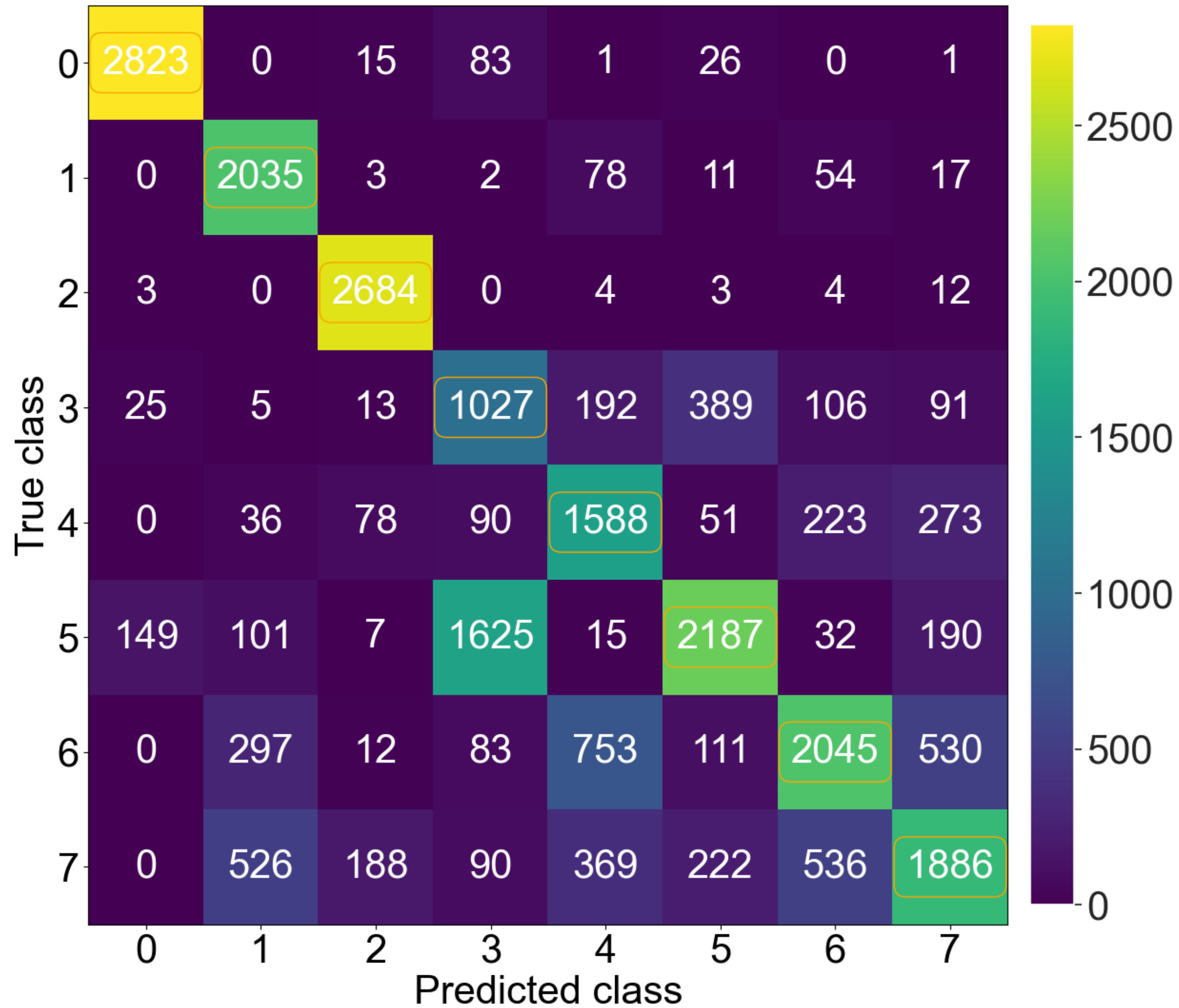
$$S_{22}(\omega) = \prod_m \frac{D_m(1/\omega)}{D_m(\omega)}$$

$$\hat{S} = \hat{1} + 2i\hat{T}$$

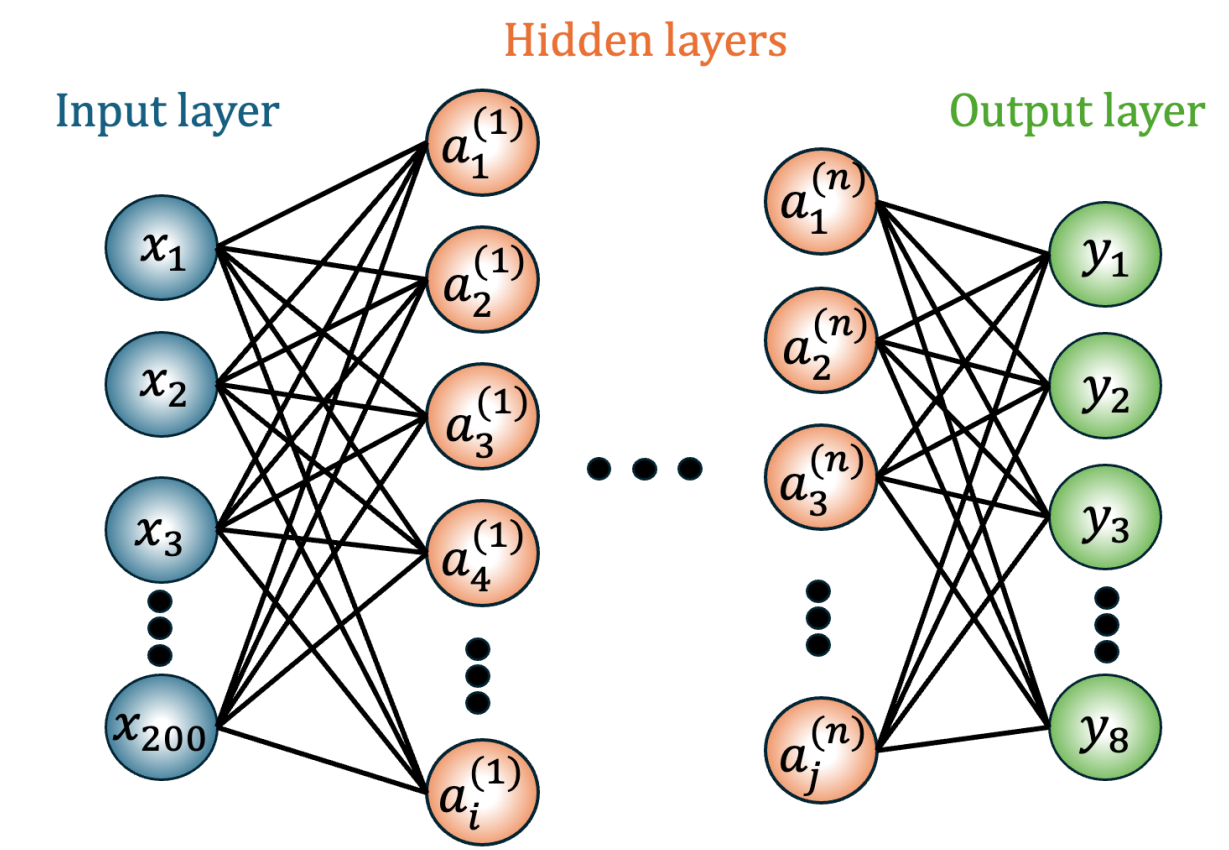
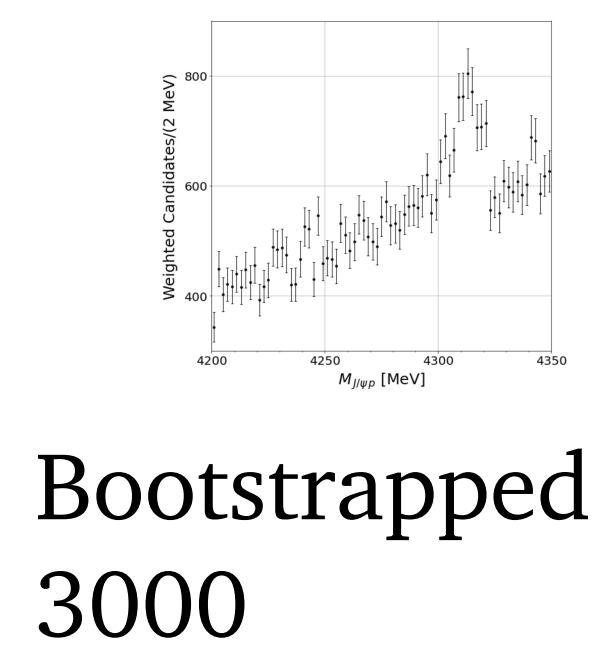


LM Santos, VAA Chavez, DLBS, JPG (2025) 52 015104

# Probe deeper: Pole structure of $P_{c\bar{c}}(4312)^+$



Class label	$S$ -matrix pole configuration
0	1 pole on $[bt]$
1	1 pole on $[bb]$
2	1 pole on $[tb]$
3	1 pole on $[bt]$ and 1 pole on $[bb]$
4	1 pole on $[bb]$ and 1 pole on $[tb]$
5	1 pole on $[bb]$ , 1 pole on $[tb]$ , 1 pole on $[bt]$
6	2 poles on $[bb]$ , 1 pole on $[tb]$
7	1 pole on $[bb]$ , 2 poles on $[tb]$



All output:  
Class 5

1 pole in each  
unphysical RS.

# Probe deeper: Pole structure of $P_{c\bar{c}}(4312)^+$

Focus only on two confusing classes: class 3 vs class 5

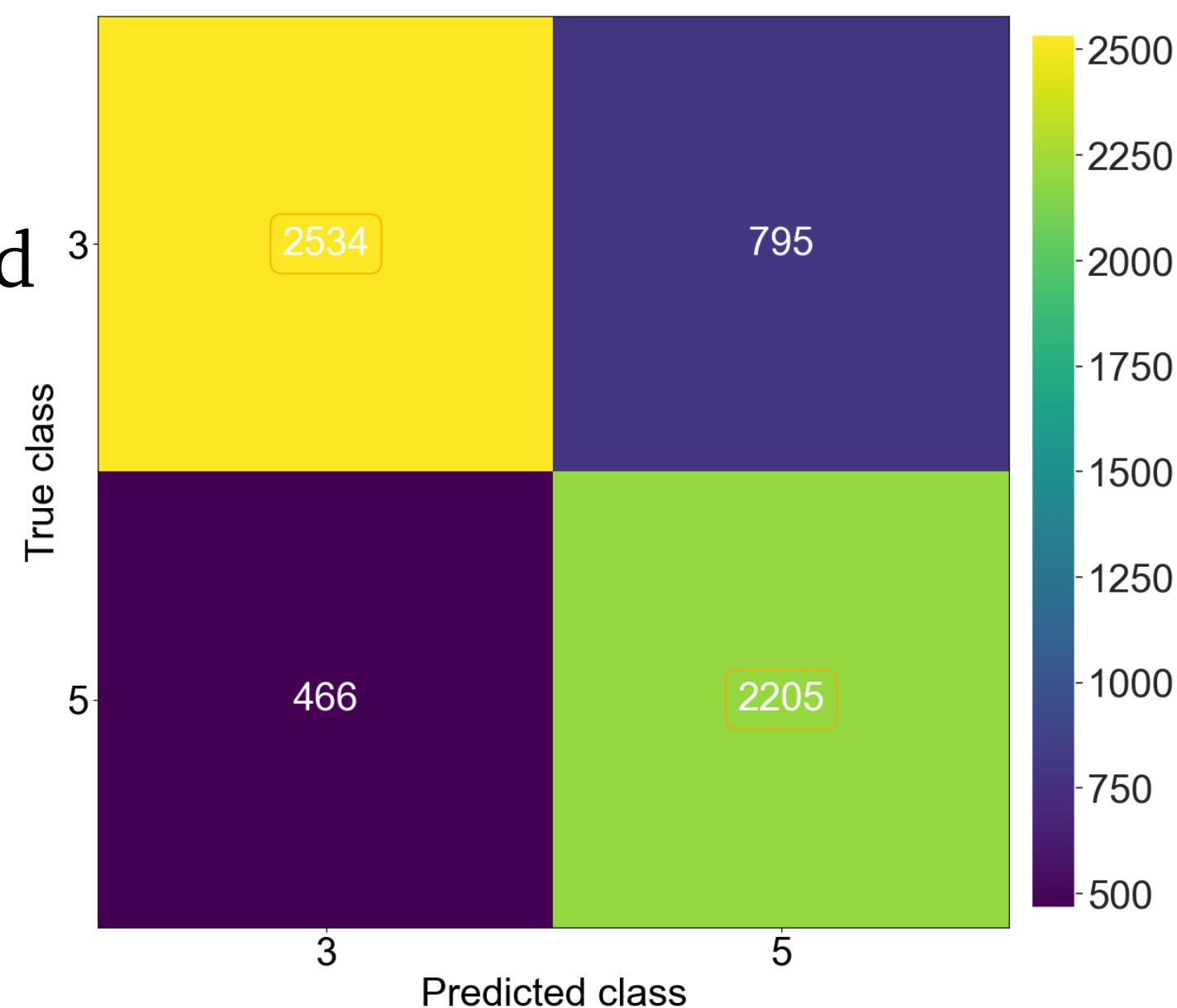
- Retrain new DNN model but with only two outputs.
- Apply again to the experimental data.

Class 3:

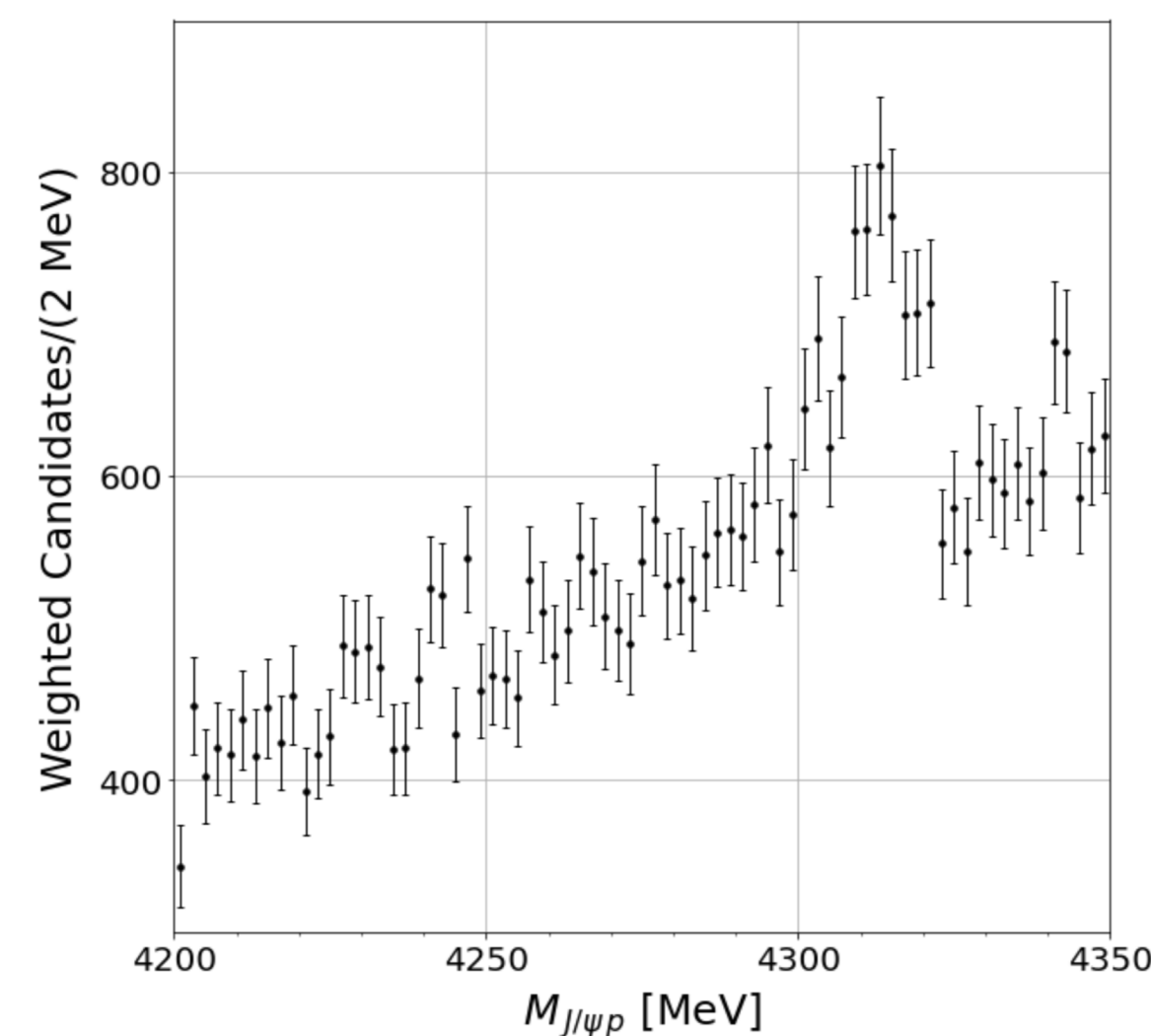
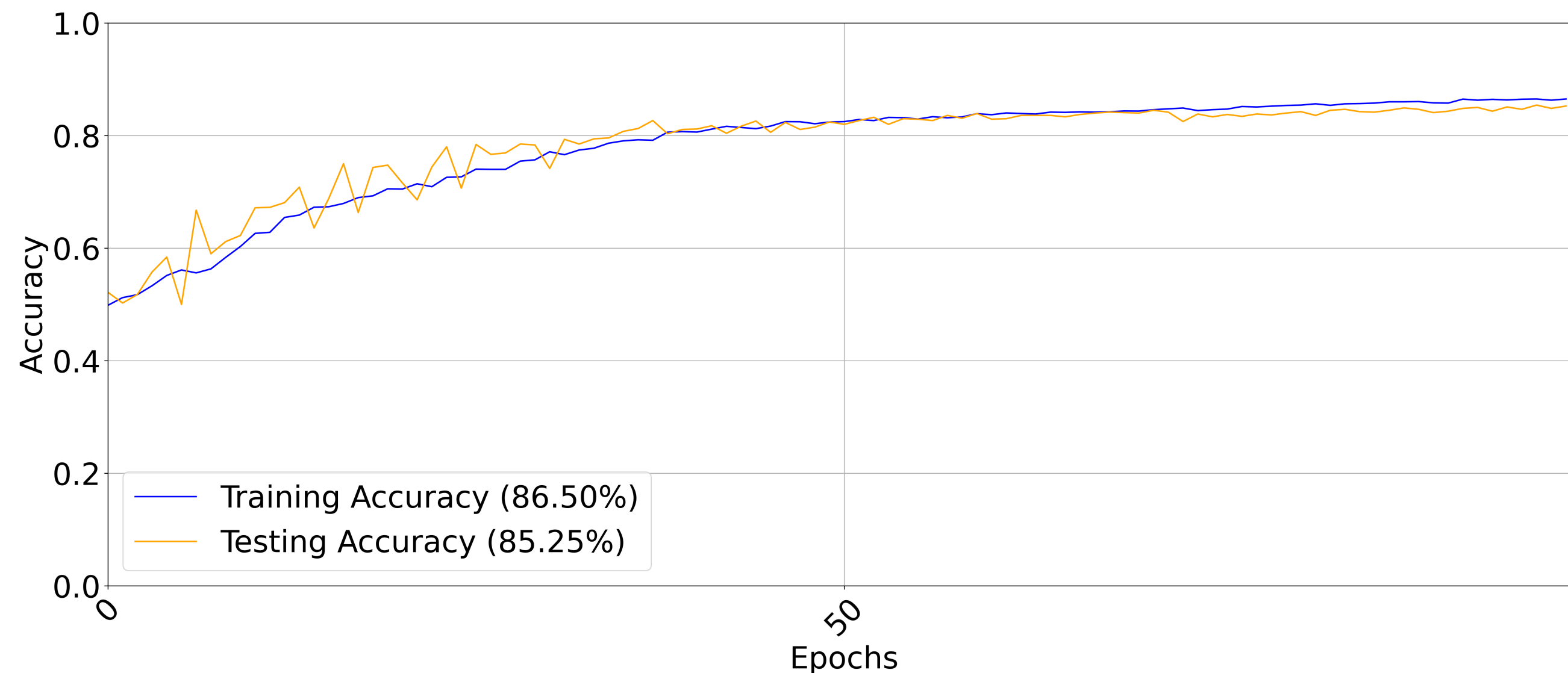
1 pole in 2nd RS and  
1 pole in the 3rd

Class 5:

1 pole in each  
unphysical RS



When the binary DNN model is applied to the experimental data, class 5 is still favored.



Pole in 2nd and 3rd RS  
-resemble pole-shadow pair  
-possible true resonance  
decaying into  $J/\psi p$

Pole in 4th RS  
-Virtual state of  $\Sigma_c \bar{D}$  coupled to  $J/\psi p$

[LM Santos, VAA Chavez, DLBS, JPG \(2025\) 52 015104](#)

# Conclusion and Outlook

- It is possible to distinguish kinematical enhancements with dynamical pole-based enhancements despite the presence of experimental uncertainty.
- To fully utilize the power of ML, use it as a model-selection framework.
  - Multi-parameter of a DNN can be used to cover a wider model space.
- Using the ML approach, we have shown that
  - $P_{c\bar{c}}(4312)^+$  is NOT due to (single) triangle singularity
  - $P_{c\bar{c}}(4312)^+$  is a possible true resonance that is contaminated by the coupled-channel interaction of  $\Sigma_c \bar{D}$  (having a virtual state) with  $J/\psi p$ .

## Outlook

- Include the Double Triangle Singularity interpretation in the ML model-selection framework.
- Apply the method to other near-threshold phenomena.
- Apply the method to correlation function.

**Thank you for your attention.**

# Back Up: General parametrization

$$S_{11}(p_1, p_2) = \prod_m \frac{D_m(-p_1, p_2)}{D_m(p_1, p_2)}$$

[KJ Le Couteur, Proc. Roy. Soc \(London\) A256 \(1960\)](#)

[RG Newton J. Math. Phys. 2, 188 \(1961\)](#)

ERE - Scattering length approx.

$$D(p_1, p_2) = (M_{11} - ip_1) (M_{22} - ip_2) - M_{12}^2$$

$D(p_1, p_2)$  can only vanish when the  $\bar{p}_1$  and  $\bar{p}_2$  have opposite imaginary parts. [W Frazer and A Hendry, Phys. Rev., 134, B1307 \(1964\)](#)

Flatté-like parametrization

$$D(p_1, p_2) = E - M + ip_1 + i\gamma_2 p_2$$

Shadow poles may appear on the physical sheet.

[RJ Eden, JR Taylor, Phys. Rev. 133, B1575 \(1974\)](#)

$$\left[ (p_1 - i\beta_1)^2 - \alpha_1^2 \right] + \lambda \left[ (p_2 - i\beta_2)^2 - \alpha_2^2 \right] = 0$$

We need a general parametrization:

- Pole position can be controlled and RS can be assigned.
- Poles are independent of each other.

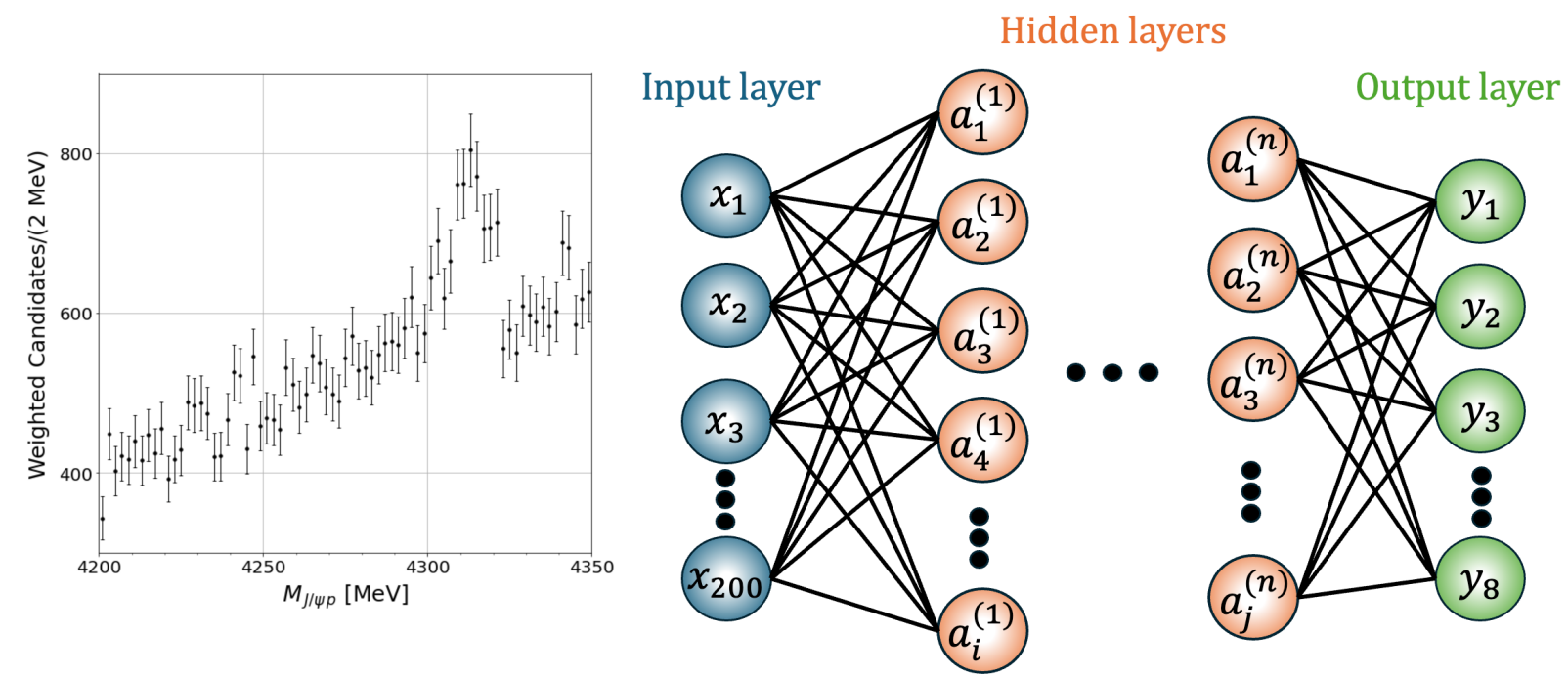
$$\left[ (p_1 - i\beta_1)^2 - \alpha_1^2 \right] \left[ \left( p_1 - i\beta_1 \frac{1-\lambda}{1+\lambda} \right)^2 - \left( \alpha_1^2 + \frac{4\lambda\beta_2^2}{(1+\lambda)^2} \right) \right] = 0$$

$$\left[ (p_2 - i\beta_2)^2 - \alpha_2^2 \right] \left[ \left( p_2 + i\beta_2 \frac{1-\lambda}{1+\lambda} \right)^2 - \left( \alpha_2^2 + \frac{4\lambda\beta_1^2}{(1+\lambda)^2} \right) \right] = 0$$

Main pole

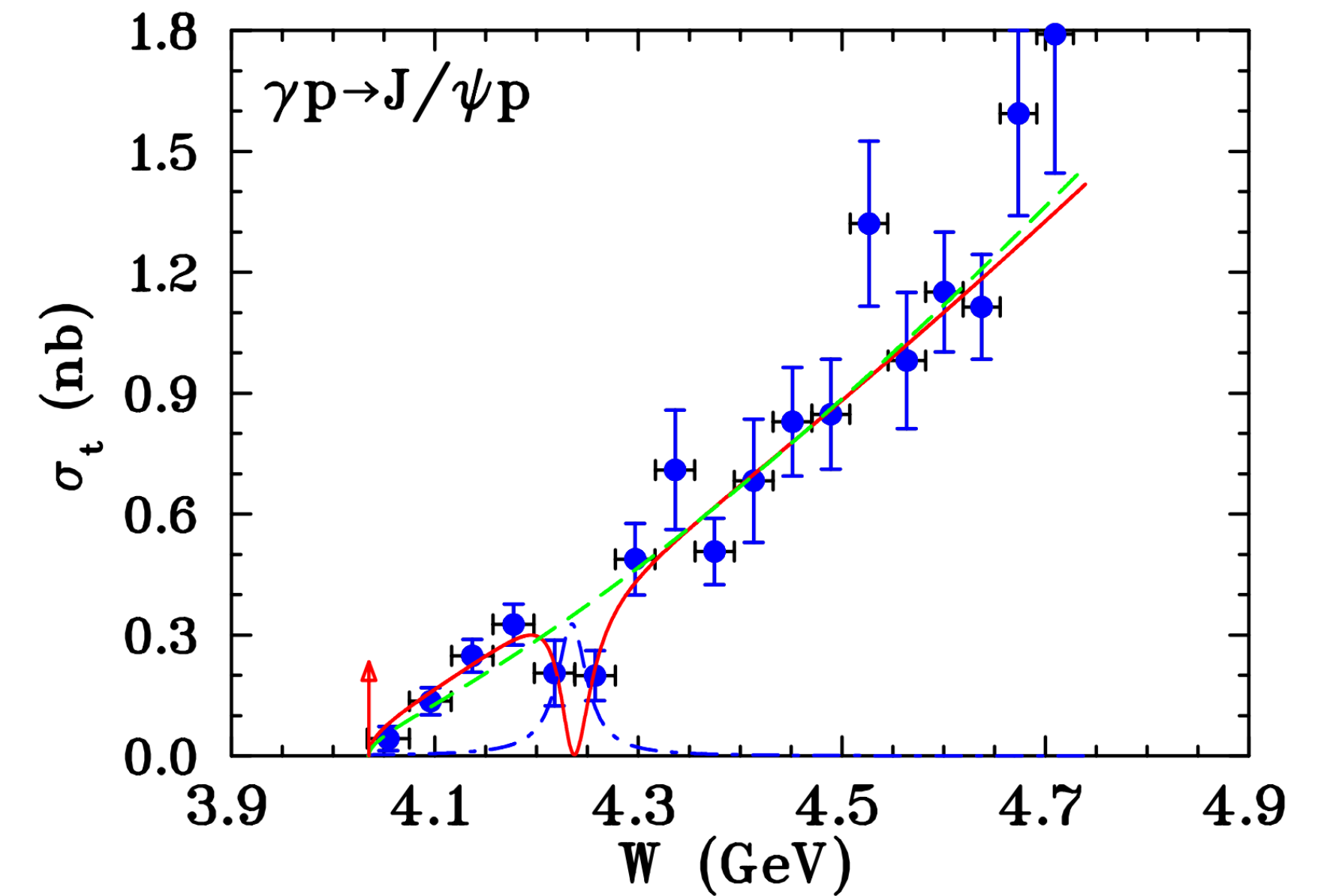
Shadow poles

# Back Up: $P_{c\bar{c}}(4312)^+$



Pole in 2nd and 3rd RS  
 -resemble pole-shadow pair  
 -possible true resonance  
 decaying into  $J/\psi p$

Pole in 4th RS  
 -Virtual state of  $\Sigma_c \bar{D}$   
 coupled to  $J/\psi p$



In contrast with the analysis of JPAC in 2019

[JPAC, PRL 123 092001 \(2019\)](#)

GlueX:  $J/\psi$  photo-production 2023 result - structure found in the  $J/\psi$ - $p$  cross-section

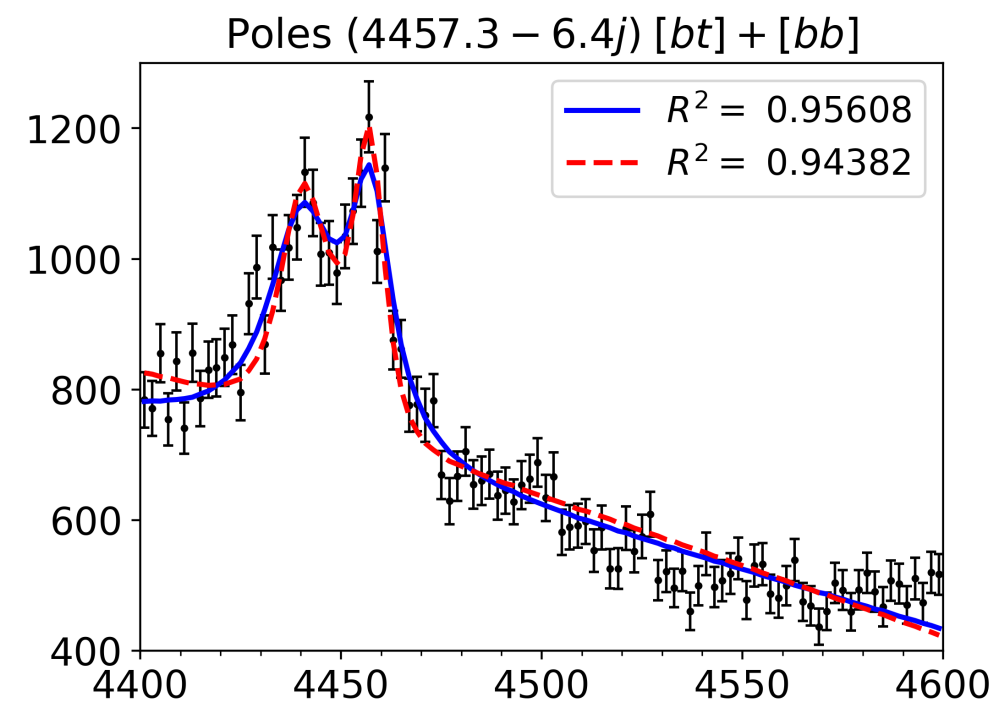
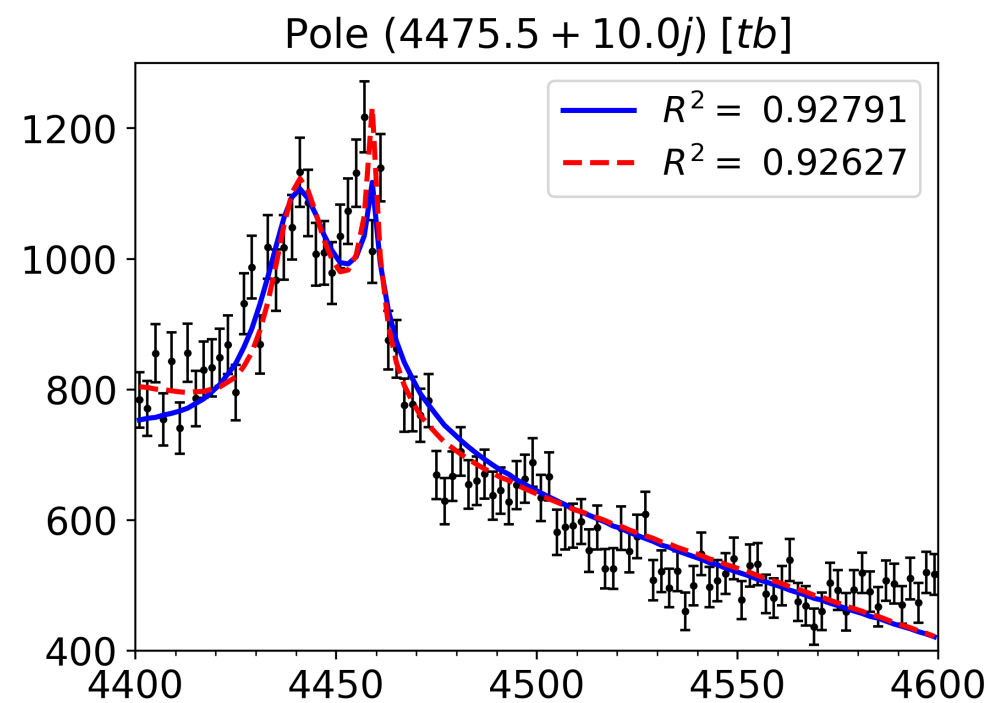
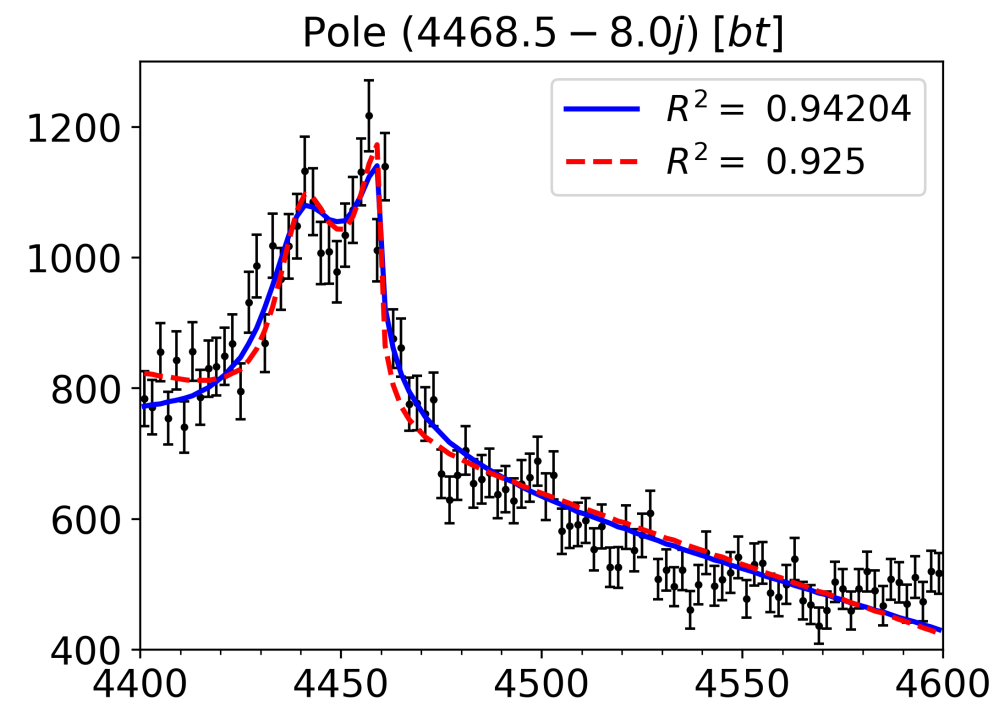
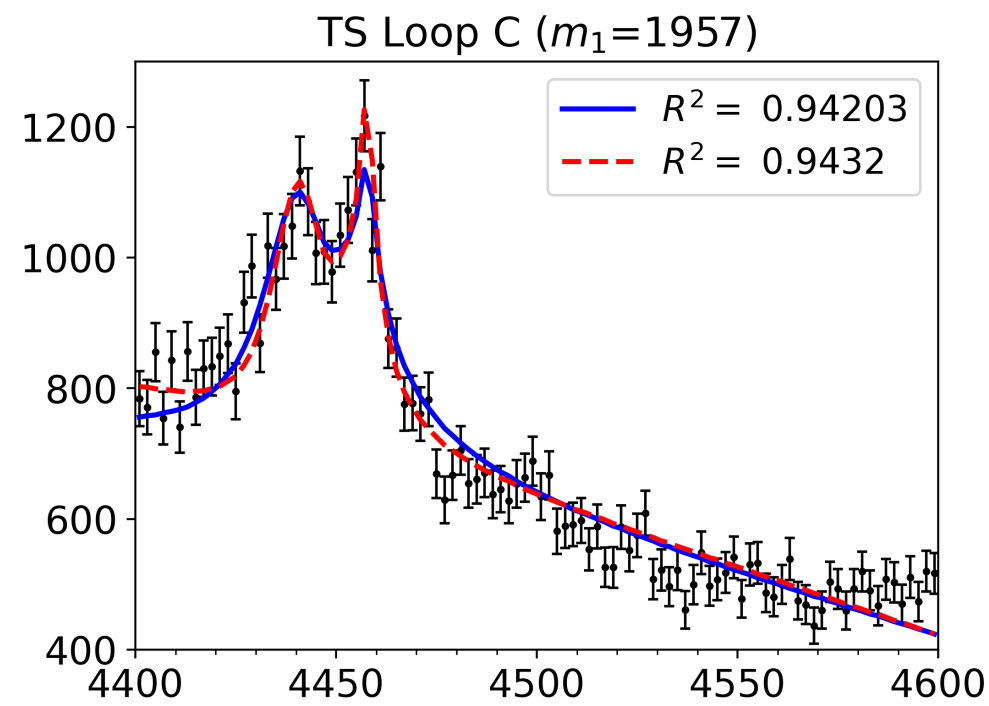
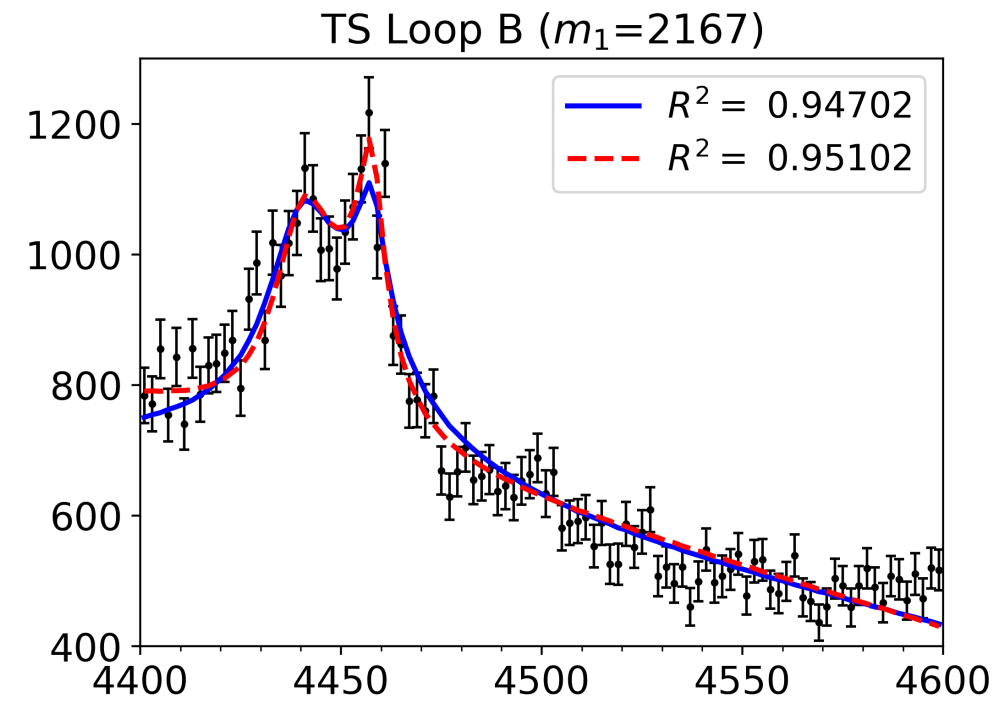
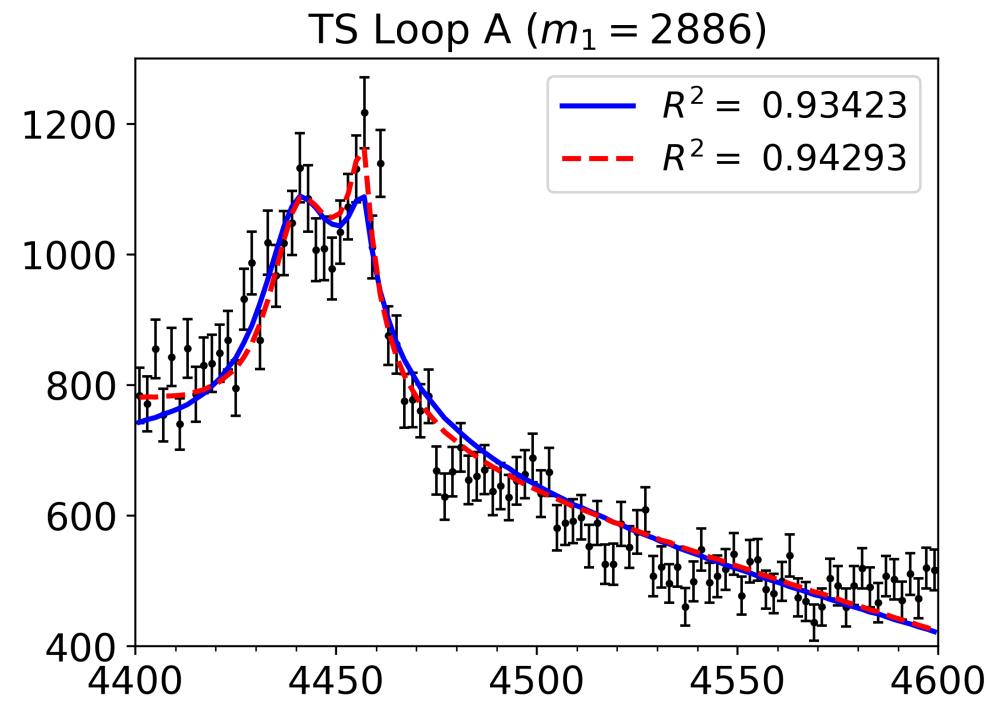
[GlueX, PRC 108 025201 \(2023\)](#)

The dip structure can be interpreted as a resonance that interfere with the non-resonant background.

[I Strakovsky, et al, PRC 108 015202 \(2023\)](#)

No contribution from the  $\Sigma_c \bar{D}$  - cannot be interpreted as molecular.

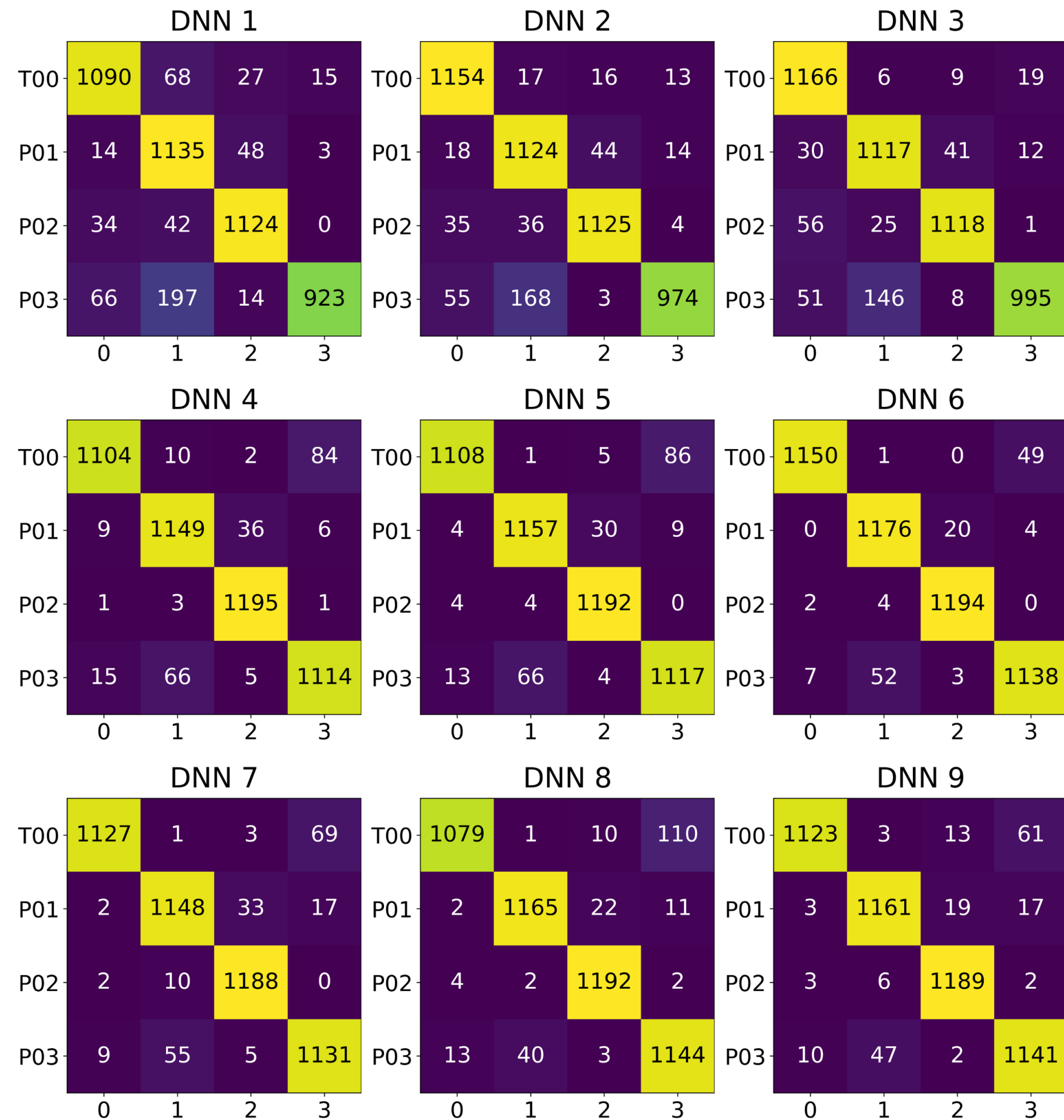
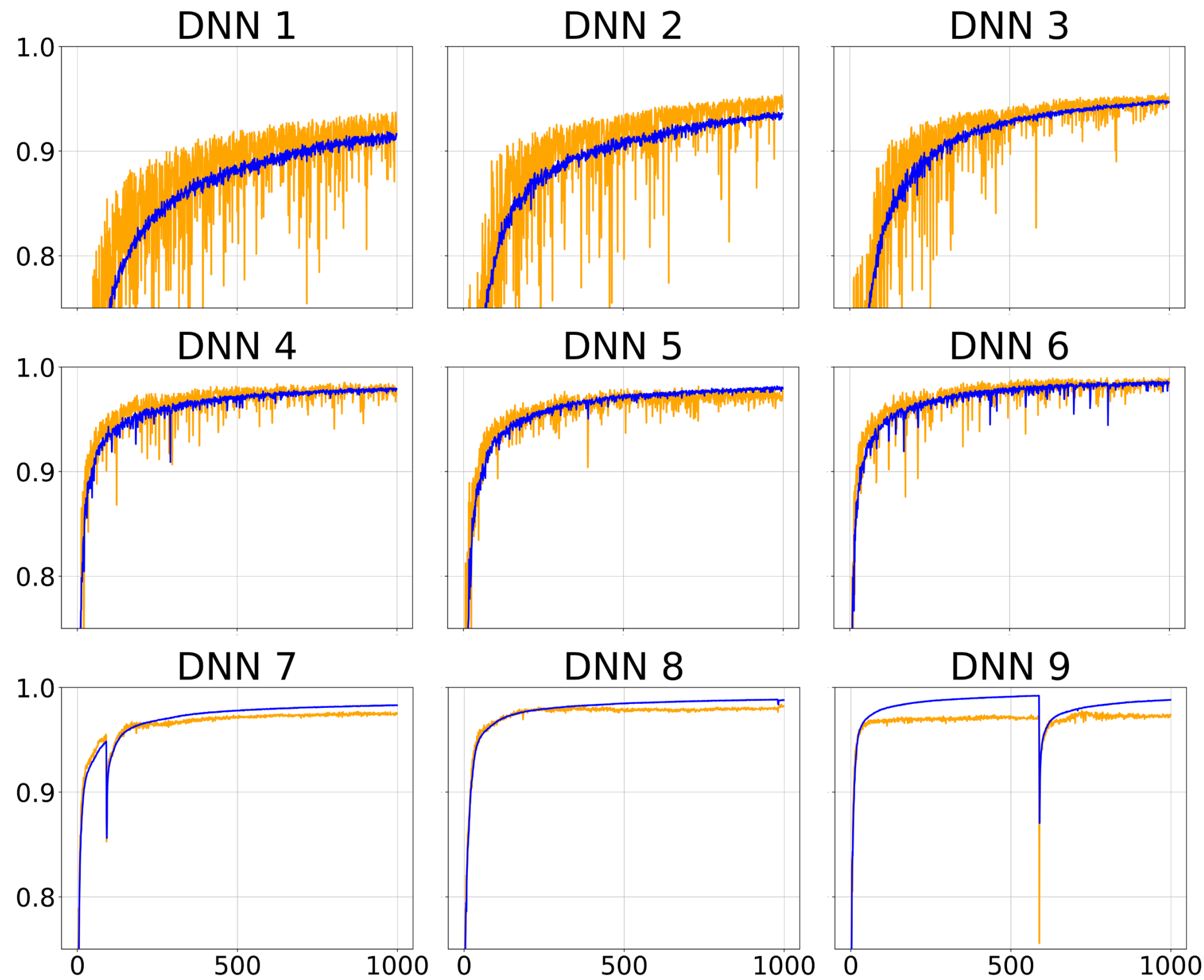
# Back Up: $P_{c\bar{c}}(4457)^+$



DNN model	Optimizer and architecture
DNN 1	AdaGrad: 200-[350-250]-4
DNN 2	AdaGrad: 200-[350-300-250]-4
DNN 3	AdaGrad: 200-[350-400-350]-4
DNN 4	AMSGrad: 200-[350-250]-4
DNN 5	AMSGrad: 200-[350-300-250]-4
DNN 6	AMSGrad: 200-[350-400-350]-4
DNN 7	SMORMS3: 200-[350-250]-4
DNN 8	SMORMS3: 200-[350-300-250]-4
DNN 9	SMORMS3: 200-[350-400-350]-4

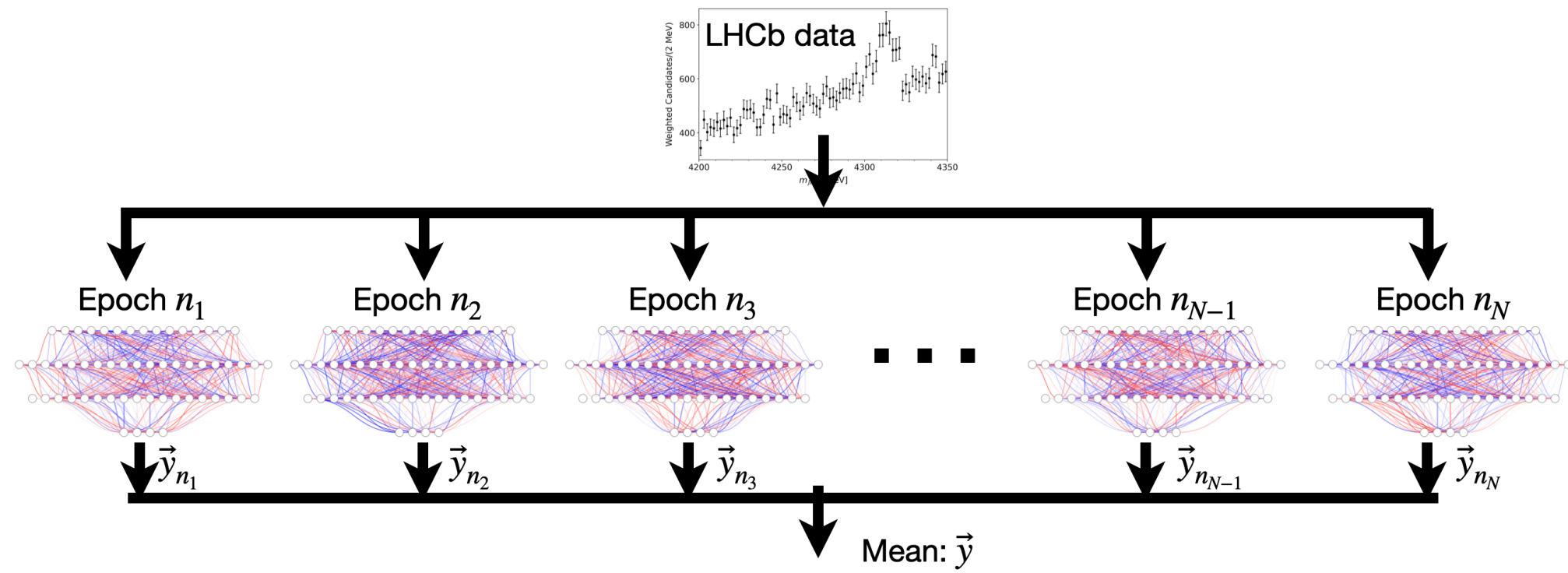
[DAO Co and DLBS, arXiv:2411.14044](https://arxiv.org/abs/2411.14044)

# Back Up: $P_{c\bar{c}}(4457)^+$



[DAO Co and DLBS, arXiv:2411.14044](https://arxiv.org/abs/2411.14044)

# Back Up: $P_{c\bar{c}}(4457)^+$



[DAO Co and DLBS, arXiv:2411.14044](https://arxiv.org/abs/2411.14044)

	<b>Triangle</b>	<b>1 pole in <math>[bt]</math></b>	<b>1 pole in <math>[tb]</math></b>	<b>1 pole each in <math>[bt]</math> and <math>[bb]</math></b>
DNN 1	376	320	1	2303
DNN 2	36	0	0	2964
DNN 3	14	287	1008	1691
DNN 4	181	317	0	2502
DNN 5	0	0	0	3000
DNN 6	0	0	0	3000
DNN 7	0	0	0	3000
DNN 8	12	2	0	2986
DNN 9	0	5	0	2995